12-2016

TARGETING PD-1/PDL-1 SIGNALING IN THE TREATMENT OF OSTEOSARCOMA LUNG METASTASIS

Pooja Dhupkar 3012359

TARGETING PD-1/PDL-1 SIGNALING IN THE TREATMENT OF

OSTEOSARCOMA LUNG METASTASIS

by

Pooja Dhupkar, M.S.

APPROVED:

_____
Eugenie Kleinerman, M.D., Supervisory Professor

_____
Nancy Gordon, M.D.

_____
Zahid Siddik, Ph.D.

_____
Michael Curran, Ph.D.

_____
Gheath Al-Atrash, D.O., Ph.D.

_____
Sonal Gupta, Ph.D.

APPROVED:

_____
Dean, The University of Texas
Graduate School of Biomedical Sciences at Houston

TARGETING PD-1/PDL-1 SIGNALING IN THE TREATMENT OF OSTEOSARCOMA LUNG METASTASIS

A

DISSERTATION

Presented to the Faculty of
The University of Texas
Health Science Center at Houston

And

The University of Texas
M.D. Anderson Cancer Center
Graduate School of Biomedical Sciences

in partial Fulfillment
of the Requirements
for the Degree of

DOCTOR OF PHILOSOPHY

by

Pooja Dhupkar, M.S.

Houston, TX

December 2016

JOHN WILEY AND SONS LICENSE TERMS AND CONDITIONS

Nov 09, 2016

This Agreement between Pooja Dhupkar ("You") and John Wiley and Sons ("John Wiley and Sons") consists of your license details and the terms and conditions provided by John Wiley and Sons and Copyright Clearance Center.

License Number	3984980441464
License date	Nov 09, 2016
Licensed Content Publisher	John Wiley and Sons
Licensed Content Publication	Immunological Reviews
Licensed Content Title	The PD-1 pathway in tolerance and autoimmunity
Licensed Content Author	Loise M. Francisco,Peter T. Sage,Arlene H. Sharpe
Licensed Content Date	Jun 15, 2010
Licensed Content Pages	24
Type of use	Dissertation/Thesis
Requestor type	University/Academic
Format	Print and electronic
Portion	Figure/table
Number of figures/tables	1
Original Wiley figure/table number(s)	Figure 2
Will you be translating?	No
Title of your thesis / dissertation	¬¬¬TARGETING PD-1/ PDL-1 SIGNALING IN THE TREATMENT OF OSTEOSARCOMA LUNG METASTASIS
Expected completion date	Dec 2016
Expected size (number of pages)	200

ELSEVIER LICENSE
TERMS AND CONDITIONS

Nov 09, 2016

This Agreement between Pooja Dhupkar ("You") and Elsevier ("Elsevier") consists of your license details and the terms and conditions provided by Elsevier and Copyright Clearance Center.

License Number	3984981202431
License date	Nov 09, 2016
Licensed Content Publisher	Elsevier
Licensed Content Publication	Trends in Pharmacological Sciences
Licensed Content Title	New immunotherapies targeting the PD-1 pathway
Licensed Content Author	Jordan M. Chinai,Murali Janakiram,Fuxiang Chen,Wantao Chen,Mark Kaplan,Xingxing Zang
Licensed Content Date	September 2015
Licensed Content Volume Number	36
Licensed Content Issue Number	9
Licensed Content Pages	9
Start Page	587
End Page	595
Type of Use	reuse in a thesis/dissertation
Intended publisher of new work	other
Portion	figures/tables/illustrations
Number of figures/tables/illustrations	1
Format	both print and electronic
Are you the author of this Elsevier article?	No
Will you be translating?	No
Order reference number	
Original figure numbers	Figure 1
Title of your thesis/dissertation	¬¬¬TARGETING PD-1/ PDL-1 SIGNALING IN THE TREATMENT OF OSTEOSARCOMA LUNG METASTASIS
Expected completion date	Dec 2016
Estimated size (number of pages)	200
Elsevier VAT number	GB 494 6272 12

DEDICATION

I would like to dedicate this dissertation to my parents, Milind and Neeta Dhupkar. You have always been an inspiration!

To my husband, Mangesh Edke, standing by my side in challenging and difficult times in this journey. Also, for supporting and motivating me to accomplish my ambitions.

ACKNOWLEDGEMENTS

I would like to sincerely extend my gratitude to my advisor, Dr. Eugenie Kleinerman. I thank her for all her support, guidance and giving me an opportunity to perform in her laboratory at a challenging time during my Ph.D. Her passion for science and compassion as a physician-scientist truly make her my role model. I am greatly thankful to my co-mentor, Dr. Nancy Gordon, who has been so kind and helpful to guide me in my dissertation project. She was always willing to discuss my concerns and kept me focused during the course of my training. Thanks to you both for making this journey easier for me!

I am grateful to my committee members, Dr. Michael Curran, Dr. Zahid Siddik, Dr. Gheath Al-Atrash and Dr. Sonal Gupta for all the suggestions and advice for my project. I would also like to thank Dr. Patrick Hwu for his guidance and being a part of my committee. I am appreciative of the support from past and current fellow lab members including Dr. Ling Yu, Dr. Gangxiong Huang, Clarissa Smith, Simin Kiany, Dr. Keri Schadler, Dr. Andrew Livingston, Dr. Zhichao Zhou, Dr. Thomas Yang, Dr. Hatel Moonat, Dr. Janice Santiago, Fei Wang and Claudia. I would also like to thank my friends and colleagues from Experimental Therapeutics program, Seema Mukherjee and Kshipra Gharpure for their support and motivation.

I am extremely lucky to be a part of a motivating family, who always believed in my ambitions and potential. Thanks to my parents Milind and Neeta Dhupkar, for trusting my goals. To my grandmother and late grandfather, for building the value of education within me. And last, but not the least, to my husband, Mangesh Edke, this would have been difficult without you being by my side. Thanks for being such and understanding and helpful partner throughout this entire Ph.D. journey!

TARGETING PD-1/PDL-1 SIGNALING IN THE TREATMENT OF OSTEOSARCOMA LUNG METASTASIS

Pooja Dhupkar, M.S.

Supervisory Professor: Eugenie Kleinerman, M.D.

Osteosarcoma (OS) manifests itself as pulmonary metastasis, which is a major cause of death in OS patients. Novel treatments like immunotherapy hold promise for the treatment of OS pulmonary metastasis. However, immunosuppressive mechanisms such as binding of immune inhibitory receptor, PD-1 with PDL-1, which is upregulated in cancer cells, may cause disease relapse.

The effect of PD-1 blockade on NK cells and macrophages has not been investigated till date. The aim of this study was to determine if PD-1 blockade leads to of OS lung metastasis regression and study the role of NK cells and/or macrophages in the anti-PD-1 responses. We demonstrated that PDL-1 is expressed in human OS cell lines and in lung metastases from OS patients, implying that its importance as a potential therapeutic target in OS. Further, *in vivo* anti-murine-PD-1 administration led to a significant decrease in the number of OS lung metastases using a human LM7 OS mouse model. Also, there was a significant increase in tumor cell apoptosis and decrease in tumor cell proliferation after *in vivo* anti-PD-1 treatment. In addition, anti-PD-1 led to blockade of p-STAT3/p-Erk1/2 and PDL-1 signaling in OS lung tumors.

We discovered that PD-1 was expressed on NK cells and macrophages in OS lung tumors. Increased infiltration of NK cells and macrophages was observed within OS lung metastatic tumors after anti-PD-1 treatment. Particularly, anti-PD-1 caused an increase in the

anti-tumor M1 macrophages and decrease in numbers of pro-inflammatory M2 macrophages in OS lung metastases. We further investigated the implication of NK cells and macrophages in the therapeutic efficacy of anti-PD-1 against OS lung metastases. NK cell depletion using anti-asialo-GM1 did not affect the efficacy of anti-PD-1. Hence, NK cells were not the crucial immune cells involved in anti-tumor responses of anti-PD-1. However, macrophage depletion using Clodrosome prior to anti-PD-1 treatment significantly compromised the regression of OS lung metastasis. Our results implied that macrophages are the crucial mediators of the anti-tumor responses of anti-PD-1 against OS lung metastasis. Overall, our data suggests that PD-1 blockade with anti-PD-1 leads to regression of OS lung metastases, primarily through activation of macrophages.

TABLE OF CONTENTS

LIST OF FIGURES

LIST OF TABLES

LIST OF ABBREVIATIONS:

4-1BB	Tumor necrosis factor receptor superfamily member 9
ALK	anaplastic lymphoma kinase
ALT	Alanine transaminase
AML	Acute myelogenous leukemia
APCs	Antigen presenting cells
AST	Aspartate aminotransferase
CAR	Chimeric antigen receptor
CBC	Complete blood count
CT	Computed tomography
CTLA-4	Cytotoxic T-lymphocyte-associated protein 4
Erk 1/2	Extracellular signal-regulated kinase ½
IDO1	Indoleamine 2,3-dioxygenase 1
IFN-γ	Interferon gamma
IL-10	Interleukin-10
IL-2	Interleukin-2
ITIM	Immunoreceptor tyrosine-based inhibitory motif
ITSM	Immunoreceptor tyrosine-based switch motif
KIR	Killer cell immunoglobulin-like receptor
LAG-3	Lymphocyte activation gene 3 protein
L-MTP-PE	Liposomal muramyl tripeptipe phosphatidyl ethanolamine
MHC	Major histocompatibility complex
MRI	Magnetic resonance imaging
mTOR	Mammalian target of rapamycin
NK	Natural killer cells
NSCLC	Non-small cell lung cancer

NY-ESO-1	New York-esophageal squamous cell carcinoma-1
OS	Osteosarcoma
OX40	Tumor necrosis factor receptor superfamily member 4
PARP	Poly ADP ribose polymerase
PBMCs	Peripheral blood mononuclear cells
PD-1	Programmed cell death protein 1
PDL-1	Programmed death ligand 1
PDL-2	Programmed cell death protein 1 ligand 2
PI3-K	Phosphatidylinositol-4,5-bisphosphate 3-kinase
SHP-1	Src homology 2-containing protein tyrosine phosphatases 1
SHP-2	Src homology 2-containing protein tyrosine phosphatases 2
STAT3	Signal transducer and activator of transcription 3
TAMs	Tumor-associated macrophages
TCR	T-cell receptor
TGF-b	Transforming growth factor-b
TILs	Tumor infiltrating lymphocytes
TUNEL	Terminal deoxynucleotidyl transferase [TdT]-mediated deoxyuridinetriphosphate [dUTP] nick end labeling
US-FDA	United States Food and Drug administration

CHAPTER 1

INTRODUCTION

Osteosarcoma

Osteosarcoma (OS) is the most frequent primary malignancy of the bone in pediatric patients. Every year, 400 new OS cases are diagnosed in the United States, which has resulted in OS becoming the eighth most common childhood malignancy (1, 2). It usually occurs in children and adolescents in the age group of 10-20 years or elderly adults above 65 years. OS primarily affects the metaphysis of the fast- growing long bones at the extremities, the most common sites of occurrence being proximal tibia (23%), distal femur (43%) or humerus (10%) (1, 3). OS arises from the mesenchymal cells of the bone and is characterized by the malignant cells producing aberrant osteoid or immature bone (2, 4). Diagnosis of OS is done using plain radiography, magnetic resonance imaging (MRI) or computed tomography (CT) scanning (5). There are several risk factors for the development of OS which include ionization radiation (cumulative high-radiation doses), chemotherapy (anthracycline or high-dose alkylating agents), Paget's disease (accelerated bone turnover), genetic abnormalities such as retinoblastoma (Rb inactivation), Li-Fraumeni syndrome (p53 deletions), Rothmund-Thomson syndrome (RECQL4 mutations), Bloom syndrome (RECQL2) and Werner syndrome (RECQL3) (5).

Due to the hematogenous spread of the disease, the most common site of OS metastasis is the lung. 15-20% of the patients have detectable metastases at the time of diagnosis and majority of the patients (85%) present with micro-metastatic disease, thus making it an aggressive life-threatening cancer (6, 7). The current standard treatment of OS includes neoadjuvant chemotherapy and subsequent surgical excision of the primary tumor as well as clinically detectable metastases. Surgery is further followed by adjuvant chemotherapy. Currently, 80% of patients are subjected to limb salvage surgery (4). The

current standard of care includes the combination chemotherapy of Cisplatin, Doxorubicin/Adriamycin and high-dose Methotrexate (MAP), with or without Ifosfamide. This combination treatment has dramatically improved the 5-year survival of patients with localized disease from 20% to 70% (4, 5). However, despite chemotherapy advances, none of the second-line therapy options for relapsed patients have shown any therapeutic benefit. The 5-year survival of patients with OS pulmonary metastasis remains as low as 20-30%, without any significant improvement in the past twenty years (2, 4). Hence, there is a pressing need to improve clinical outcomes for relapsed disease patients through the discovery of novel therapeutic options for this lethal malignancy. **Table 1** lists the current clinical trials that are ongoing for OS (https://clinicaltrials.gov/)

.

Table 1. Current clinical trials in OS

(https://clinicaltrials.gov/)

Target population	**Agent**	**Phase**	**Study started**
Bone metastasis in solid tumors, advanced pretreated OS	Chemotherapy combination of Sirolimus with cyclophosphamide, methotrexate, zoledronic acid	Phase 1 (Prospective)	February 2015
Osteosarcoma metastasis	Apatinib (small-molecule VEGFR tyrosine kinase inhibitor)	Phase 2 Phase 3	March 2016

Target patient population	**Agent**	**Phase**	**Study started**
OS	Combination of neo-adjuvant chemotherapy and Lithium Carbonate (GSK3β inhibitor)	Phase 4	January 2013
Metastatic/ recurrent OS	Combination of Dinutuximab (Anti-disialoganglioside monoclonal antibody and Sargramostim (GM-CSF)	Phase 2	November 2015
Lung metastasis in Soft Tissue Sarcoma and Bone sarcomas	Doxorubicin (*In vivo* lung perfusion)	Phase 1	February 2016
GD2+ solid tumors (OS, neuroblastoma)	Anti-GD2-CAR T cells (3rd generation)	Phase 1	February 2014
OS, CNS tumors, Neuroblastoma, Ewings Sarcoma, Rhabdomyosarcoma	Allogenic hematopoietic cell transplantation and Donor NK cell infusions	Phase 2	March 2014

Target patient population	Agent	Phase	Study started
Solid tumors (non-CNS) including OS	HSV1716 (mutant herpes simplex virus (HSV) type I)	Phase 1	March 2010
Relapsed OS	Docetaxel and Gemcitabine combination versus Ifosfamide	Phase 2	April 2016
Relapsed OS	Thiotepa (Alkylating agent) and stem cell rescue with chemotherapy	Phase 2	July 2009
Metastatic OS	Pazopanib	Phase 2	April 2013
Recurrent, metastatic OS	Denosumab (RANK ligand antibody)	Phase 2	October 2015
High grade OS	Regorafenib (Multi-kinase inhibitor)	Phase 2	September 2014
Sarcomas including OS	Combination of cyclophosphamide and MM-398 (Irinotecan Sucrosofate Liposome Injection)	Phase 1	December 2013
Relapsed/ Recurrent OS	Combination of erlotinib and temozolomide	Phase 2	August 2016

Target patient population	Agent	Phase	Study started
Sarcomas including advanced/metastatic OS	***Combination of Pembrolizumab (anti-PD-1) and Metronomic Cyclophosphamide***	***Phase 2***	***March 2015***
Sarcomas including recurrent OS	***Combination of Nivolumab (anti-PD-1) and Ipilimumab (anti-CTLA-4)***	***Phase 1/Phase 2***	***February 2015***

Immunotherapy for Osteosarcoma treatment

Immunotherapy is one of the promising approaches to target minimal residual and relapsed disease. Our laboratory has previously successfully discovered novel immunotherapeutic strategies for treatment of OS in preclinical and clinical settings.

L-MTP-PE

We have shown that the immunomodulator L-MTP-PE activates the macrophages and monocytes to eradicate metastases in human and canine models of OS (8-10). L-MTP-PE is known to induce inflammatory responses like activation of macrophages, stimulation of anti-tumor monocytes, and cause an increase in levels of cytokines and inflammatory molecules (11). Recently, data from clinical trials showed that L-MTP-PE given in combination with standard adjuvant chemotherapy resulted in 8% improvement in the overall survival of

patients with OS metastatic disease (12-14). L-MTP-PE has been approved by European Medical Agency and in other countries for the treatment of surgically resectable non-metastatic OS in combination with chemotherapy. L-MTP-PE has been the only novel therapeutic agent that has made a significant impact on the survival of OS patients.

NK cell therapy

Immune-based cell therapy, in particular, natural-killer (NK) cell therapy has shown to be cytolytic as NK cells express several activating receptors (15). NK cells are the major drivers of the innate immune system and have an advantage over T-cells as they kill target cells without prior tumor-antigen recognition or major histocompatibility complex (MHC)-restriction (16). Adoptive NK cell immunotherapy has shown to be effective against multiple cancer types including acute myelogenous leukemia (AML), metastatic melanoma, renal cell carcinoma and Hodgkin's disease (17-19). NK cell infusions require *ex vivo* expansion to generate large numbers of NK cells to elicit the necessary clinical therapeutic effect. Several platforms such as membrane bound IL-21–expressing K562 antigen presenting cells (APCs) have been implemented to generate a high number of proliferating activated NK cells (20). It has been found that lower NK cell numbers correlated with poor outcomes in OS patients (21, 22). *In vitro* cytotoxicity studies with NK cells have also demonstrated activity against a panel of OS cells and other pediatric solid tumor cell lines (23-25). Further, it has been previously shown that the number and activity of NK cells positively correlated with the clinical outcomes in OS patients treated with Interleukin-2 (IL-2) (22). This implied the role of NK cells in the control of osteosarcoma.

Aerosol IL-2

IL-2 is a crucial cytokine for the NK and T-cell activation, proliferation and maintenance of immune responses (26, 27). Systemic high-dose IL-2 has been previously approved by the United States Food and Drug administration (US-FDA) for the treatment of metastatic renal cancer and metastatic melanoma (28, 29). However, IL-2 treatment has been associated with a plethora of systemic toxicities such as 'capillary leak syndrome' culminating in extravasation of fluid into the organs, pulmonary congestion, hypotension, pre-renal azotemia, adult respiratory distress syndrome and myocardial infarction (30). Hence, alternative approaches such as aerosolized route of delivery of IL-2 have been studied for certain conditions such as lung diseases. Aerosol IL-2 offers an advantage of producing the organ (lung)-specific delivery with minimal toxicity enabling the use of lower dosages. Aerosolized IL-2 has also demonstrated therapeutic benefit in dogs with OS lung disease (31, 32). Previous studies have shown the modest efficacy and safety of aerosol IL-2 in renal cell carcinoma metastasis due to the activation of lymphocytes in the lung (33). Our laboratory has shown the efficacy of single agent aerosol IL-2 in a human OS pulmonary metastasis model (34). However, as the complete elimination of metastases was not observed and relapse was observed, we used a combination approach of aerosol IL-2 along with NK cells. Guma. S *et al.* discovered that aerosolized IL-2 increased the number of human NK cells in the lung and the combination NK and aerosol IL-2 had significant effect against OS lung metastases as compared to NK cell therapy alone (34). Also, the overall survival of mice was significantly improved by the combination therapy and provided benefit compared to the single agent treatments (35).

T-cell therapy

Adoptive T-cell therapy involves the modulation of the adaptive immune system by the transfer of T cells into the patients to induce antitumor responses. It also involves *ex vivo* expansion of T cells before infusing in patients. Recently, genetically engineered T cells such as T-cell receptor (TCR)-modified T cells, chimeric antigen receptor (CAR)-modified T cells have been used to help in accurately redirecting the T cells to the target antigens (36). Adoptive T-cell therapy demonstrated success in in early studies in melanoma, where using autologous polyclonal T cells expressing melan-A (MART-1) specific α/β TCRs were administered and 2 of 15 patients showed objective responses against metastatic lesions (37). Clinical trials using New York-esophageal squamous cell carcinoma-1 (NY-ESO-1)-specific TCR T cells showed objective clinical responses in 4 out of 6 synovial cell carcinoma patients and melanoma patients after chemotherapy (38). Similarly, Ahmed *et al*. showed that HER-2 specific CARs caused regression of OS xenografts in local and metastatic mouse models (39). Our lab demonstrated that IL-11Rα is highly expressed in patient specimens of OS lung metastasis. Hence, administration of IL-11Rα -CAR-specific T cells in nude mice resulted in regression of lung metastases (40).

In summary, a number of immunotherapeutic strategies have demonstrated success in exhibiting an antitumor role in OS. This promotes a better understanding of immune-tumor cell interactions in the OS lung tumor microenvironment in order to develop better immune targeting agents.

Role of PD-1 (Programmed cell death protein 1) and PDL-1 (Programmed death ligand 1) pathway in Cancer

PD-1 and PDL-1 Background

Immune evasion has been recently accepted as one of the hallmarks of cancer. A dynamic interplay exists between the tumor and the host in the tumor microenvironment and the ability of the tumor cells to evade immune recognition (immune surveillance) determines disease progression (41). Immune inhibitory or 'checkpoint' pathways have been known to play a role in limiting the antitumor immune responses against cancer as well as in maintenance of tolerance to self-antigens. The two well-studied negative co-stimulatory molecules are CTLA-4 (cytotoxic T-lymphocyte-associated protein 4) and PD-1. PD-1 is an immune-inhibitory receptor that was first isolated in 1992 by the Ishida group, from the murine T-cell hybridoma undergoing programmed cell death (42). PD-1 is primarily expressed on the membrane, but cytoplasmic expression has also been observed (43). PD-1 is expressed on immune cells such as T cells, B cells, natural killer cells, monocytes on activation (44). Further, PD-1 is an inducible receptor as its expression can be modulated by various cytokines such as IFN-γ (Interferon gamma), IL-2, IL-15 IL-21 (45). On the contrary, CTLA-4 is a recently discovered inhibitory receptor expressed exclusively on T cells and is involved in limiting memory and naive T-cell early activation (46).

Two ligands, PDL-1 (B7-H1) and PDL-2 (programmed cell death protein 1 ligand 2) or B7-H2 were discovered, PDL-1 being the primary ligand responsible for PD-1 mediated immunosuppression (47, 48). PDL-1 is known to be expressed in a wide variety of tissues on both hematopoietic and non-hematopoietic origin. Specifically, PDL-1 is expressed on

immune cells such as T cells, macrophages, B cells and dendritic cells, endothelial cells and muscle cells and also on normal tissues such as placenta, heart, lung and liver (46, 49). Thus, PD-1-PDL-1 pathway controls the immune responses in both secondary lymphoid organs as well as peripheral tissues.

Structure of PD-1 and PDL-2

The length of PD-1 cDNA is 2,106 nucleotides and the protein consists of 288 amino acid residues. It is positioned on chromosome 2 at band q37 (50). Human PD-1 gene is a homologue of murine PD-1 and is known to share 70% homology at the nucleotide level and ~60% identity at the amino acid level with the murine version (51, 52). PD-1 is a 50-55 kDa type I transmembrane glycoprotein of the Ig superfamily. It contains IgV extracellular region, transmembrane domain and cytoplasmic tail. The cytoplasmic region is composed of immunoreceptortyrosine-based inhibitory motif (ITIM), and the immunoreceptor tyrosine-based switch motif (ITSM), which are essential for the inhibitory signaling (53).

The human PDL-1 gene is located on 9p24, the PDL-1 cDNA is 870 bp and it encodes a protein of 290 amino acids (50). PDL-1 is a type I transmembrane glycoprotein and contains IgV-like and C-like domains, a hydrophobic transmembrane domain and a cytoplasmic tail of 30 amino acids (47).

PD-1/PDL-1 signaling and function

The PD-1/PDL-1 pathway plays an important role in the maintenance of peripheral and central 'self' tolerance (54-56). **Figure 1** A. illustrates a typical T-cell activation response after exposure to a foreign antigen. Peptide antigen is presented by antigen-presenting cells (APCs) to T-cell receptor (TCR) cells through MHC proteins and then co-stimulation occurs as CD80 and CD86 on APCs to CD28 on T cells. This results in T-cell proliferation and enhanced cytotoxicity exerted by T cells. In response to continuous antigen presentation in chronic infection or acute inflammatory responses, PD-1 is upregulated on T-lymphocytes ($CD4^+/CD8^+$). PD-1 on T cells binds to PDL-1 on APCs or tumor cells, thus, blocking the CD28 mediated T-cell activation (**Figure 1 B**.). After the antigen is cleared, PD-1 expression decreases accordingly. Thus, the main function of PD-1 signaling is to protect the host tissue damage by limiting the immune response to pathogens. PD-1 signaling also prohibits the auto-immune responses by promoting tolerance to self-antigens. In cancer, various immunosuppression mechanisms in tumor microenvironment prevent the development of anti-tumor immune responses. Immune evasion may occur due to upregulation of PDL-1 expression on the tumors, due to the release of cytokines such as IFN-γ from T-cells (57). Immunosupressive cytokines such as transforming growth factor-b [TGF-b], interleukin-10 [IL-10]) or immunosuppressive enzymes (indoleamine-2,3-dioxygenase) are produced which prevent T-cell activation. **Figure 1 C.** demonstrates that PD-1 or PDL-1 blocking antibodies can result in uncoupling of binding of PD-1 with PDL-1, thus resulting in activation of T-cell responses against cancer. Studies have shown that PD-1 is expressed on exhausted T-cells and that blocking PD-1-PDL-1 pathway may result in T-cell activation in different cancer types (58-63).

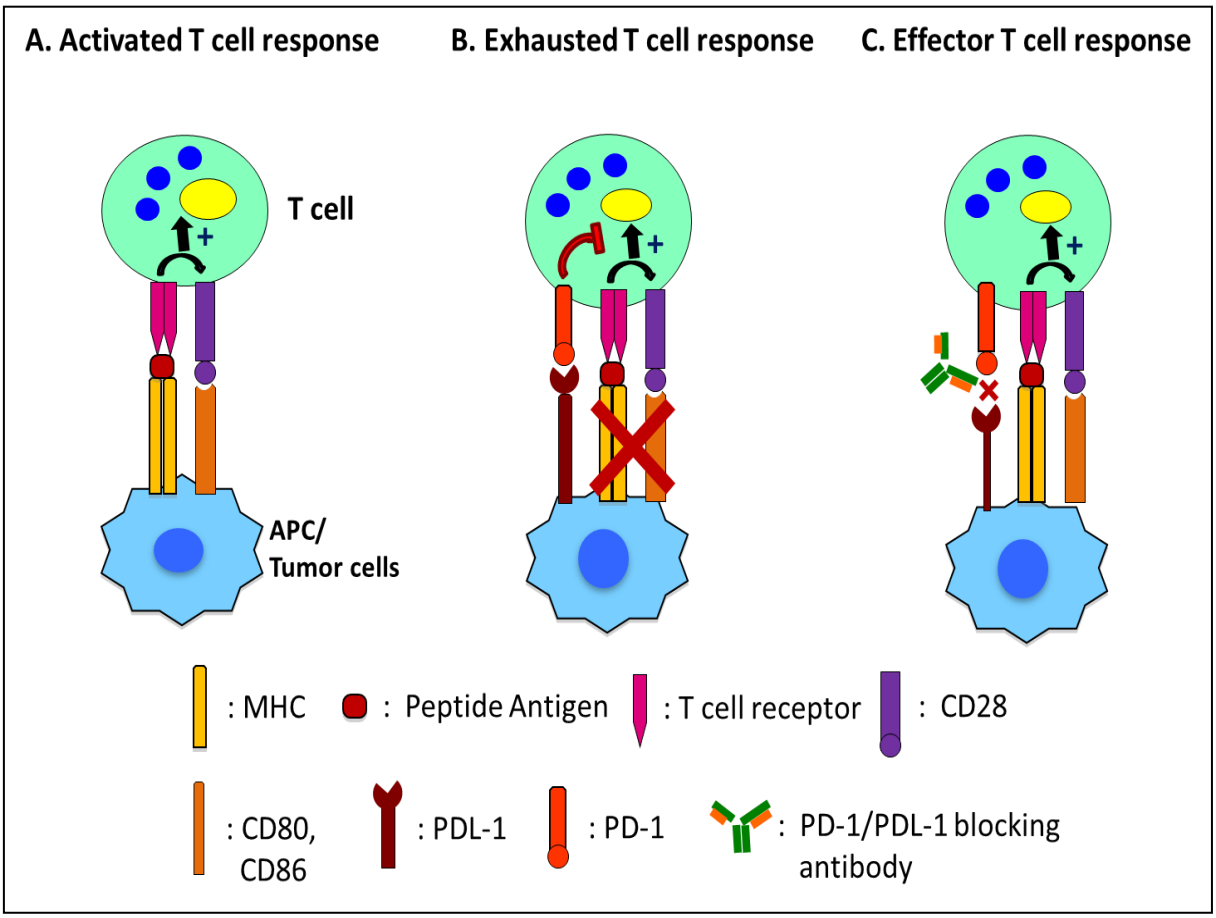

Figure 1. PD-1 in T-cell responses.
A. T-cell activation occurs with the MHC bound-peptide antigen presentation to the T-cell receptor, followed by co-stimulation with the binding of CD80 and CD86 to CD28 on T cells; **B.** PD-1 is induced on T cells in chronic infection and persistent antigen exposure. PDL-1 is upregulated on APCs, which then binds to PD-1 on T cells to inhibit the CD28-mediated T-cell activation. PDL-1 is also upregulated on cancer cells, which binds to PD-1, resulting in T-cell exhaustion and evasion of immune responses; **C.** PD-1 or PDL-1 antibodies inhibit the binding of PDL-1 on tumor cells with PD-1, resulting in activation of tumor-specific T cells, T-cell proliferation and increased cytotoxicity of T cells against cancer cells. *(Adapted from Harvey R. D. et al., Clin Pharmacol Ther, 2014).*

The function of PD-1 has been best characterized in T cells, although its role in other cell types has been studied as well. The ligation of PD-1 with PDL-1 functionally results in decreased immune cell proliferation, cell survival, cytolytic function and cytokine production and promotes apoptosis of antigen-specific T cells (64). The detailed signaling pathway is

illustrated in **Figure 2**. At the molecular level, interaction of PD-1 with PDL-1 results in the recruitment of SHP-1 and SHP-2 phosphatases (Src homology 2-containing protein tyrosine phosphatases 1 and 2). SHP-1 and SHP-2 bind to the ITSM motif and induce de-phosphorylation of downstream molecules as well as augmentation of PTEN expression. Inhibition of PI3-K (Phosphatidylinositol-4,5-bisphosphate 3-kinase) activity causes the blocking of PI3-K/Akt pathways, resulting in decreased T-cell survival, proliferation, protein synthesis, and IL-2 production (65).

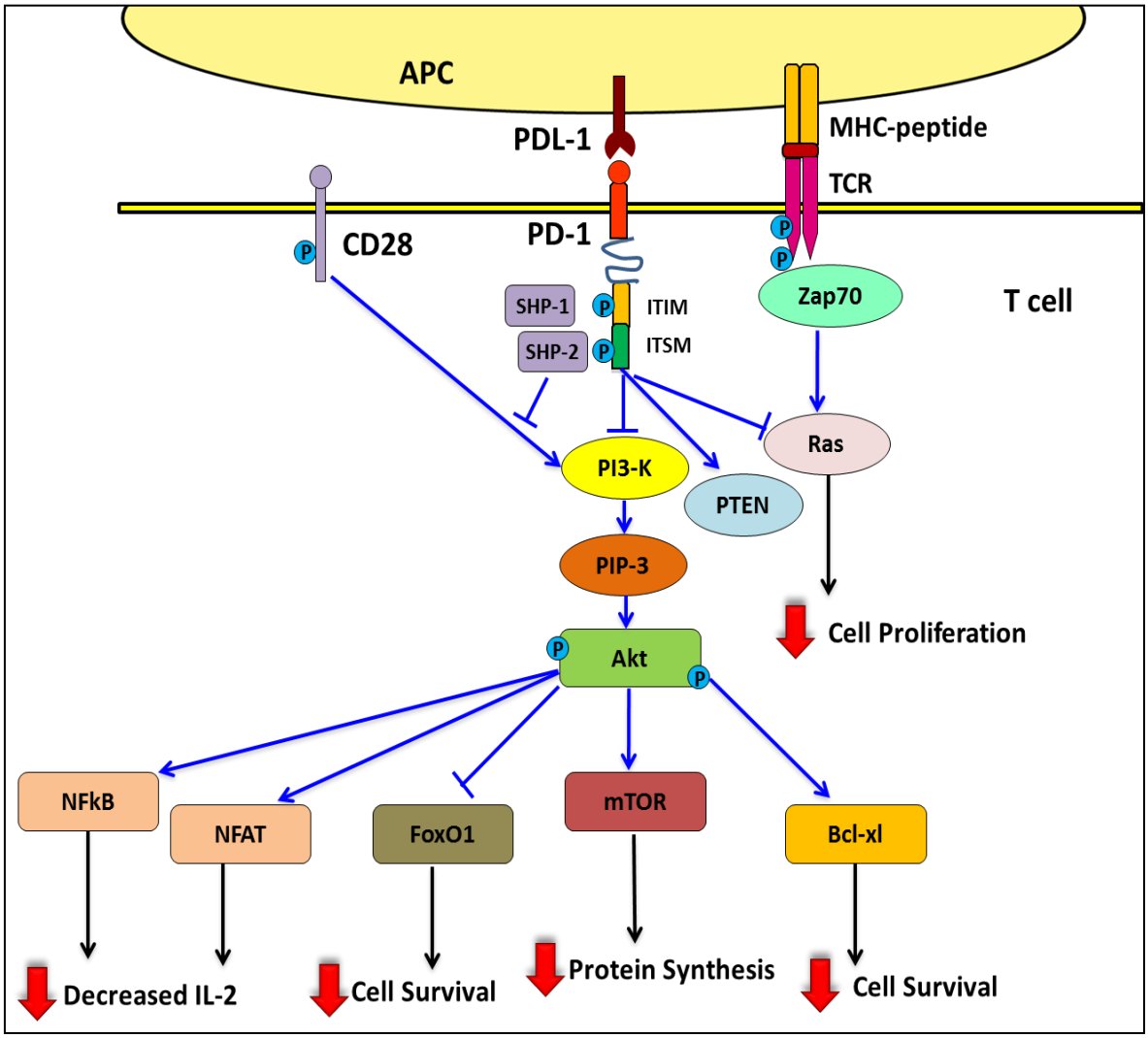

Figure 2. The PD-1 signaling pathway.
Ligand binding to PD-1 results in inhibition of TCR signaling through dephosphorylation of TCR CD3ζ chains and Zap-70, resulting in decreased Ras activation and cell proliferation. PD-1 signaling may also block CD28-mediated Akt activation through PI3-K inhibition. This occurs due to phosphorylation of ITIM and ITSM PD-1 motifs resulting in binding of SHP-1/SHP-2. This causes inactivation of PI3-K and downstream Akt pathways, resulting in decreased mTOR, Bcl-xL NFκB, increased FoxO1 causing decrease in protein synthesis, T-cell survival and cytokine release. PD-1 signaling also results in augmentation of PTEN. *(Adapted from Chinai J. M et al., Trends Pharmacol Sci. 2015; Francisco L. M. et al,. Immunol Rev. 2010).*

PDL-1 expression in cancer types

The major ligand for PD-1, PDL-1 is overexpressed on tumor cells. PDL-1 is upregulated on tumor cells by two mechanisms, innate and adaptive resistance (66). Specific oncogenic mutations drive the PDL-1 expression in certain cancers, which is called as innate resistance. PTEN mutations resulting in PI3-K activation result in elevation of PDL-1 expression in glioblastomas while anaplastic lymphoma kinase (ALK) mutations in lymphomas and lung cancer, have been known to drive PDL-1 expression through signal transducer and activator of transcription 3 (STAT3) signaling (67, 68). BRAFV600 mutations along with STAT3 signaling caused activation of MAPK signaling in melanoma (69). The second mechanism of PDL-1 upregulation, adaptive immune resistance, occurring in the tumor microenvironment, is through physiological stimuli that normally occur to protect tissue from immune-mediated damage. PDL-1 can be induced on tumor cells through induction by IFN's. Gajewski and colleagues showed that certain tumors possess the 'inflammatory gene' signature, which involved the genes of IFN pathway. Recently, it was also demonstrated that a correlation exists between intra-tumoral IFN and PDL-1 expression and lymphocyte infiltration (70, 71). This indicated that a negative feedback loop exists, where IFN-γ induces PDL-1 expression, thereby suppressing the activation of $PD\text{-}1^{+}$ T cells.

PDL-1 is overexpressed on tumor cells in a number of different cancer types such as melanoma, renal, non-small cell lung cancer, head and neck, ovarian, breast, gastric cancer, pancreatic cancer and glioblastomas (72-76). PDL-1 expression has also been associated with worse prognosis and resistance to therapeutic agents in certain cancers such as renal cancer, pancreatic, bladder, liver, breast, stomach, lung, and ovarian cancers (72, 74, 77-79). On the contrary, PDL-1 may also correlate with improved survival and lymphocyte infiltration in

some cancers (71). There has been no association of PDL-1 found with prognosis in certain cancers (80, 81).

Many studies have demonstrated a correlation between PDL-1 tumor expression and the clinical activity of anti-PD-1/anti-PDL-1 antibodies. Topalian *et al*. first showed a positive co-relation of PDL-1 expression with objective response rates of patients as patient popultaion with positive PDL-1 expression (>= 5%) showed a good objective response rate (36%). On the other hand, patients with low PDL-1 expression did not show any objective responses (82). Similarly, in KEYNOTE 001 study, tumor PDL-1 expression was associated with response to pembrolizumab therapy (83). A Phase I trial of anti-PDL-1 antibody (MPDL3280A) in various solid tumors showed that the best clinical responses were observed in patients, when PDL-1 was expressed by tumor-infiltrating immune cells (84). This implies that PDL-1 expression in the tumor microenvironment is also an important factor in determining clinical responses. Another Pembrolizumab study in melanoma showed that immune cells at the invasive front of the tumor expressing PD-1 and PDL-1 correlated with clinical response (85). However, a recent Phase 3 multicentric study and a study by Gettinger S. N. and colleagues showed that PDL-1 was not a prognostic factor and did not determine the therapeutic responses of Nivolumab in patients with NSCLC (non-small cell lung cancer) (86, 87). Thus, PDL-1 analysis may vary according to the staining platform and protocols, antibody clones as well as cut-offs for positivity. Similarly, there is a variability in PDL-1 expression due to the tumor heterogenity and differences in spatial expression (stroma versus tumor). Thus, determining PDL-1 expression is crucial, but it's role as a biomarker needs to be carefully considered.

PD-1/PDL-1 targeting agents and other checkpoint inhibitors

Checkpoint blockade for PD-1/PDL-1 pathway has been employed in two ways. Blockade of PD-1 with antibodies impedes the inhibitory signaling from ligation of both PDL-1 and PDL-2. On the other hand, PDL-1 blockade hinders the negative signaling from the binding of PD-1 and CD80 (B7-1) (88). Based on early clinical studies, it was observed that targeting PDL-1 may exert less toxicity as compared to PD-1 blockade. On the contrary, PD-1 blockade was found to be more effective than PDL-1 by itself, because of the cumulative effect of inhibiting PDL-1 and PDL-2 binding (88).

Nivolumab

Nivolumab (BMS-936558 or MDX1106b) is the most widely studied PD-1 targeted antibody. It is a fully monoclonal human IgG4 antibody that has been shown to lack antibody dependent cellular cytotoxicity. In initial Phase 1 studies, Nivolumab has been shown to demonstrate efficacy in a number of cancers including NSCLC, melanoma, Hodgkin's lymphoma, colorectal, prostate and renal cell carcinomas. Of total 294 patients, 18% objective responses were observed in NSCLC, 28% in melanoma and 27% in renal cell carcinoma. Nivolumab was administered at the doses of 0.1 mg/kg to 10 mg/kg every 2 weeks for 8 weeks. Stable disease (greater than 24 weeks) was observed in some melanoma, non-small cell lung cancer and renal cell carcinoma patients. Owing to the remarkable regression observed, phase 3 trials were conducted and it was observed that overall survival benefit in metastatic melanoma patients was as compared to Ipilimumab and Dacarbazine (89, 90)). Similarly, Phase II studies also showed that there was a significantly improved overall survival and progression-free survival in previously treated metastatic squamous cell-

NSCLC patients as compared to Docetaxel (86). Thus, Nivolumab was approved for the treatment of metastatic squamous NSCLC patients after platinum-chemotherapy as well as for metastatic melanoma by United States Food and Drug Administration (US-FDA) (91, 92).

Pembrolizumab (MK-3475)

Pembrolizumab is also PD-1 blocking, humanized monoclonal IgG4 kappa isotype antibody. It was approved by the FDA in 2014 for unresectable, metastatic melanoma after Ipilimumab. Phase I trial studies have demonstrated its anti-tumor activity in non-small cell lung cancer patients (83). Pembrolizumab has also shown better prolonged progression-free and overall survival and lesser toxicities as compared to Ipilimumab in advanced melanoma patients (89). It has also received an accelerated FDA-approval for patients with metastatic NSCLC, whose tumors express PDL-1 and who have had disease progression after platinum chemotherapy and targeted therapy (93). Other promising PD-1 targeted antibodies which are currently in Phase II trials include Pidilizumab (CT-011) and MEDI0680 **(Table 2).**

Early clinical trial results of the SARC028 study evaluating anti-PD-1 antibody Pembrolizumab in advanced sarcomas revealed partial responses in 1 out of 20 OS patients after 8 weeks as per RECIST criteria (NCT02301039), *Tawbi HA, Burgess MA, Crowley J, et al. Safety and efficacy of PD-1 blockade using pembrolizumab in patients with advanced soft tissue (STS) and bone sarcomas (BS): Results of SARC028—A multicenter phase II study. J Clin Oncol 34, 2016 (suppl; abstr 11006).* Longer follow-up of these patients is currently being pursued as delayed responses may be observed in immunotherapy. The inclusion criteria of patients in SARC028 study involved measurable disease as defined by RECIST

1.1 criteria. Since OS is a fast-growing tumor type, this may not be the most accurate way of pre-selection. Particularly, the size of lesion at the initiation of treatment should be considered in the design of clinical trial as PD-1 targeting agents would work in micrometastatic disease and not in case of bulky tumors.

PDL-1 inhibitors

Durvalumab (MED14736)

It is an IgG_1k monoclonal antibody directed towards PDL-1. Durvalumab has shown promise in patients with non-small cell lung cancer. Currently, phase 3 trials of Durvalumab are ongoing for pretreated patients with advanced NSCLC (94). There are also trials ongoing for urothelial bladder cancer and squamous cell cancer of the head and neck (95).

MPDL3280A

MPDL3280A is an engineered humanized IgG1k monoclonal antibody. Phase I trials have depicted the efficacy of MPDL3280A in different tumor types (84). Further, Phase I trials in NSCLC and renal cell carcinoma have shown objective responses of 23% and 14% respectively. (84, 96). MPDL3280A has also shown activity against patients with advanced bladder cancer with objective response rates of 26% (97). Currently, the drug is in Phase II clinical trials for non-small cell lung cancer.

Other PDL-1 inhibitors in clinical development are BMS-936559 (MDX1105), which is currently under Phase I trials for advanced tumors and MSB0010718C, which is under Phase II trials for various tumors. (96, 98).

Other checkpoint inhibitors

The first checkpoint inhibitor which was successfully developed was Ipilimumab, a fully humanized monoclonal antibody against CTLA-4. CTLA-4 primarily is the checkpoint protein which also plays a crucial role in limiting T-cell responses against tumor cells. Ipilimumab was approved by the FDA for patients with advanced melanoma (99, 100) **(Table 2).**

As illustrated in **Table 2,** modulation of other checkpoints such as TIM3 and lymphocyte activation gene 3 protein (LAG-3), KIR (killer cell immunoglobulin-like receptor), IDO1 (indoleamine 2,3-dioxygenase 1), 4-1BB (tumor necrosis factor receptor superfamily member 9) and OX40 (tumor necrosis factor receptor superfamily member 4) are currently under investigation (101).

Table 2. Current checkpoint inhibitors in development

(101, 102)

Drug	Target	Tumor type	First Indication	Development
Nivolumab (Opdivo)	PD-1	NSCLC, pancreatic cancer, renal cancer, Glioblastoma, lymphomas, SCLC, gastric cancer, melanoma, ovarian, multiple myeloma	Malignant melanoma, Non-small cell lung cancer	Marketed
Pembrolizumab (Keytruda)	PD-1	NSCLC, head and neck squamous cell cancer, renal cell cancer, glioblastoma, lymphoma, pancreatic cancer, other advanced solid tumors.	Malignant melanoma, Non-small cell lung cancer	Marketed

Drug	Target	Tumor type	First Indication	Development
Pidilizumab (CT-011)	PD-1	Multiple myeloma, glioblastoma, lymphoma	Hematological/Solid tumors	Phase II
MEDI14736	PDL-1	NSCLC, glioblastoma, head and neck squamous cell cancer, advanced solid tumors	Non-small cell lung cancer	Phase III
MPDL3280A	PDL-1	Bladder cancer, NSCLC, renal cell carcinoma, advanced solid tumors	Urothelial bladder cancer/NSCLC	Phase III
Ipilimumab	CTLA-4	NSCLC, melanoma, Glioblastoma, renal cancer, SCLC, multiple myeloma, gastric cancer, ovarian, pancreatic cancer, lymphomas	Advanced Melanoma	Marketed
BMS-986016	LAG-3	Chronic lymphocytic leukemia, multiple myeloma, Hodgkin and non-Hodgkin lymphoma, Advanced solid tumors	Hematologic/solid tumors	Phase I
Lirilumab	KIR	Acute myeloid leukemia, multiple myeloma, Hodgkin and non-Hodgkin lymphoma, advanced solid tumors	Acute myeloid leukemia	Phase II
PF-05082566	41BB (CD137)	-	Hematologic/solid tumors	Phase I
MEDI6469	OX40 (CD134)	-	Solid tumors	Phase I
NLG-919	IDO1	-	Solid tumors	Phase I

Aim of the Study

Immunotherapy is an emerging type of treatment approach for cancer. Previously published studies have focused on checkpoint blockade inhibitors targeted towards CTLA-4 or PD-1 in various tumor types. PD-1 blocking antibodies, Nivolumab and Pembrolizumab, have been approved by the FDA for metastatic melanoma and NSCLC. Recently, PDL-1 blockade has shown to enhance the function of tumor infiltrating lymphocytes (TILs) in an osteosarcoma metastatic mouse model (103). However, the implication of PD-1-PDL-1 pathway in the immunotherapeutic efficacy of NK cells and/or macrophages in OS has not been established.

Hence, our central hypothesis is that PD-1 blockade using anti-PD-1 antibody leads to regression of OS lung metastasis through the activation of macrophages and/or NK cells. Thus, to this end, we proposed to investigate PDL-1 expression in OS cells and tissues from patients with OS lung metastasis. After validating PDL-1 as a potential therapeutic target in various OS cell lines, we determined the therapeutic efficacy of anti-PD-1 therapy against OS lung metastases using a human LM7 OS mouse model. We further delineated the novel mechanisms implicated in the effectiveness of anti-PD-1. We assessed PD-1 expression on NK cells and macrophages in OS lung tumors and hypothesized that the activation of NK cells and/or macrophages could be the major contributing factors for regression of OS lung metastasis.

The study of PD-1 blockade in OS lung metastasis preclinical models and the understanding of mechanisms involved can provide a rationale for translating anti-PD-1 antibodies either alone or in combination with other immunotherapies (e.g. macrophage

activating agents or adoptive NK cell therapy) to improve the clinical outcome of metastatic OS patients.

CHAPTER 2

Materials and Methods

Cell lines

Human osteosarcoma cell lines LM7, KRIB, U2OS, 143B, SAOS-2, C-CH-OSD, CCH-OS-O and MG63.2 were cultured in complete Dulbecco's modified Eagle's medium (Whittaker Bioproducts Inc. Walkersville, MD) containing 10% fetal bovine serum (Intergen, Purchase, NJ) and 1X antibiotic-antimycotic (Fisher Scientific, Pittsburg, PA) at 37°C in 5% CO2 (104, 105). SAOS-2, KRIB, U2OS, 143B and MG63.2 cells were obtained from the American Type Culture Collection (ATCC). LM7 cell line is a metastatic cell line, created in our laboratory from SAOS-2 cells by intravenous recovery from lungs of nude mice (106). C-CH-OSD and CCH-OS-O are cell lines obtained from patient samples, derived from pre-treatment biopsies and were obtained from Dennis Hughes laboratory (M.D. Anderson Cancer Center). Cells used were between the 3rd and 10th passages and were verified to be mycoplasma-negative using the MycoAlert™ Mycoplasma Detection Kit (Lonza, Allendale, NJ).

OS patient samples

Paraffin-embedded tissues of lung metastases from 10 OS patients and primary tumors were obtained to determine PDL-1 expression. The patient protocol approval was done by the Institutional Review Board at The University of Texas M. D. Anderson Cancer Center. PDL-1 expression in OS lung metastases and primary tumors was assessed as described in immunohistochemistry section.

Animal Model

Athymic female *nu/nu* mice were purchased from National Cancer Institute (Bethesda, MD) and housed 5 per cage in an animal facility approved by the American Association of Laboratory Animal Care, in accordance with the current regulations and standards of the U.S. Department of Agriculture, Department of Health and Human Services and the NIH. Experiments were conducted in accordance with the protocols and procedures in compliance with the Institutional Animal Care and Use Committee (IACUC) at The University of Texas M. D. Anderson Cancer Center. Mice were held 2 weeks before being used in experiments. LM7 cells ($2x10^6$) were intravenously injected via the tail vein of *nu/nu* mice and the treatment was started 6-7 weeks after intravenous injection, when the formation of micrometastases was confirmed by hematoxylin and eosin (H&E) staining of the lung tissues from sacrificed mice. *In Vivo* MAb anti-mPD-1 (RMPI-14), was purchased from Bio X Cell (West Lebanon, NH). Mice were randomly divided in two groups (5 mice per group) and treated intraperitoneally with either PBS or anti-PD-1 antibody (200 μg/mouse) twice a week, for five weeks. The dose chosen was comparable to the dose used in other animal tumor models (107-109). Mice were sacrificed at the end of the treatment using 5% CO2 and lungs, spleen, liver, heart and kidney were resected. Tissues were either fixed with 10% formalin acetate (Fisher Scientific, Pittsburg, PA) and paraffin-embedded or were snap-frozen in 1:1 Tissue-Tek OCT (VWR, Radnor, PA) and PBS.

Toxicity Studies

Tissues collected from all the animal groups were used to assess toxicity of anti-PD-1 therapy. Analysis was performed by a pathologist blinded to the study. Serum samples from

all the groups were also analyzed for evidence of toxicity. Complete blood count (CBC) and chemistry profile was determined in all serum samples collected and compared.

Immunohistochemistry

Paraffin-embedded lung tissue sections were heated at 55°C for 30 min, deparaffinized using xylene and ethanol solutions and then rehydrated. Antigen retrieval was performed either by using 0.1 M sodium citrate (pH 6.0) buffer or the buffer as per manufacturer's protocol. Slides were heated in pressure-cooker at 100°C for 30 min, allowed to cool, washed with PBS and then incubated with 3% H_2O_2 for 12 minutes to block exogenous peroxidases. For staining frozen sections, tissues were first fixed using cold acetone for 5 min. Blocking was performed by using either 4% fish skin solution (Electron Microscopy Sciences, PA, USA) for 20 min or goat-serum for 1 hour. Primary antibodies against hPDL-1 (1:100) (Cell signaling Technology, Danvers, MA), h-Ki-67 (1:100) (Neomarkers, Fremont, CA), cleaved caspase-3 (1:50) (Biocare Medical, Concord, CA), m-F4/80 (1:200) and CD163 (1:100) (Abcam, Cambridge, MA), m-NKp46 (1:50) (Biolegend, San Diego, CA), or CD68 (1:50) (BD Biosciences, San Jose, CA) were added overnight at 4°C **(Table 3)**. Incubation with anti-rabbit-IgG-HRP (Santacruz Biotechnology, Dallas, TX) or anti-rat-IgG HRP (Jackson Immunoresearch, Westgrove, PA) secondary antibodies (1:1000) was performed for 1 hour at room temperature. Alternatively, amplifier combination of biotinylated anti-rabbit or anti-rat antibody with streptavidin-HRP label (Biocare Medical, Concord, CA) was added for 25 min, followed by PBS washes and streptavidin-HRP solution for 25 min. Lastly, detection was performed using 3,3′-diaminobenzidine (DAB) and counterstaining with hematoxylin. For negative controls, no primary antibody was added. Images were captured using a light microscope (Leica, Wetzlar, Germany) and quantification

for positive staining was performed using Simple PCI software (Hamamatsu) as previously described (110).

TUNEL Staining

TUNEL assay was performed using DeadEnd Flourometric TUNEL System (Promega, Madison, WI). Paraffin-embedded tissues were deparaffanized, treated with Proteinase K for 10 min followed by blocking of endogenous peroxidases with 3% H_2O_2 for 12 minutes. The reaction was then performed using recombinant terminal transferase and biotin-16-dUTP (Roche Applied Sciences) for 1 hour at 37°C. Further, sections were incubated with 2% bovine serum albumin and 5% normal horse serum for 10 min and then Streptavidin-HRP label (Biocare Medical, Concord, CA) for 30 min. Finally, detection was performed using DAB and counterstaining with hematoxylin. Quantification of images was performed using Simple PCI software (Hamamatsu).

Flow cytometry Staining

Single cell suspensions were obtained from lung tumor nodules and spleens isolated from mice from different groups. Tissues were washed with PBS, immediately passed through 100 μm syringe filter (Corning Inc.) and treated with Ammonium-Chloride-Potassium (ACK) lysing buffer (Fisher Scientific, Pittsburg, PA). Cell suspensions were suspended in FACS buffer (PBS, containing 2% FBS) and stained with antibodies or isotype-matched IgG controls for 30 min. The antibodies used included: anti-m-F4/80-APC and CD11b-FITC (E-Bioscience, San Diego, CA), anti-mPD-1-PE and anti-m-NKp46-PerCP (Biolegend, San Diego, CA). Cells were washed in FACS buffer before detection. 10,000

gated-events per sample were acquired using FACS Calibur (Becton Dickinson, Mountain View, CA) and analysis was performed using FlowJo software (Ashland, OR).

In vivo NK and macrophage depletion studies

To deplete endogenous NK cells, 50µl of anti-asialo-GM1 (Wako, Richmond, VA), was injected i.p. into mice, twice a week for a total of 5 weeks. Treatment with anti-PD-1 was given 24 hours after injecting anti-asialo-GM1. Combination treatment of anti-asialo-GM1 and anti-PD-1 was performed for 5 weeks. Similar treatment scheme was used for macrophage depletion studies. Liposomal Clodronate (Encapsula NanoSciences, Brentwood, TN) was injected (200 µl, i.p., twice a week) followed by treatment with anti-PD-1 24 hours later. After treatment was completed, mice were sacrificed; organs were resected and analyzed as described above.

Western blotting

Tumor lysates were obtained from lung nodules excised from mice, snap-frozen in liquid nitrogen and stored at -80°C. Tissues were homogenized and lysed using RIPA lysis buffer (Santa Cruz Biotechnology, Dallas, TX). Protein concentration in lysates was determined using a Bio-Rad protein assay (Hercules, California). Protein lysate (40 µg) was boiled for 5 min and resolved using 10% SDS-/PAGE followed by nitrocellulose membrane transfer. Membranes were blocked using 5% milk in TBST followed by overnight incubation with either of primary antibodies (1:1000 in 5% milk in TBST): PDL-1, p-Stat3-705, total Stat3, phospho-p44/42 MAPK (Thr202/Tyr204), p44/42 MAPK, cleaved caspase-3 (Asp175) and total caspase-3 (Cell Signaling, Danvers, MA) **(Table 3)**. Membranes were washed and

incubated with the respective secondary antibody for 1 hour. Detection was performed using autoradiography and quantified using Image J software.

Table 3. List of Primary Antibodies

Antibody	Application	Dilution	Company
PDL-1 (Rabbit monoclonal)	IHC	1:100 (mouse OS lung metastases) 1:50 (OS patient samples)	Cell Signaling
	Western Blotting	1:500	
Ki-67 (Rabbit monoclonal)	IHC	1:100	Neomarkers
Cleaved caspase-3 (Rabbit Polyclonal)	IHC	1:100	Biocare Medical
Anti-mF4/80 (Rat monoclonal)	IHC	1:200	Abcam
Anti-mNKp46 (Rat)	IHC	1:50	Biolegend
CD86 (Rat)	IHC	1:50	BD Pharmingen
CD163 (Rabbit polyclonal)	IHC	1:200	Abcam
Anti-mF4/80-APC	Flow Cytometry		E-Biosciences
Anti-mCD11b-FITC	Flow Cytometry		E-Biosciences
Anti-mNKp46-PerCP	Flow Cytometry		Biolegend
Anti-mPD-1-PE	Flow Cytometry		Biolegend
Phospho-Stat3 (Tyr 705) (Rabbit monoclonal)	Western Blotting	1:1000	Cell Signaling
Stat3 (Rabbit monoclonal)	Western Blotting	1:1000	Cell Signaling
Phospho-Stat1-701 (Rabbit monoclonal)	Western Blotting	1:1000	Cell Signaling
Stat-1 (Rabbit monoclonal)	Western Blotting	1:1000	Cell Signaling
Phospho-p44/42 MAPK (Rabbit monoclonal)	Western Blotting	1:1000	Cell Signaling

Antibody	Application	Dilution	Company
p44/42 MAPK (Rabbit polyclonal)	Western Blotting	1:1000	Cell Signaling
Cleaved caspase-3 (Asp175) (Rabbit monoclonal)	Western Blotting	1:1000	Cell Signaling
Caspase-3 (Rabbit monoclonal)	Western Blotting	1:1000	Cell Signaling

CHAPTER 3

PDL-1 and PDL-2 expression in human OS cell lines

Rationale

Previously published studies have demonstrated upregulation of PDL-1 expression on cancer cells in certain cancers such as melanomas, renal, pancreatic and non-small cell lung cancer (72-76). *Shen J. K. et al.* recently showed that PDL-1 transcript levels were upregulated in human OS tumor samples as well as patient cell lines (111, 112). As PDL-1 expression has been studied as an immune escape mechanism utilized by cancer cells, we sought to determine if this may be a potential therapeutic target in OS. In addition, as PD-1 is known to bind to two ligands PDL-1 and PDL-2, we also tested PDL-2 expression in OS cell lines.

Hence, in Chapter 3, the major objective was to determine the basal PDL-1 and PDL-2 expression in human OS cell lines *in vitro*. For this purpose, we used a panel of OS cell lines including LM7, KRIB, U2OS, 143B, SAOS-2, C-CH-OSD, CCH-OS-O and MG63.2 with varying metastatic potential. Initially, Flow cytometry assays were performed to determine and compare the surface levels of PDL-1and PDL-2 in OS cells. Since PDL-1 is a transmembrane receptor, we also assessed if there are any differences between surface localization and total protein expression of PDL-1. We determined the total PDL-1 levels by western blotting.

As PDL-1 is an inducible receptor, and its expression can be modulated by the cytokines such as IFN-γ *in vitro*, we determined if PDL-1 expression on OS cell lines can be induced by IFN-γ by performing Flow cytometry assays (113, 114)

Results

PDL-1 is expressed in OS cell lines and total PDL-1 expression levels co-relate with surface expression levels

PDL-1 expression was determined in human OS cell lines KRIB, LM7, SAOS-2, C-CH-OSD, C-CH-OSO and MG63.2. MDA-MB-231, a triple-negative breast cancer cell line, known to express high levels of PDL-1 was used as a positive control. **Figure 3 A.** represents the PDL-1% positivity as compared to IgG controls and **Figure 3 B.** depicts the MFI normalized to isotype IgG. We found constitutive PDL-1 expression in 5 out of 8 OS cell lines, with the highest constitutive expression seen in KRIB, U2OS and 143 B cell lines (MFI of 29.2, 25.2, 16.8) **(Figure 3 A and B).** C-CH-OSD, C-CH-OSO and MG63.2 had very low levels of baseline PDL-1 expression (MFI of 2.1, 1.1 and 1.9). LM7 and SAOS-2 cell lines had intermediate-high PDL-1 expression levels (MFI of 5.9 and 5.0). Total PDL-1 levels in OS cell lines were also examined by western blotting. It was observed that PDL-1 is expressed in KRIB, U2OS, 143 B, LM7 and SAOS-2 cells **(Figure 3 C and D).** Further, the total PDL-1 expression pattern was similar to that of surface levels of PDL-1, which indicated that PDL-1 at the surface reflected the total PDL-1 protein. Variable PDL-1 expression levels were observed in OS cell lines, possibly due to the intrinsic differences between the OS cells.

A.

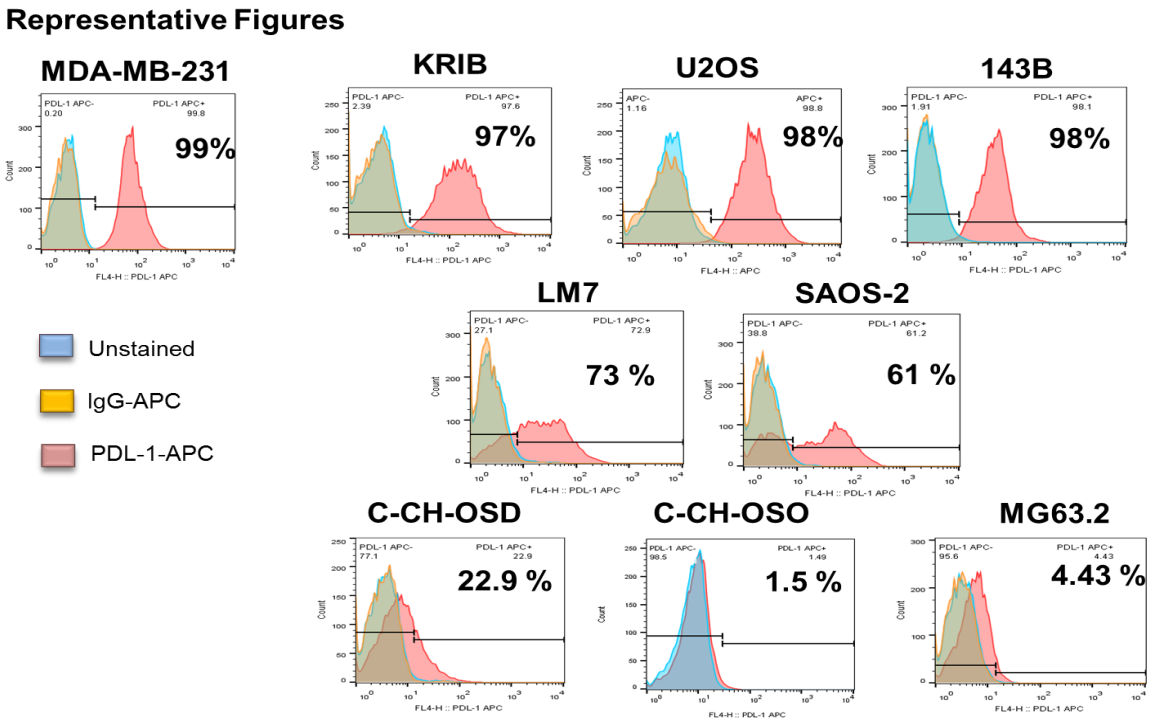

B.

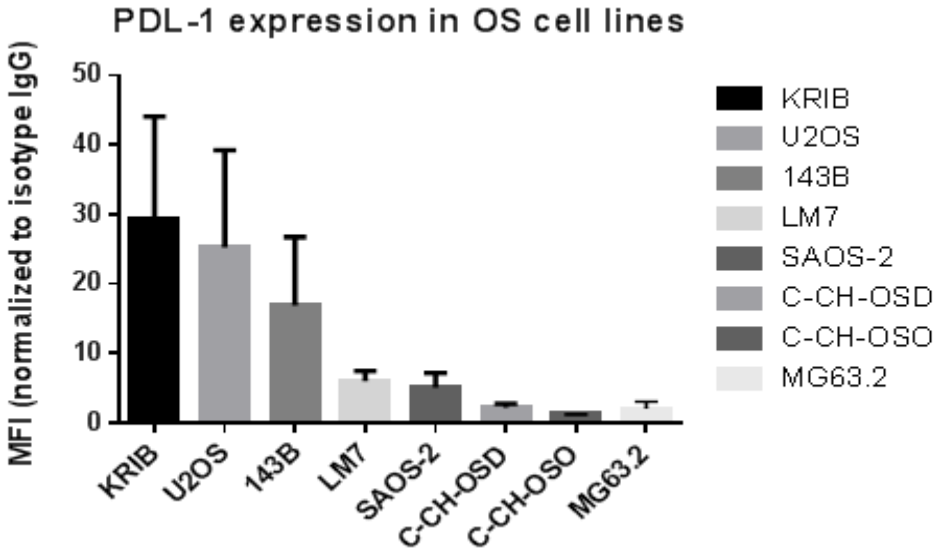

C.

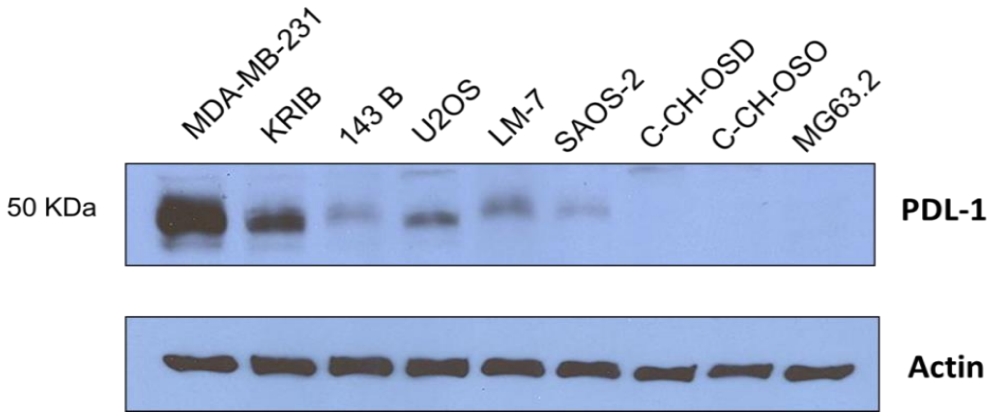

D.

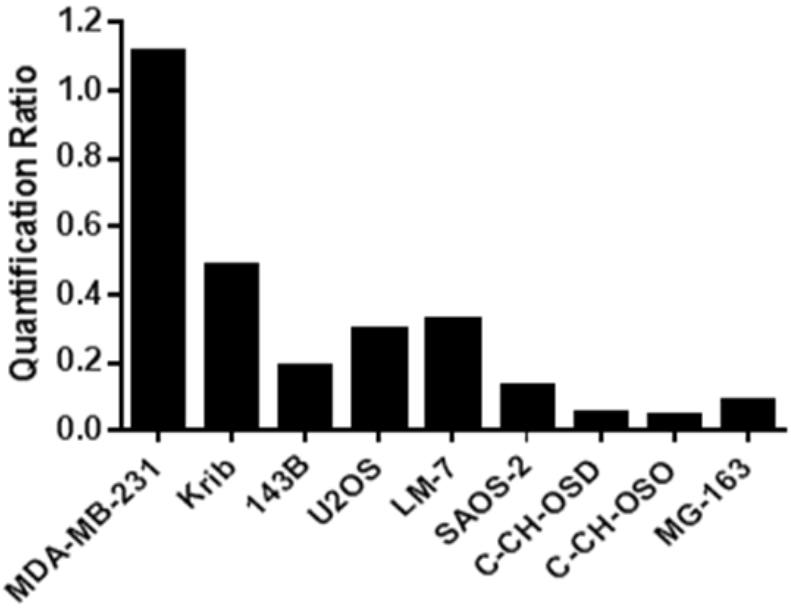

Figure 3. PDL-1 is expressed in OS cell lines.
A. Flow cytometry analysis was performed to assess surface PDL-1 expression in a panel of OS cell lines and MDA-MB-231 cells as a positive control. Staining was performed using either IgG-APC or PDL-1-APC antibody for 30 min. Representative flow charts are shown; B. Mean and standard deviation of PDL-1 positivity compared to IgG controls as determined by flow cytometry from three independent experiments; C. OS cell lines were cultured, lysates were collected using RIPA buffer and proteins were resolved using 10% SDS-PAGE followed by probing with anti-hPDL-1 antibody. MDA-MB-231 cells were used as a positive control and Actin served as a loading control; D. Quantification of PDL-1 levels in OS cell lines was done relative to actin levels using Image J analysis

IFN-γ causes an upregulation of PDL-1 expression in OS cells in vitro

We further investigated if PDL-1 expression on OS cells with intermediate and low baseline expression was inducible. There was a significant increase in PDL-1 expression after IFN-γ addition in SAOS-2 (11 to 118), LM7 (4.3 to 46) and C-CH-OSD (4.4 to 68.9). **(Figure 4 A and B)**. There was also an increase in PDL-1 after IFN-γ induction in C-CH-OSO (1.0 to 11.9), although not significant. The significant increase in PDL-1 expression after IFN-γ indicates that PDL-1 expression could be further modulated by the cytokine microenvironment *in vivo*. Thus, cells with lower baseline PDL-1 expression *in vitro* could potentially show a significant response towards PD-1 blockade *in vivo*.

A.

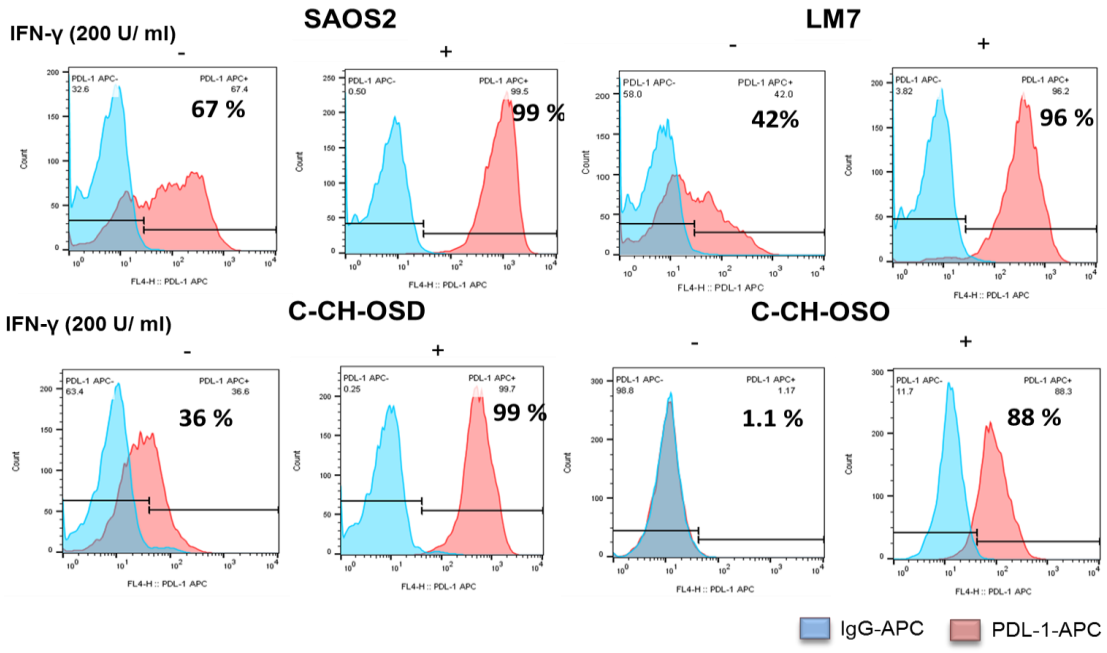

B.

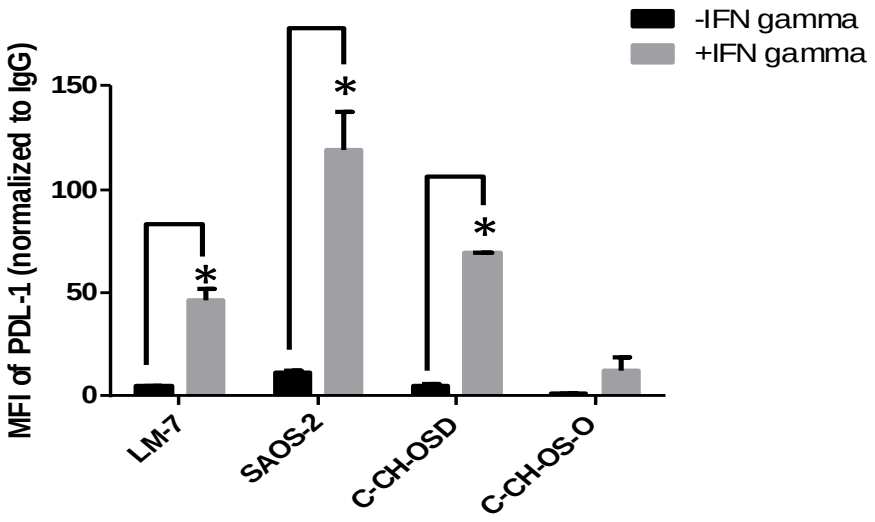

Figure 4. IFN-γ induces PDL-1 expression in OS cells.
A. LM7, SAOS-2, C-CH-OSD, C-CH-OSO cells were treated with IFN-γ (200U/ml) for 24 hours. Flow cytometry analysis was performed using anti-PDL-1-APC antibody or IgG-APC isotype control. Representative flow charts are shown; B. Summary from two independent experiments showing mean and standard deviations for PDL-1 positivity (*: $p<0.05$).

Very low levels of PDL-2 are expressed in OS cell lines

PDL-2 expression on OS cell lines was determined using flow cytometry analysis with custom-made anti-human PDL-2-APC antibody using B-16 cells overexpressing PDL-2 (B16-PDL-2) as a positive control. **Figure 5** depicts that very low levels of PDL-2 were expressed in all OS cell lines (LM7: 1.3, KRIB: 1.07, SAOS-2: 1.21, U2OS: 1.14, C-CH-OSD: 1.1, C-CH-OSO: 0.98, MG63.2: 1.08), as compared to the positive control cells (MFI=11.3). LM7 had relatively the highest PDL-2 (MFI=1.31) expression amongst all OS cell lines. This corroborates the published data that PDL-1 is the major dominant PD-1 ligand that is expressed on a variety of hematopoietic and non- hematopoietic cells and that PDL-2 expression is expressed in very few cells and tissues (115, 116).

A.

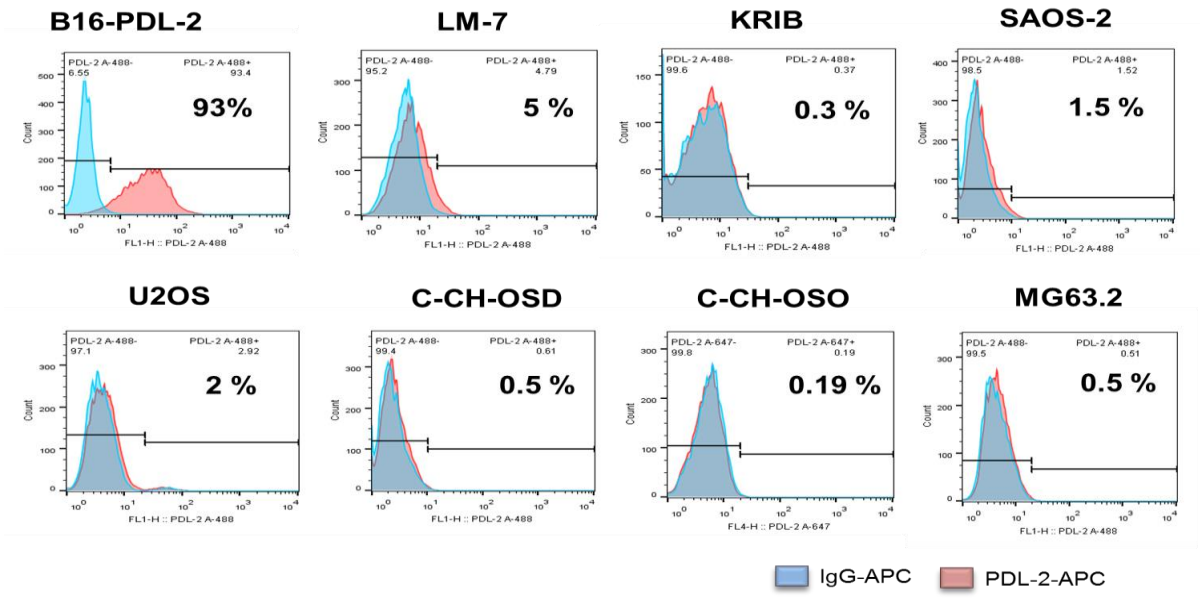

B.

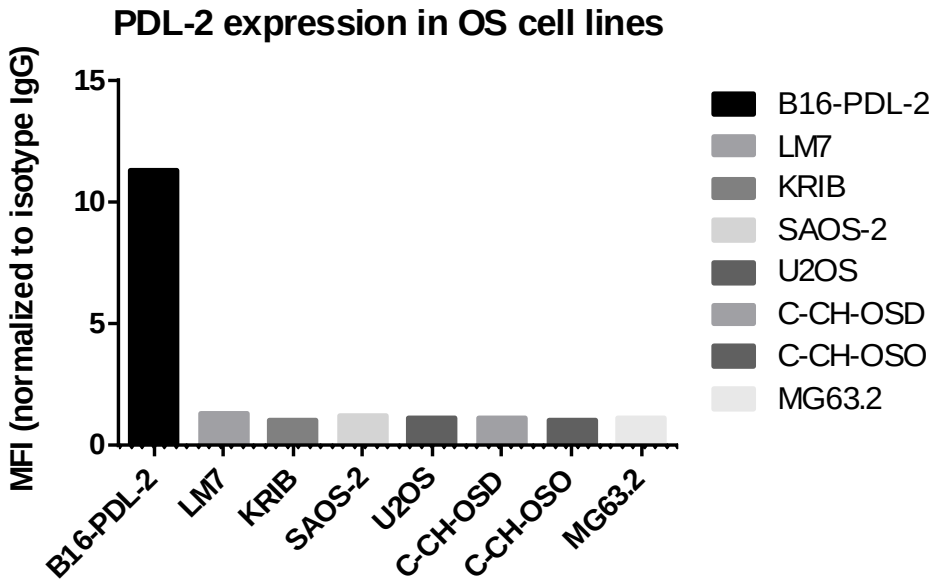

Figure 5. PDL-2 expression was low in OS cells.
Flow cytometry analysis was performed in OS cells with anti-hPDL-2-APC antibody using B-16 overexpressing PDL-2 cells as a positive control. Representative flow charts are shown above.

Summary

These data support our hypothesis that PDL-1 is a key potential therapeutic target is OS. We showed that PDL-1 is expressed in a majority of the OS cell lines *in vitro* at the surface as well as at the total protein level as demonstrated by flow cytometry and western blotting analysis. PDL-1 is variably expressed in OS cells, possibly due to the genomic differences in between the cell lines. Atefi M. *et al.* demonstrated similar findings of variable PDL-1 expression in a panel of 51 melanoma cancer cell lines. They further showed that PDL-1 expression did not co-relate with the oncogene-driver mutations (PTEN, MAPK or PI3-K-Akt activation mutations) in these cell lines (117).

We also demonstrate that the OS cell lines with lower PDL-1 levels (C-CH-OSO, C-CH-OSD LM7 and SAOS-2) express higher PDL-1 levels when exposed to the cytokine IFN-γ, thus proving that PDL-1 is inducible in OS cells. Other studies such as those in breast cancer and multiple myeloma have also revealed an induction of PDL-1 with IFN-γ (118, 119). This is particularly crucial as it shows that the expression of PDL-1 may be upregulated in the *in vivo* microenvironment, even if it is not present at higher levels *in vitro.* IFN-γ from immune cells (e.g. T cells and macrophages) has been shown to increase PDL-1 expression on tumor cells *in vivo* (57, 120). This data further provided a stimulus for our study to target PDL-1 using *in vivo* OS models. We used the LM7 (with intermediate, but inducible PDL-1 expression) human OS mouse model for our studies. Finally, we confirmed that the expression of the second ligand for PD-1, i.e., PDL-2 is minimal in OS cells, suggesting that it is not the crucial regulator for immune escape mechanisms in OS.

CHAPTER 4

PDL-1 expression in human OS patients

Rationale

Our data from Chapter 3 indicate that PDL-1 is highly expressed in human OS cell lines *in vitro*. Numerous studies have reported PDL-1 upregulation in numerous cancer types such as melanoma, renal, non-small cell lung cancer, head and neck, ovarian, breast, gastric cancer, pancreatic cancer and glioblastomas (72-76). PDL-1 expression has also been associated with poor clinical outcomes such as worse prognosis, poor survival or metastasis (72, 74, 121). For example, Thompson *et al*. and Krambeck *et al*. showed PDL-1 expression in 24% paraffin-embedded renal carcinoma tumor tissues, primarily at the cell surface. It was also demonstrated in these studies that PDL-1 was associated with clinicopathological characteristics such as higher grade, advanced tumor-nodal-metastatic (TNM) stage, metastatic progression and increased risk of death (73, 122). Similarly, in breast cancer, intra-tumoral PDL-1 expression on the surface and cytoplasm was seen in 50% of patients and was associated with poor prognostic factors (123, 124). PDL-1 was also discovered to be an independent prognostic factor for pancreatic cancer patients, overall survival and progression-free survival in patients with ovarian cancer, and disease-free survival in patients with hepatocellular carcinoma (76, 79, 125). Thus, a plethora of recent studies reflect the importance of PDL-1 in cancer and it's co-relation to the patient clinical outcomes.

PDL-1 expression in primary and metastatic lung OS has not been addressed till date. Hence, the aim of this chapter was to determine the role of PDL-1 as a potential target in the translational setting by evaluating the PDL-1 expression in patients with OS lung metastasis. PDL-1 expression and it's localization pattern was determined by IHC staining using paraffin-embedded tissues of lung metastases and primary tumors from OS patients.

Results

PDL-1 is expressed in lung metastases and primary tumors from OS patients

In order to determine PDL-1 expression in OS patients, we obtained paraffin-embedded tissues of lung metastases and primary tumors from OS patients. IHC analysis was performed using rabbit monoclonal anti-human PDL-1 antibody using appropriate negative and positive control (lung adenocarcinoma) tissue slides. The staining was examined and confirmed by a pathologist. Our results showed that PDL-1^{+} tumor cells were observed in 8 out of 10 patients (~80%) in comparison with the negative controls **(Figure 6 A)**. Further, PDL-1 expression was present in the membrane and cytoplasm of the OS lung metastases. There were variable patterns of expression (focal or scattered) seen within different OS patients. The quantification data revealed that an average of ~30% PDL-1 positivity was observed in the lung metastases from the patient group **(Figure 6 B)**. Also, 6 out of 10 patients (60%) showed PDL-1 expression below 30% whereas 4 out of 10 patients (40%) showed PDL-1 expression above the median 30%. Our data demonstrated that PDL-1 is expressed in lung metastases from OS patients and the expression pattern is variable.

Similarly, we found that PDL-1 was also expressed in the bone tumors of OS patients. We used three representative OS primary bone tumor paraffin-embedded samples for PDL-1 staining. We found variable levels and pattern of PDL-1 expression in primary samples as well **(Figure 6 C)**.

C.

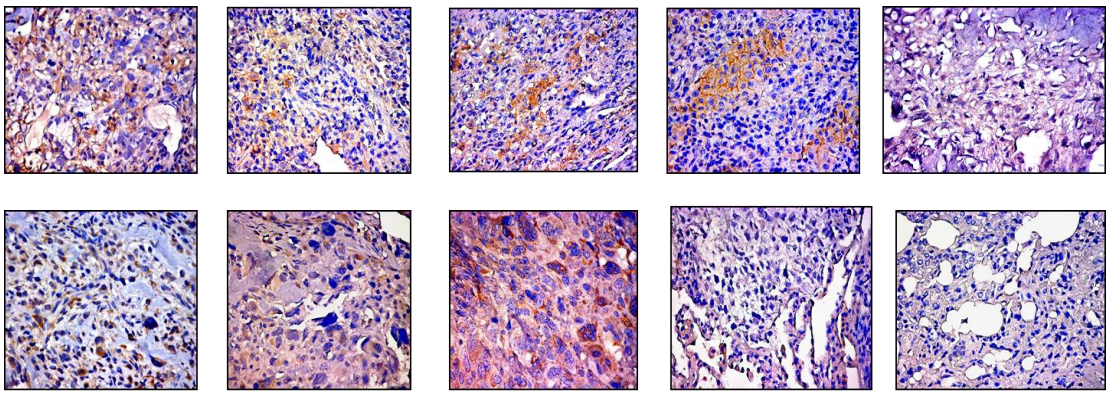

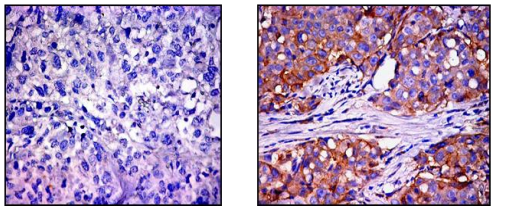

D.

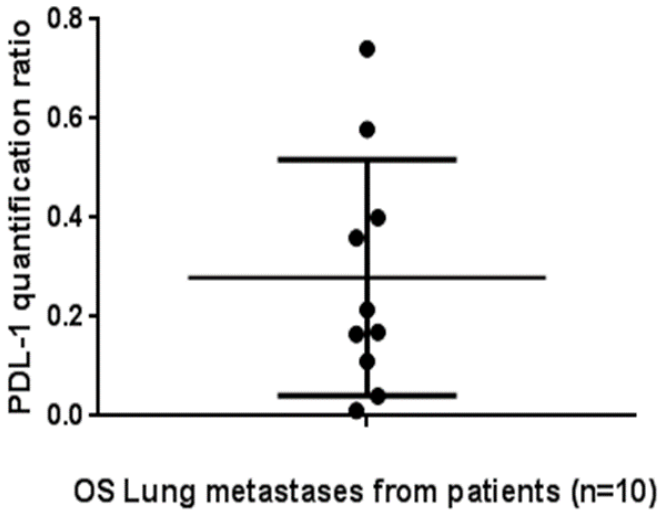

E.

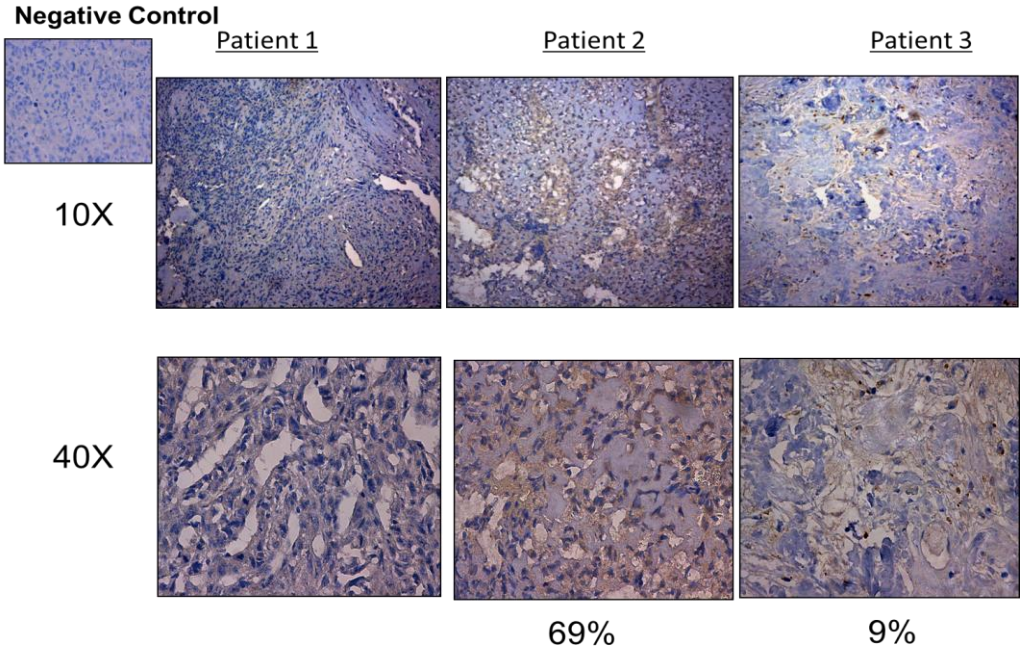

Figure 6. PDL-1 is expressed in OS patient lung metastases and primary bone tumors. A. IHC staining was performed on paraffin-embedded tisssues for lung metastases from 10 OS patients, using anti-hPDL-1 antibody and lung adenocarcinoma tissue as a positive control; B. Quantification of PDL-1 positivity as analyzed by Cell Quest software. Mean PDL-1 expression is ~30%; C. IHC staining for primary bone tumor slides from OS patients was also performed using anti-hPDL-1 antibody.

Summary

Our *in vitro* data demonstrated PDL-1 expression in the various human OS cell lines. Further, we also noted that PDL-1 expression was variable within the panel of cell lines. Here, we wanted to evaluate whether PDL-1 is expressed in the actual tumor microenvironment of OS patients and if it contributes to lung metastatic disease. Hence, we examined PDL-1 expression in OS patients in the primary tumors and lung metastases.

Our results demonstrate that PDL-1 is expressed in OS patients, indicating that it may play a role in immunosuppression of OS lung metastatic disease. We found PDL-1

expression in both primary tumors and lung metastases from OS patients, implying that PDL-1 may play a role in both the growth of primary tumors as well as metastatic spread to the lungs. PDL-1 expression has been previously shown in other cancers in other studies; however, our group has been the first to demonstrate PDL-1 expression in paraffin-embedded tissues in OS patients in both primary and metastatic state. Another study has shown PDL-1 expression in 75% of OS metastatic patients using immunofluorescence assays, but could not detect PDL-1 in primary OS patients (103).

In our studies, we have not only shown PDL-1 expression but have also uncovered the finding that there is a variable expression of PDL-1 within OS patient samples and that the pattern of membrane/cytoplasmic expression may differ within various OS patients. This may be due to the fact that OS entails a very complex group of cancer sub-types with variable genomic characteristics. These findings are particularly important as PDL-1 is being used as a biomarker for clinical studies using PD-1 targeting therapies. Various cut-offs have been used to define PDL-1 positivity for IHC staining method. Recently, Checkmate-057 phase III study demonstrated that patients with >1% PDL-1 positivity showed better clinical responses such as objective response rate (ORR), overall survival and progression-free survival in pre-treated NSCLC patients (126).

Thus, it is crucial to evaluate PDL-1 expression in OS patients to enable even patients with as low as 1% PDL-1 expression to have access to PD-1 targeted therapies. Hence, evaluation of PDL-1 in different OS patient sub-types is of translational significance as it will help in pre-selection of patients with PDL-1 expression for the treatment with anti-PD-1 or anti-PDL-1 antibodies.

CHAPTER 5

Therapeutic efficacy against OS lung metastases *in vivo* through inhibition of tumor cell proliferation and increased tumor cell apoptosis

Rationale

Our data obtained using OS cell lines and OS patients, as demonstrated in Chapters 3 and 4, led us to the discovery that PDL-1 is a novel therapeutic target in OS. The efficacy of anti-PD-1 or anti-PDL-1 antibodies either alone or in combination with other checkpoint inhibitors *in vivo* has been shown in several cancers such as melanoma, colon cancer and pancreatic cancer (60, 76, 127-130). Recently, the effect of blocking PDL-1 was demonstrated against OS lung metastasis in K7-M2 mouse model (103). Most of the studies have focused on T cells as a mechanism of immune-suppression in the tumors. Here, we investigate the effect of blocking the interaction of PD-1 receptor on macrophages and NK cells with PDL-1 on OS cells *in vivo* in a human xenograft model using an anti-murine-PD-1 (anti-mPD-1) antibody.

Our data reveals that PDL-1 is expressed in LM7 cells and earlier findings from our lab have demonstrated that LM7 cells are susceptible to NK cell cytotoxicity (34). In addition, our lab has previously established the nude mouse metastatic model showing that spontaneous metastasis of LM7 cells to the lungs (106). Since this model can be utilized to form pulmonary micro-metastatic disease, it is an ideal model for assessing the efficacy of immune-modulating agents. Most of the earlier studies have focused on the significance of T-cell activation in the therapeutic responses of anti-PD-1. However, the effect of blockade of PD-1 on NK cells and macrophages has not been investigated till date. Hence, we were interested in studying the role of NK cells and macrophages in the immunosuppressive OS lung microenvironment. With this aim, we used LM7 human xenograft nude mouse model for the purpose of studying the therapeutic responses of anti-PD-1 against OS lung metastasis.

Anti-mPD-1 was used with the intent of blocking the endogenous PD-1 receptor on murine NK cells and macrophages. It has been shown that the binding affinities of mPD-1 to mPDL-1 and mPD-1 to hPDL-1 are equivalent, due to the 77% homology between murine and human PDL-1. Also, there is a significant homology between mPD-1 and hPD-1 receptor (52, 131, 132). Hence, we hypothesized that mPD-1 on immune cells can bind to hPDL-1 on tumor cells (LM7) and this interaction can be blocked using anti-mPD-1 antibody.

LM7 cells were intravenously injected in *nu/nu* mice to establish micro-metastatic disease. After 7 weeks, lungs were excised to confirm micro-metastases by H and E staining. Mice were randomly divided in two groups of n=5 before starting treatment. Anti-mPD-1 (RMPI-14) antibody, with the previously published dose of 200 μg/mouse, twice weekly regimen, intraperitoneally (i.p.), was used for treatment for 5 weeks (60, 108). Following the treatment, the animals were sacrificed and the lungs and other organs were obtained for further analysis.

Results

Anti-PD-1 decreases the number of OS pulmonary macro-metastases and micro-metastases

Anti-PD-1 treatment was used to target OS micro-metastatic disease. As shown in **Figure. 7**, treatment of mice with anti-PD-1 (RMPI-14) for 5 weeks (n=5) resulted in significant decrease in the mean number of LM7 macro-metastases (visual) and micro-metastases (microscopic) ($p < 0.05$). This showed that PD-1 blockade significantly reduced the prevalence of lung metastases in LM7 mouse model.

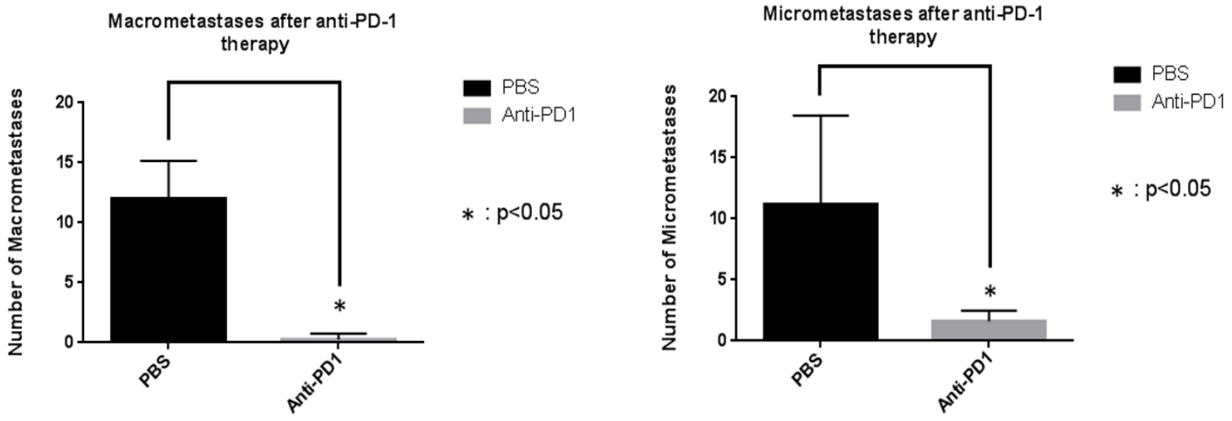

Figure 7. *In vivo* anti-PD-1 administration led to a decrease in the number of OS lung metastases.
Mice with established micrometastases were administered either PBS or anti-PD-1 (i.p., 200 μg/mouse), twice weekly for 5 weeks. Lungs were excised and the number of OS lung macrometastases and micrometastases were counted. Statistical analysis was performed using student's t-test (*: $p < 0.05$).

Anti-PD-1 decreases OS tumor cell proliferation

To determine the mechanisms involved in the therapeutic efficacy of anti-PD-1, we determined the effect on tumor cell proliferation by performing IHC staining of Ki-67 for paraffin-embedded tissues of LM7 lung metastases. Ki-67 is a used as a marker for cell proliferation *in vivo* (133). Ki-67 is strictly associated with cell proliferation and is present in all phases of the cell cycle, but absent in the resting phase (134). **Figures 8 A and B.** depict that the number of Ki-67^{+} proliferating tumor cells were significantly decreased in anti-PD-1 treatment mice group as compared to the PBS controls ($p<0.05$). The quantification of Ki-67 positivity was calculated from three random fields in slide sections from mice in PBS and anti-PD-1 treated groups by Cell Quest Software.

A.

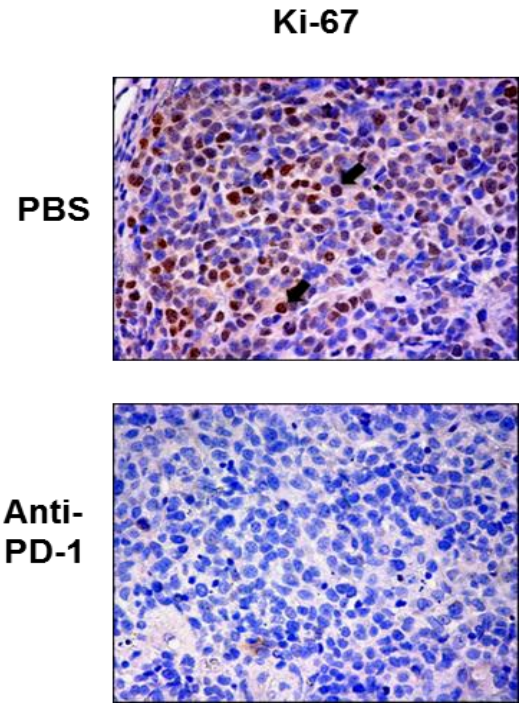

B.

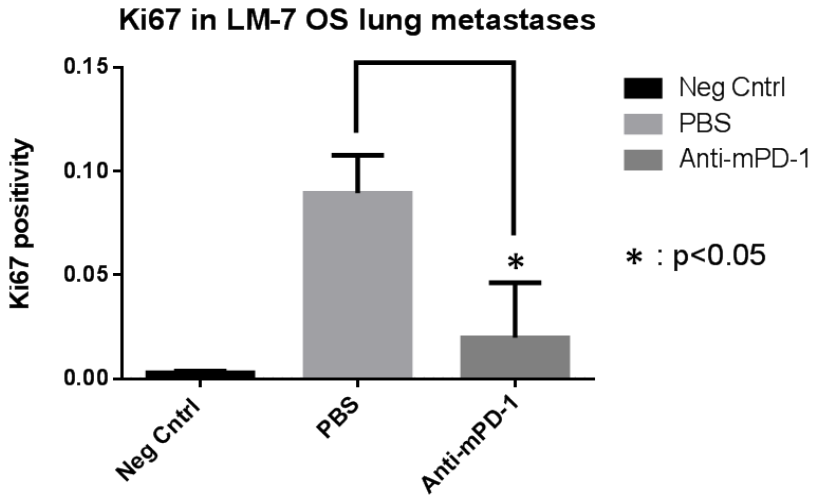

Figure 8. *In vivo* anti-PD-1 administration led to a decrease in LM7 tumor cell proliferation.

A. IHC staining was performed for lung metastasis sections from mice using anti-human-Ki-67 antibody. Representative sections are shown. (Magnification: 40X). B. Quantification for Ki-67 positivity was done in 3 random microscopic fields using Cell Quest Software and student's t-test was performed. ($p<0.05$)

Anti-PD-1 treatment leads to enhanced OS tumor cell apoptosis in vivo

In order to assess if anti-PD-1 antibody led to increased tumor cell death, we quantified apoptosis by IHC staining of cleaved caspase-3 and TUNEL. Caspase-3 is the central 'effector' activated death protease that activates the cleavage of other proteins in the programmed death pathway. As it is a crucial mediator in the apoptosis signaling pathway, the active or cleaved form of caspase-3 acts as an important readout in apoptosis assays including IHC staining of paraffin tissues (135, 136). Similarly, TUNEL (terminal deoxynucleotidyl transferase [TdT]-mediated deoxyuridinetriphosphate [dUTP] nick end labeling) assay detects double-strand DNA fragmentation in samples (137, 138)). Apoptotic nuclei can be easily identified in fixed paraffin tissue sections by TUNEL, thus providing a measure of cell death (139, 140). Here, we show that tumor sections from anti-PD-1 treated mice displayed significantly higher levels of cleaved caspase-3 **(Figure 9 A and B)** and TUNEL **(Figure 9 C and D)** positivity as compared to respective PBS treated control sections. Positive staining is seen as brown nuclear dots. The quantification results of staining obtained from three random fields from mice in both groups show that these results are statistically significant ($p<0.05$)**.**

A.

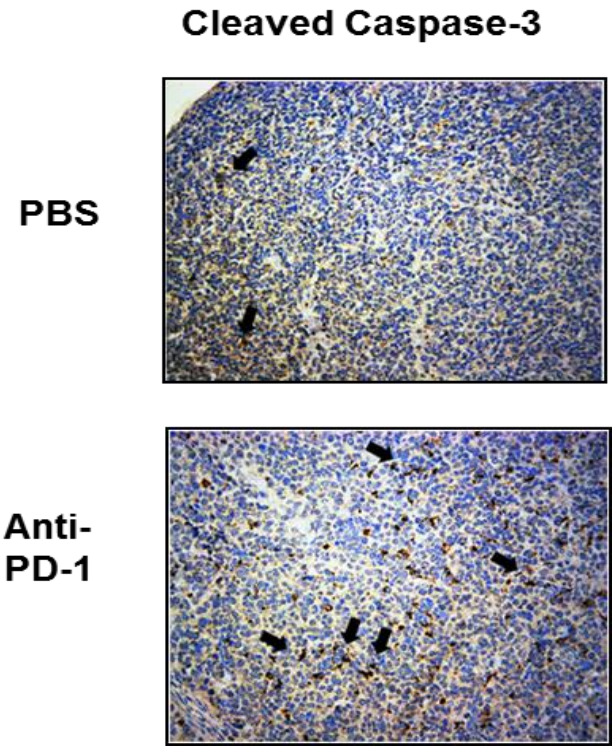

B.

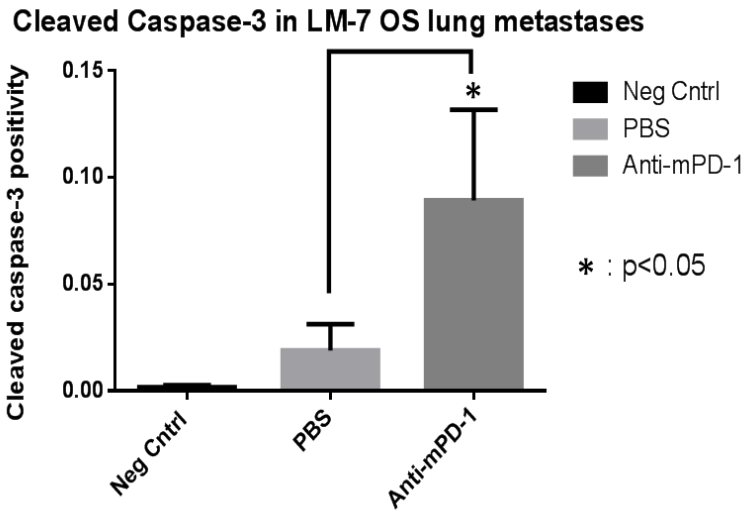

C.

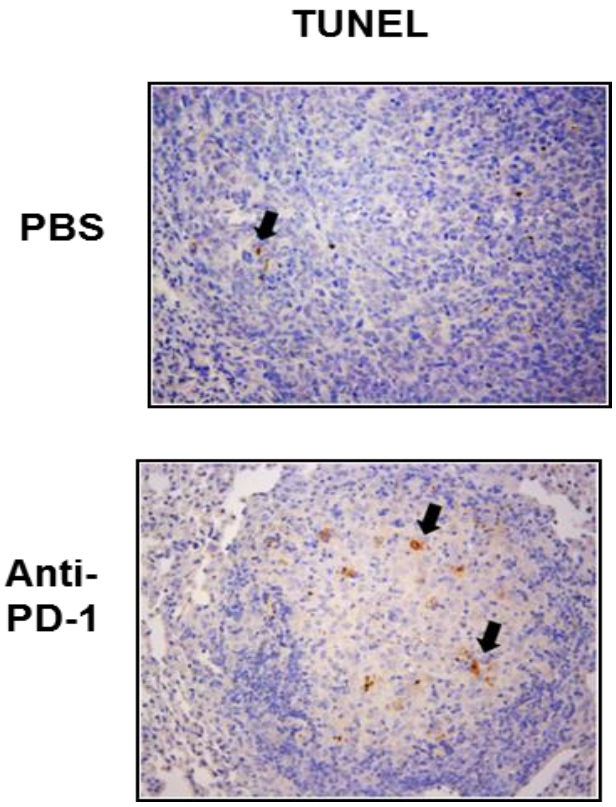

D.

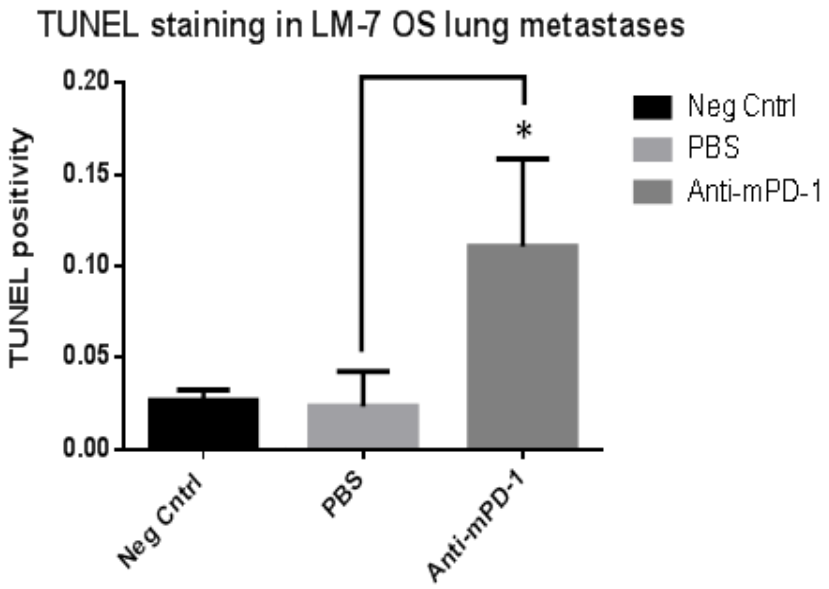

Figure 9. Anti-PD-1 treatment increased apoptosis in LM7 OS lung metastases.
A, C. Cleaved caspase-3 and TUNEL staining was performed to assess apoptosis in paraffin-embedded LM7 lung metastasis tissues from mice treated with PBS or anti-PD-1. Representative sections are shown (Magnification: 40X); B, D. Quantification was done using Cell Quest Software and student's t-test was performed. ($p<0.05$)

In addition, we also confirmed the cleaved caspase-3 expression in the OS lung tumors from anti-PD-1 treated mice versus PBS control mice using an alternative technique. As IHC represents expression at the tissue level, we assessed the overall expression in lung tumors using western blotting. Cleaved caspase-3 and total caspase-3 expression was assessed in the lysates from lung tumor nodules of mice. As expected, there was an increase in cleaved caspase-3 and decrease in total caspase-3 expression in lysates from anti-PD-1 treated mice as compared to PBS treated mice **(Figure 10).** These data indicated that anti-PD-1 treatment led to cell death by triggering tumor apoptosis.

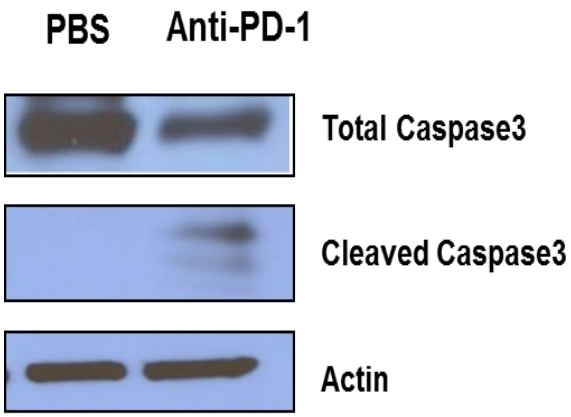

Figure 10. Anti-PD-1 treatment enhanced apoptosis in LM7 OS lung tumors.
Lysates were obtained from LM7 lung tumor nodules of mice treated with PBS or anti-PD-1 for 5 weeks. Western blotting was done to evaluate total and cleaved caspase-3 expression.

In vivo anti-PD-1 treatment was not associated with any significant systemic toxicities

In order to ensure that anti-PD-1 does not cause systemic toxicities after 5 week treatment, we performed complete blood count (CBC) and liver enzyme chemistry tests. Serum was obtained from 5 mice after 5 weeks of anti-PD-1 treatment and parameters such as hemoglobin (Hb), hematocrit, platelets and WBC counts were computed. It was found that there were no significant differences in the mean values of hemoglobin, hematocrit, platelets and WBCs between the PBS treated and anti-PD-1 treated mice groups ($p>0.05$) **(Figure 11).** In addition, the values obtained for these parameters were within the normal ranges found in healthy *nu/nu* mice (Hb: 14.4-15 g/dL, Hematocrit: 44-44.6%, Platelets: 813-1100*10^3, WBCs: 5.7-7*10^3). These data indicated that anti-PD-1 treatment did not induce any significant systemic inflammation.

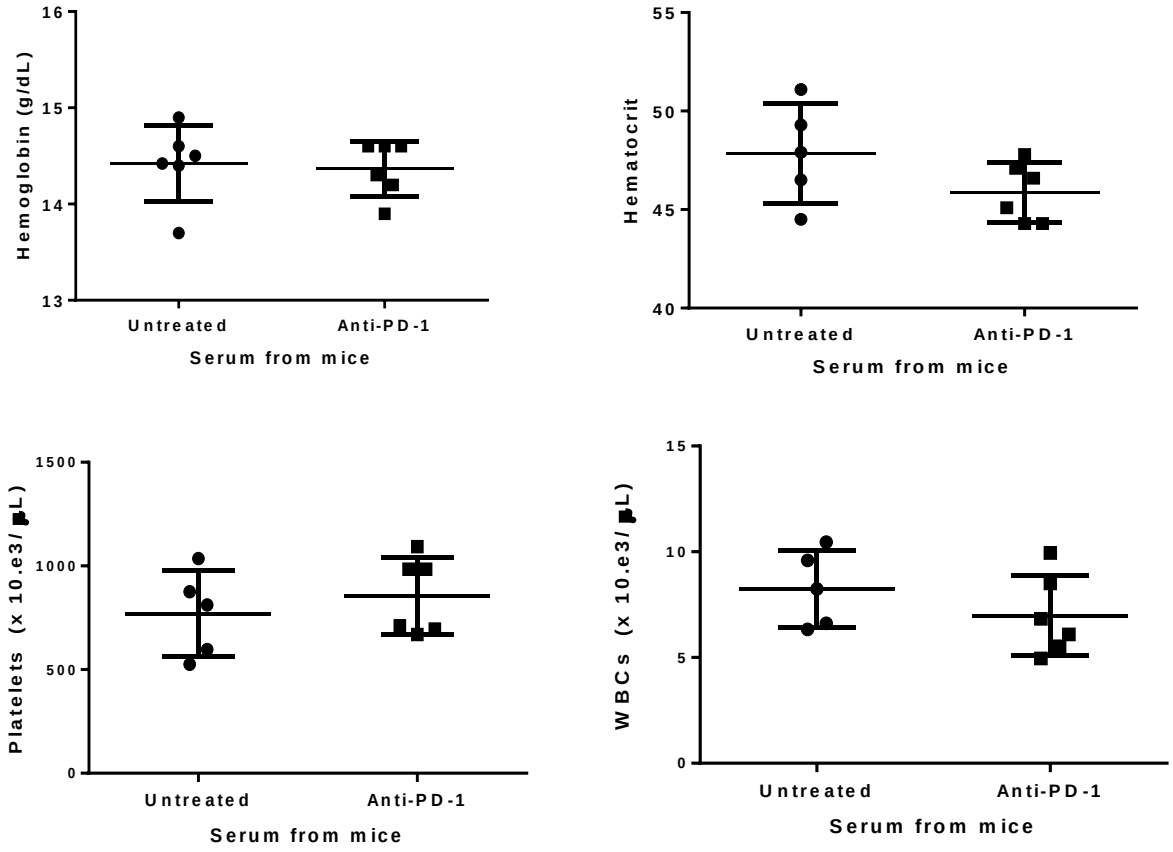

Figure 11. No significant differences of CBC functions were observed after anti-PD-1 treatment in mice.
CBC tests included analysis for hemoglobin, hematocrit, platelets and WBC counts from blood of PBS and anti-PD-1 treated mice after 5 weeks. Statistical analysis was performed using student's t-test ($p>0.05$).

Also, liver enzyme chemistry levels of the control and treated animals were determined in a similar way. Specifically, serum was obtained and tested for AST (aspartate aminotransferase) and ALT (Alanine transaminase) liver enzymes. We found no significant differences in AST, ALT and AST/ALT ratio between the control and treated mice groups **(Figure 12).** Also, these values are within the normal ranges found in healthy *nu/nu* mice (AST: 110-174 U/L, ALT: 33.4-60 U/L, AST/ALT: 2.9- 3.4). This implied that anti-PD-1 did

not induce any significant liver damage. Overall, we conclude that there were no significant systemic toxicities induced by anti-PD-1 treatment.

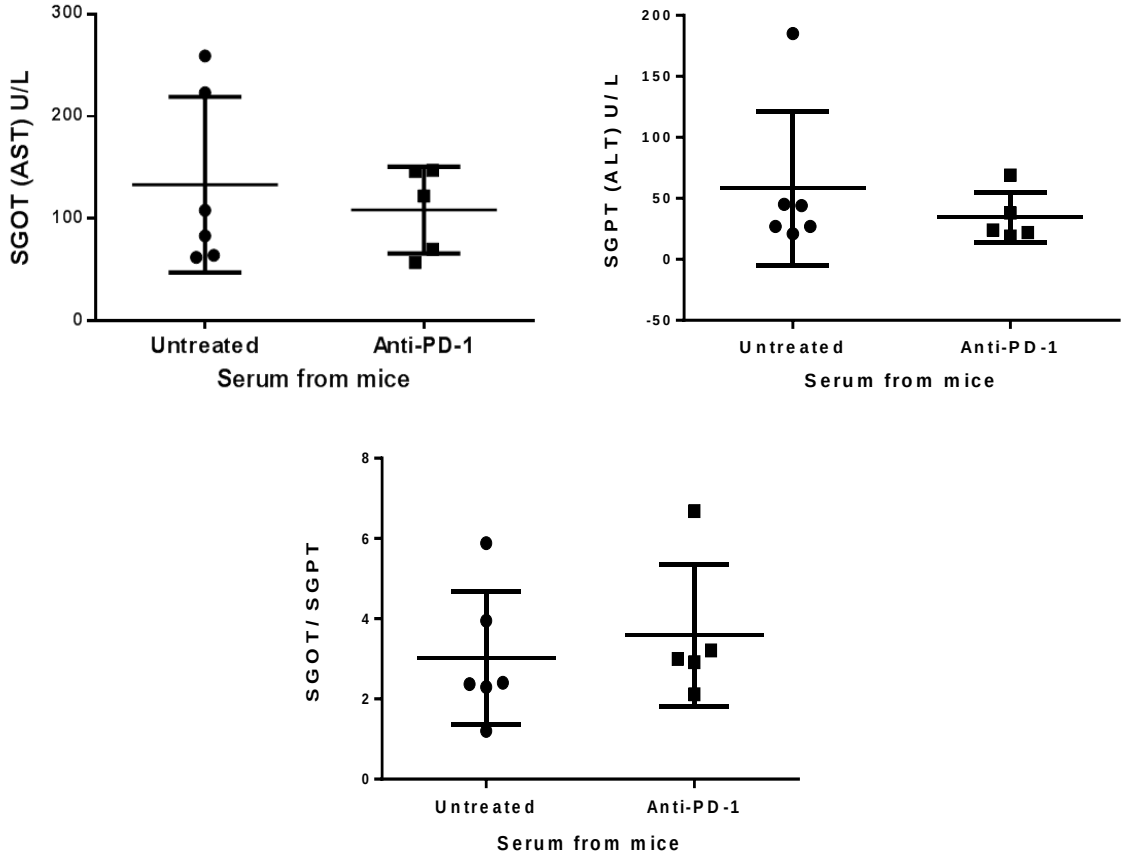

Figure 12. No significant differences were observed in liver enzyme chemistry tests after anti-PD-1 treatment in mice.
Liver enzyme chemistry included tests for AST and ALT liver enzymes from serum of PBS and anti-PD-1 treated mice after 5 weeks. Statistical analysis was performed using student's t-test ($p>0.05$).

Anti-PD-1 treatment did not cause acute or chronic toxicities as evaluated by histological examination

In order to determine the toxic effects at the tissue level, we performed histological examination of organs by sacrificing the animals treated for 5 weeks with either PBS or anti-PD-1 treatment. We obtained lungs, spleen, liver, heart and kidneys from mice followed by H

and E staining. Pathological examination was performed under the supervision of Dr. John Stewart (Department of Pathology, MD Anderson Cancer Center). There were no significant toxicities, inflammation or necrosis/scarring observed in the various organs after anti-PD-1 treatment **(Figure 13)**. This showed that anti-PD-1 therapy was efficacious without causing non-specific effects on the mouse organs.

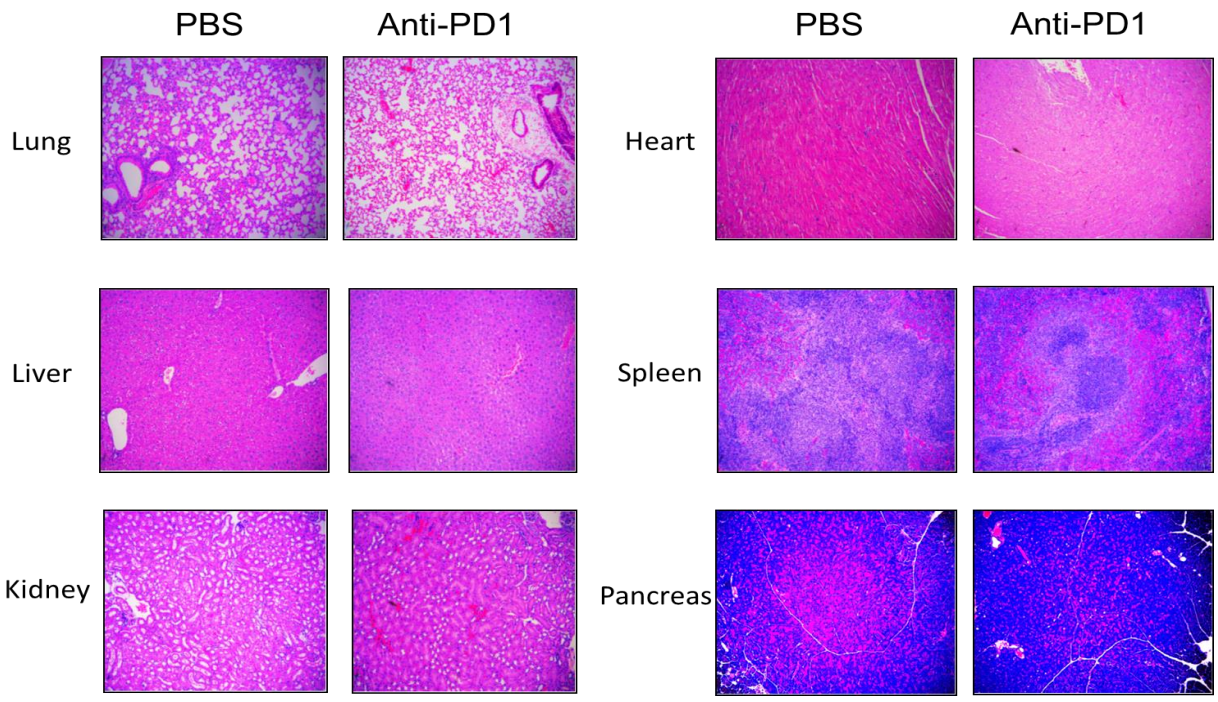

Figure 13. No specific pathological changes in the mouse tissues were observed after anti-PD-1 treatment for 5 weeks.
H and E staining was performed for lungs, spleen, liver, heart and kidneys from mice after PBS or anti-PD-1 treatment for 5 weeks. Pathological examination was performed to examine toxicities in tissues microscopically.

Summary

In this chapter, we demonstrated that anti-PD-1 was effective in inducing regression of OS lung metastases in mice. Using a human OS model, we observed that there was a significant inhibition in the development of lung metastasis after anti-PD-1 treatment. We interpret this to mean that the therapeutic efficacy of anti-PD-1 measured by the number of macro and micro-metastases formed was secondary to the blockade of the PD-1-PDL-1 interaction. Further, this was accompanied by induction in tumor cell apoptosis, represented by cleaved caspase-3 activation. We also found that there was a significant decrease in the tumor cell proliferation, as seen by the cell proliferation marker, Ki-67. It has been shown

that there is an imbalance of apoptosis and proliferation during cancer progression (141). Apoptosis and proliferation are linked by cell-cycle regulators and apoptotic stimuli can affect both the processes (142). The degree of apoptosis and proliferation occurring in a particular cell milieu ultimately determines the cellular outcome. Our data indicates that the mechanisms involved in the efficacy of anti-PD-1 include both induction of the apoptotic pathway as well as inhibition of tumor cell proliferation, which ultimately lead to the inhibition of growth of metastatic tumors. The effects of anti-PD-1 treatment on cell cycle may be performed in future. Since there is an enhancement of apoptosis, we can predict that there would be G1 arrest and a sub-G1 peak after anti-PD-1 treatment. In addition, since there is a decrease in tumor cell proliferation, we could also predict that there may be an decrease in the percentage of tumor cells in the S phase and/or G2/M phase. This can be confirmed *in vivo* through reduced expression of cell cycle regulators, Cyclin D/Cyclin E that are crucial in G0/G1 phase transition, by western blotting. Cyclins D and E are involved in progression though G1 and G1/S phases. Similarly, since pRb is involved in G1/S phase entry, reduced levels of pRb may be assessed in tumor lysates (143, 144) .

Anti-PD-1 drugs have been known to cause immune-related side-effects including pneumonitis, thyroiditis, hypophysititus in the clinic (82, 145, 146). Hence, we determined if anti-PD-1 caused significant toxicities when used for treatment in nude mice at the dose at which it resulted in efficacy. However, no hematologic toxicity as determined by CBC. Anti-PD-1 drugs such as Nivolumab are known to cause hepatic and gastrointestinal effects like hepatitis, colitis in the clinic. Certain patients have also shown elevation of alanine aminotransferase (ALT) levels and aspartate aminotransferase (AST) (82, 145). Hepatotoxicity is indicated by an increase in liver enzymes such as AST and ALT. We

observed no changes in the liver enzyme levels or any pathological changes in the liver, lung, spleen, kidney, heart or pancreas after anti-PD-1 treatment. Our data showed that there were no significant toxicities (systemic or pathological) observed on anti-PD-1 treatment. This is of crucial importance as it demonstrated that anti-PD-1 exerted targeted organ-specific effect at the lung tumor site, without affecting other organs to cause side-effects or toxicities. Thus, we established that anti-PD-1 was safe for administration at the dosage we administered.

CHAPTER 6

Enhanced NK cell and macrophage infiltration in OS lung tumors after PD-1 blockade

Rationale

Many studies have previously demonstrated the anti-tumor efficacy of PD-1/PDL-1 inhibitors in several mouse tumor models like melanoma, NSCLC, renal cancer, colon cancer and pancreatic cancer (60, 147, 148). Anti-PD-1 antibodies have also shown therapeutic efficacy in combination with other checkpoint inhibitors such as CTLA-4 and LAG-3 (129, 149). Recently, the effect of blocking PDL-1 was shown against OS lung metastasis in K7-M2 mouse model (103). However, all these studies have demonstrated that blockade of PD-1/PDL-1 leads to an increase in the T-cell infiltration, activation of tumor-specific T cells and recruitment of effector T cells to the tumor sites, decrease in the number and deactivation of Tregs at the tumor site, upregulation of pro-inflammatory cytokines and downregulation of immunosuppressive cytokines (60-63). In addition, PD-1 has been known to be upregulated on tumor infiltrating T cells and has been associated with T-cell dysfunction in tumors (150, 151). PD-1 expression has not been well characterized in tumor-associated macrophages as well as NK cells in mouse tumor models till date.

Our data in Chapter 5 showed anti-tumor efficacy of anti-PD-1 against human LM7 OS lung metastases in a nude mouse model devoid of T cells, which was accompanied by increased apoptosis. We therefore hypothesized that PD-1 blockade might be inducing the migration of non-T immune cells (NK and macrophages) into the lung tumors, which ultimately lead to tumor cell apoptosis. Thus, in Chapter 6, we analyzed PD-1 expression on NK cells and macrophages in the OS lung tumors. We further determined the number of NK cells and macrophages from mice in the lung tumor nodules and in OS lung metastases by utilizing two techniques, flow cytometry and IHC respectively. We also determined the number of immune cells in spleen, the lymphoid organ which initiates immune responses

towards antigens. This was to ascertain if there was any overall systemic increase in the number of immune cells after anti-PD-1 treatment. Flow cytometry analysis was performed by obtaining single-cell suspensions of lung tumor nodules and spleens from mice. We used mNKp46 and mF4/80 as markers for murine NK cell and macrophages respectively. Similarly, IHC was performed on paraffin-embedded tissues of OS lung metastases and NK and macrophages were stained using antibodies against mNKp46 and mF4/80.

Results

PD-1 expression is upregulated on NK cells and macrophages in OS lung tumors

Figure 14 A. shows the macrophage population within LM7 lung tumor nodules identified as $F4/80^{+}/CD11b^{+}$. We observed that PD-1 was upregulated on macrophages in OS lung tumor nodules in nude mice. $F4/80^{+}/CD11b^{+}$ stained for PD-1 showed that most of the macrophages (98.8%) had PD-1 positivity. We also showed that anti-PD-1 treatment led to a significant increase in the number of $F4/80^{+}CD11b^{+}$ macrophages (7.6% to 34%) double positive). Thus, the total number of macrophages in the tumor nodules increased on anti-PD-1 treatment; however, the PD-1 expressing macrophage population remained the same after anti-PD-1 treatment.

Similarly, double staining of NKp46 and PD-1 and using flow cytometry analysis revealed that PD-1 is upregulated on NK cells **(Figure 14 B).** Further identification of PD-1 expression amongst NK cells subset showed that all of the cells (100%) expressed PD-1. We further showed that anti-PD-1 treatment led to a significant increase in the number of NK cells (31% to 80%). PD-1 expressing NK cell subset population remained the same after anti-PD-1 treatment.

A.

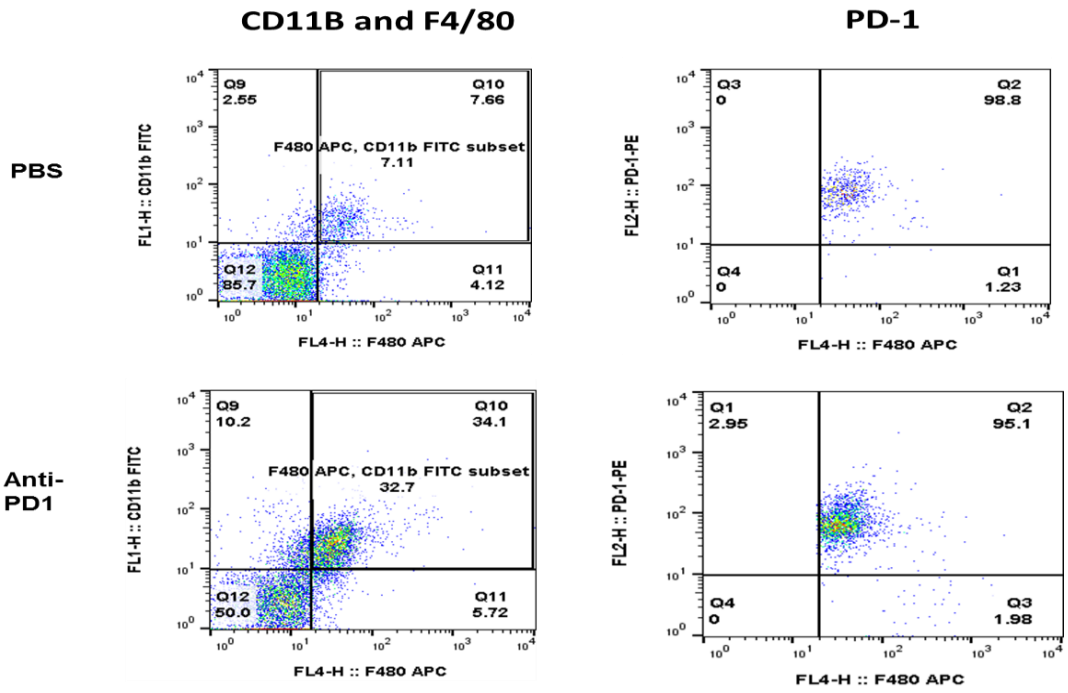

B.

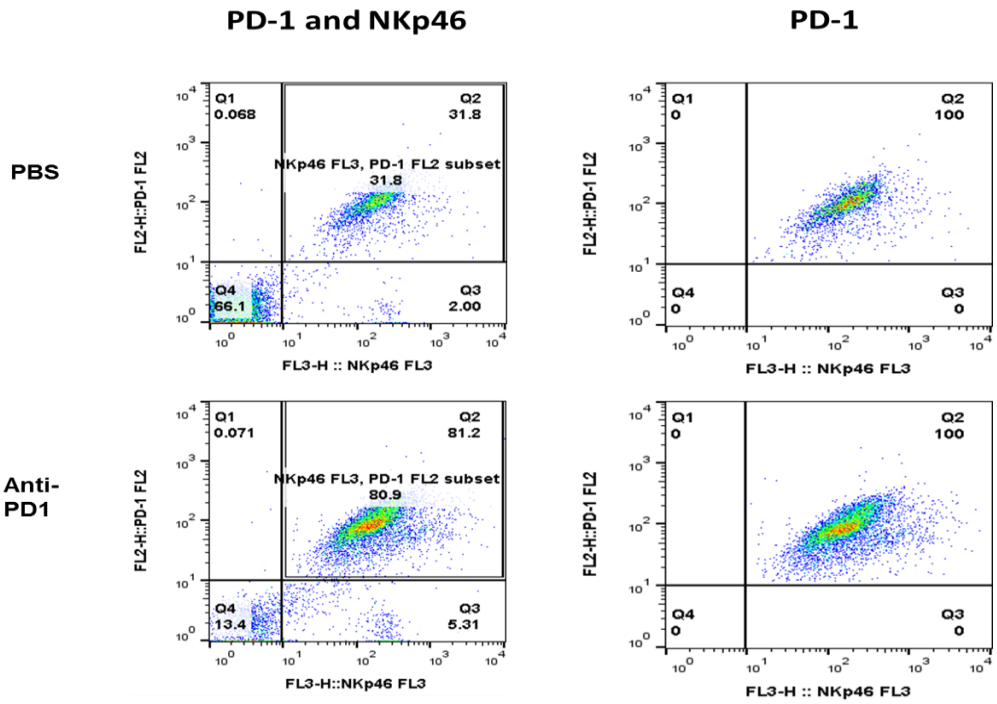

Figure 14. PD-1 was upregulated on macrophages and NK cells in OS lung tumors. A. Flow cytometry analysis was performed after obtaining single cell suspensions from lung tumor nodules from mice treated with anti-PD-1. Staining was done using anti-F4/80-APC, anti-CD11b-FITC, and anti-PD-1-PE antibodies and respective isotype IgG controls. PD-1 expressing macrophages were identified by PD-1-PE, F4/80-APC and CD11b-FITC positively stained population; B. NK cells were identified from single cell suspensions of lung tumors by staining with anti-NKp46-PerCP. PD-1 expressing NK cells were identified by double staining of PD-1-PE and NKp46.

Lower levels of PD-1 are expressed on NK cells and macrophages in the spleen from mice as compared to OS lung tumors

Figure 15 A shows that amongst the macrophage sub-set population (~ 2.6%) in the spleens of nude mice, only 56% of the cells expressed PD-1. The numbers of macrophages in the spleens were unchanged on anti-PD-1 treatment (3.3% to 5.39%) and the PD-1 expressing macrophage sub-populations remained unchanged (56.3 to 64.1%).

Similarly, amongst the NKp46^{+} (~7.7%) in the spleen, only 35% of NK cells express PD-1 **(Figure 15 B)**. Also, the numbers of NK cells (7.7% to 9.5%) remains unchanged after anti-PD-1 treatment as the number of immune cells remained the same. Also, PD-1 expressing NK cell population remained unchanged (35% to 32.6%) after anti-PD-1 treatment in the spleens of mice. Our data reflected that PD-1 receptor was highly upregulated at the lung tumor sites compared to that in the spleen, suggesting that immunosuppression was specific to the tumor microenvironment.

A.

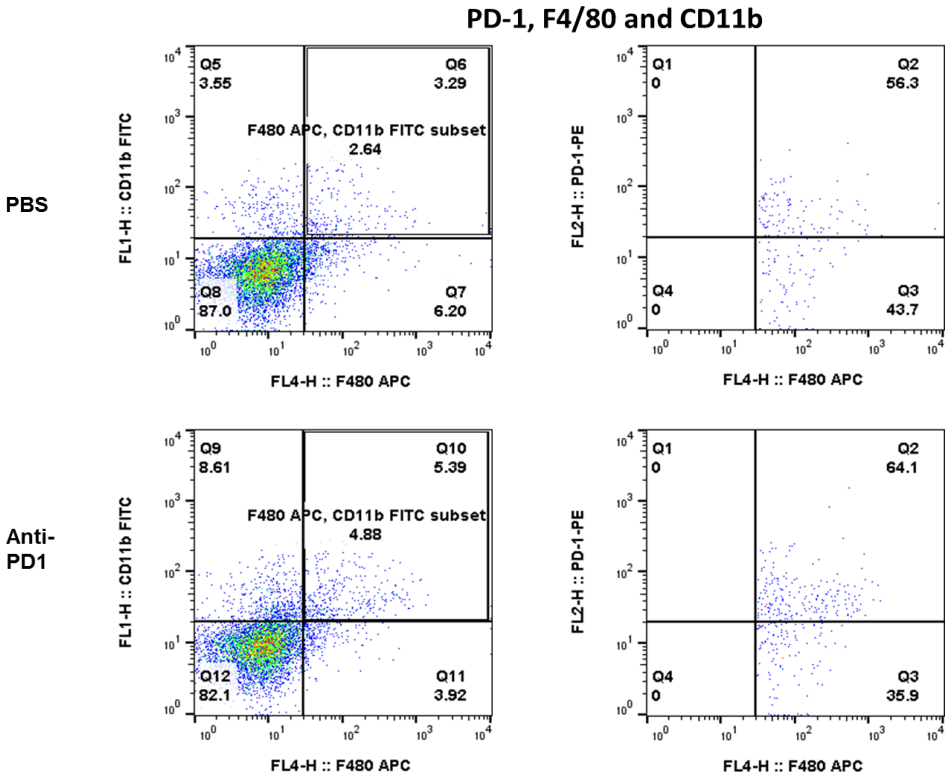

B.

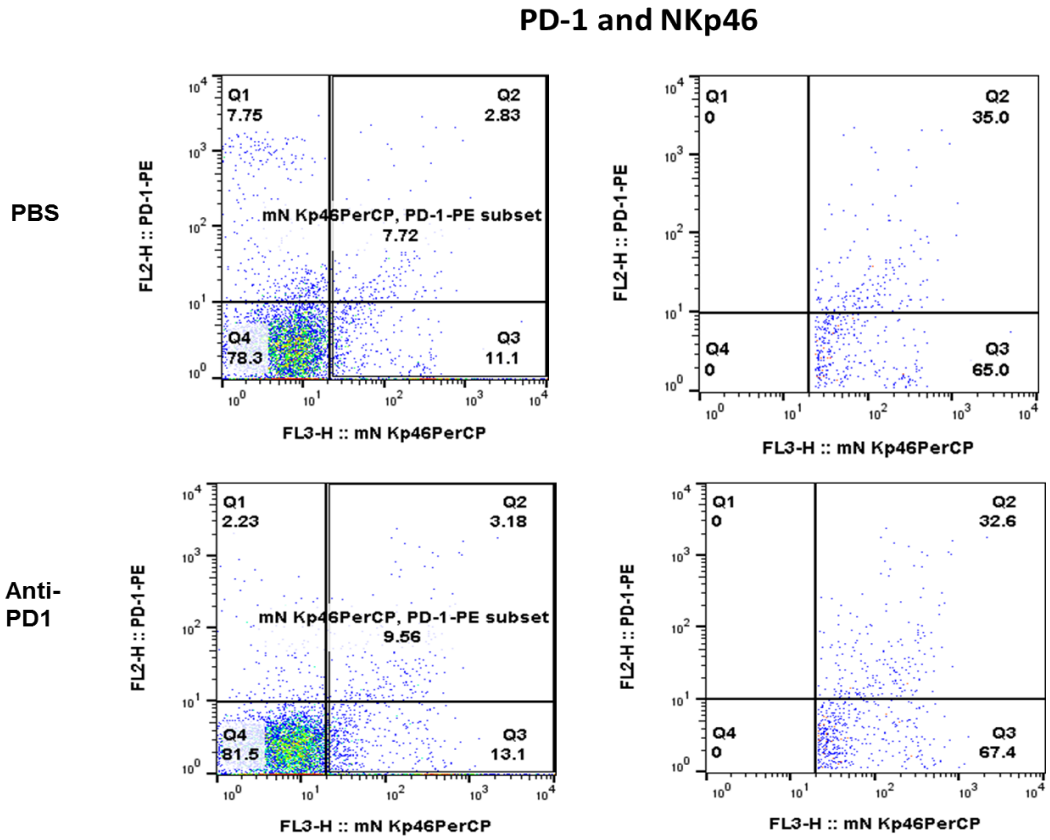

Figure 15. Lower levels of PD-1 are expressed on NK cells and macrophages in spleen as compared to OS lung tumors.

A. Flow cytometry analysis was performed after obtaining single cell suspensions from spleens of mice treated with either PBS or anti-PD-1. Staining was done using anti-F4/80-APC, anti-CD11b-FITC and anti-PD-1-PE antibodies and isotype IgG controls, PD-1 expressing macrophage subpopulation was identified within $F4/80^{+}CD11b^{+}$ population; B. Flow cytometry analysis was performed after obtaining single cell suspensions from spleens followed by staining using anti-NKp46-Percp and PD-1-PE to identify PD-1 expressing NK cells after anti-PD-1 treatment.

Anti-PD-1 increases the number of NK cells in OS lung metastases

Figure 16 A. depicted a 2.5 fold increase ($NKp46^+$: 19% to 44%) in the number of NK cells in the lung tumor suspensions of anti-PD-1 treated group compared to the control group. This data showed that there was a significant increase in NK infiltration in lung tumors after anti-PD-1 treatment.

IHC analysis of OS lung metastases of untreated versus anti-PD-1 treated mice using NKp46 staining also showed significantly increased NKp46 staining in anti-PD-1 treated group. (**Figure 16 B and C).** The $NKp46^+$ cells *(indicated by arrowheads)* were limited to the tumor periphery in the lung metastases of PBS treated mice, as opposed to enhanced staining within the entire tumor area after anti-PD-1 treatment. Negative control tissue showed absence of non-specific secondary antibody staining. This corroborated our flow cytometry data, reiterating that there was increased NK cell recruitment within the OS lung metastases with PD-1 blockade.

A.

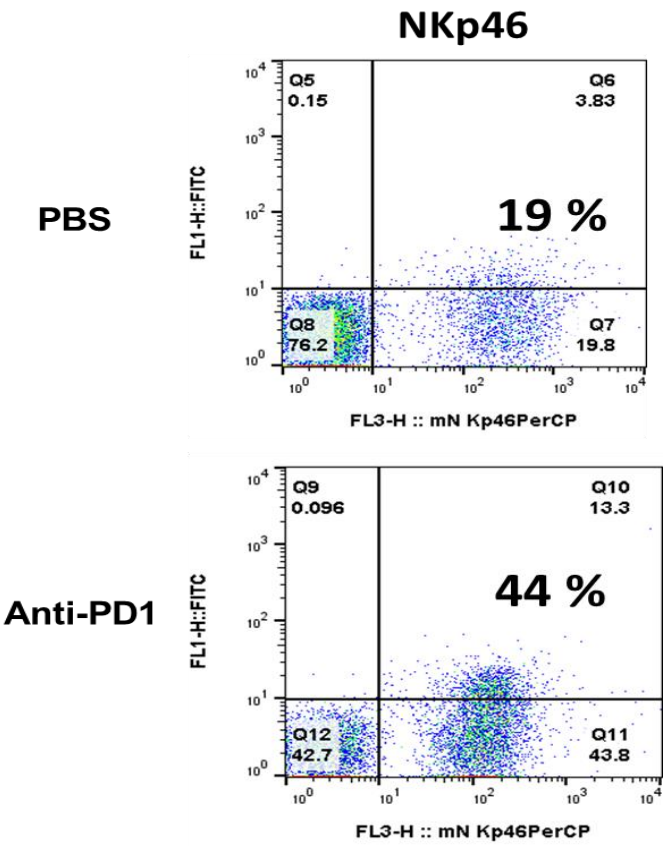

Δ (PBS):**0.43**, Δ (Anti-PD-1):**0.49**

B.

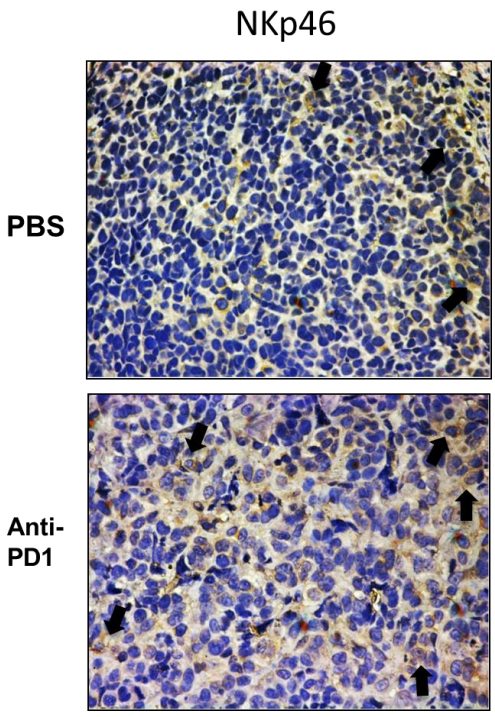

C.

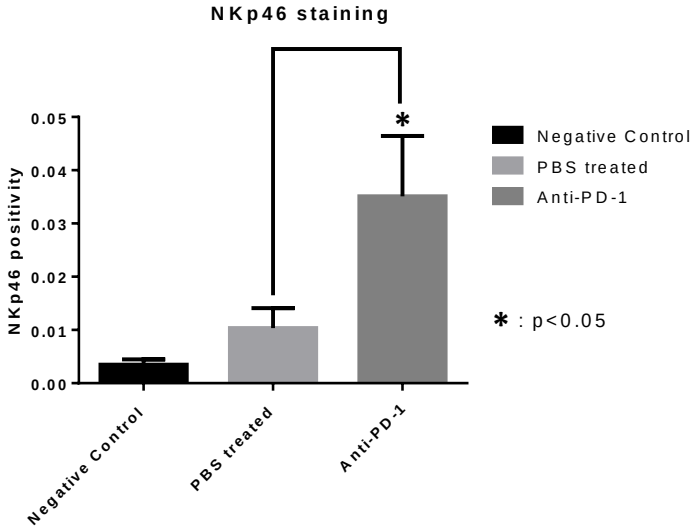

Figure 16. Anti-PD-1 treatment increases the number of NK cells in OS lung tumors.
A. Flow cytometry was performed in single cell suspensions from lung tumor nodules of mice treated with either PBS or anti-PD-1. Staining was done with either anti-mNKp46-PerCP or isotype IgG control antibodies; B. NKp46 staining was performed in paraffin-embedded LM7 OS lung metastases from mice treated with PBS or anti-PD-1.

Representative sections are shown (Magnification: 40X); C. Quantification for was done using Cell Quest Software and student's t-test was performed, (*: $p<0.05$).

Anti-PD-1 increases the number of macrophages in OS lung metastases

We also analyzed the number of macrophages in the lung tumor suspensions of anti-PD-1 treated group and PBS treated group. We found a threefold increase in the percentage of macrophages ($F4/80^+$: 11.8% to 31.4 %, $F4/80^+CD11b^+$: 15.6% to 33.4%) in the lung tumors of mice receiving anti-PD-1 antibody compared to those receiving PBS **(Figure 17 A).**

Similarly, IHC analysis of F4/80 of paraffin-embedded tissues from anti-PD-1 treated and PBS treated mice was used to determine overall infiltration of macrophages within LM7 OS metastases. As seen in representative tissue sections, we noted that the ratio of the cells staining positive for F4/80 was significantly higher in metastases from anti-PD-1 treated mice as compared to PBS treated mice **(Figure 17 B and C).** The F4/80 positivity *(indicated by arrowheads)* was confirmed by comparing to the negative control tissue without primary antibody staining. Thus, this data validated the findings by flow analysis, indicating that there were significantly higher numbers of macrophages migrating into OS lung tumors upon anti-PD-1 treatment.

A.

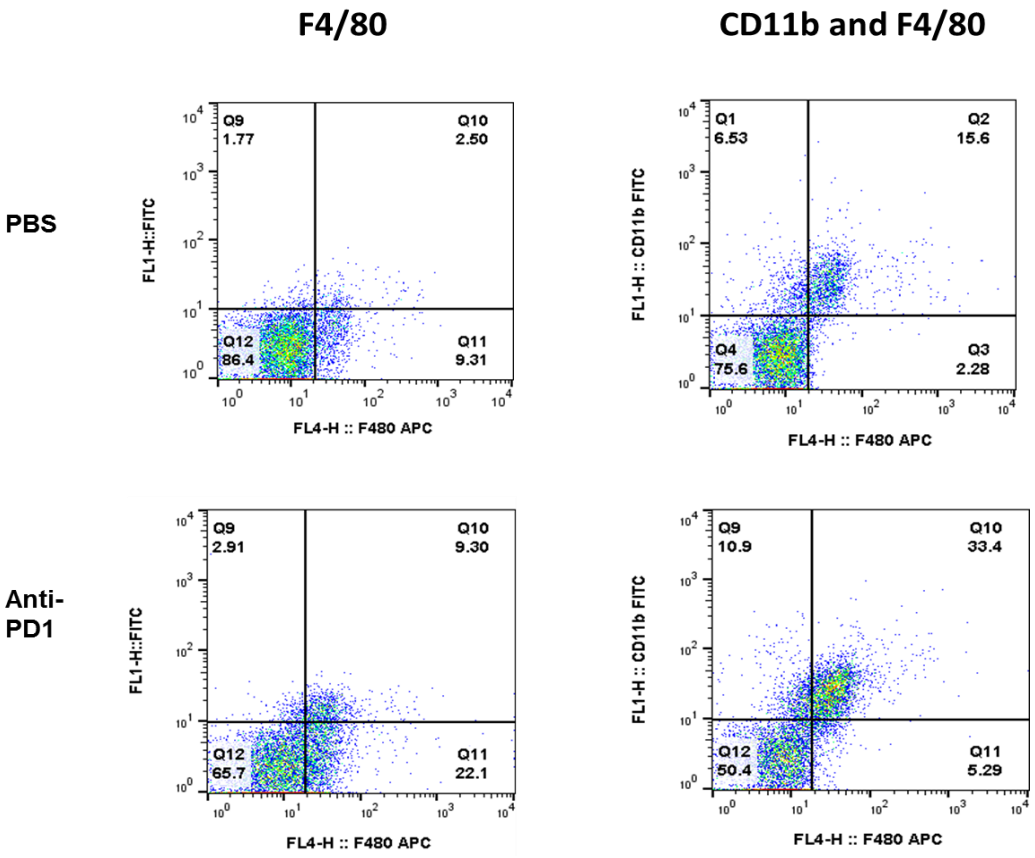

$CD11b^{+}F4/80^{+}$: Δ (PBS):**0.51**, Δ (Anti-PD-1):**0.02**

B.

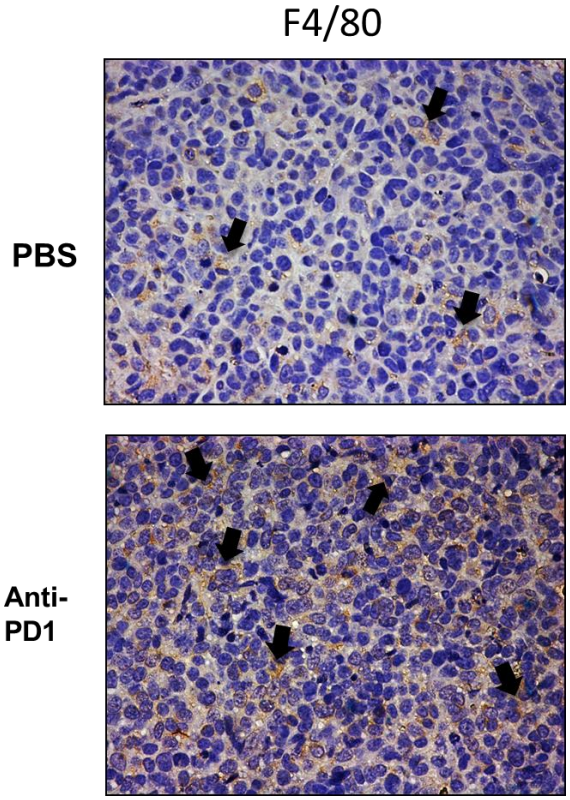

C.

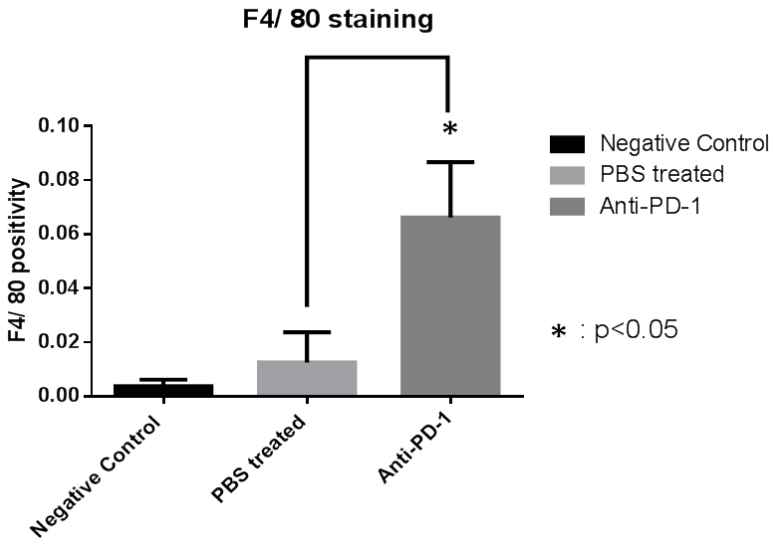

Figure 17. Anti-PD-1 treatment increases the number of macrophages in OS lung tumors.
A. Flow cytometry was performed in single cell suspensions from lung tumor nodules of mice treated with either PBS or anti-PD-1. Staining was done with either anti-mF4/80 and/or anti-mCD11b-FITC along with isotype IgG control antibodies; B. F4/80 staining was performed in paraffin-embedded LM7 OS lung metastases from mice treated with PBS or anti-PD-1. Representative sections are shown (Magnification: 40X); C. Quantification for was done using Cell Quest Software and student's t-test was performed, (*: $p<0.05$).

Anti-PD-1 does not alter the number of NK cells and macrophages in the spleens of mice

Figures 18 A and B. represent the number of NK cells and macrophages in the spleens from two groups of mice, PBS treated and anti-PD-1 treated group. We showed that there was no change in the number of NK cells (7.6% to 6%) after anti-PD-1 treatment. Similarly, the number of macrophages also did not change after PD-1 blockade (4% to 3%). This data reflected that the effect of anti-PD-1 was specific to the lung tumor site and it did not induce a global immune response in other organs.

A.

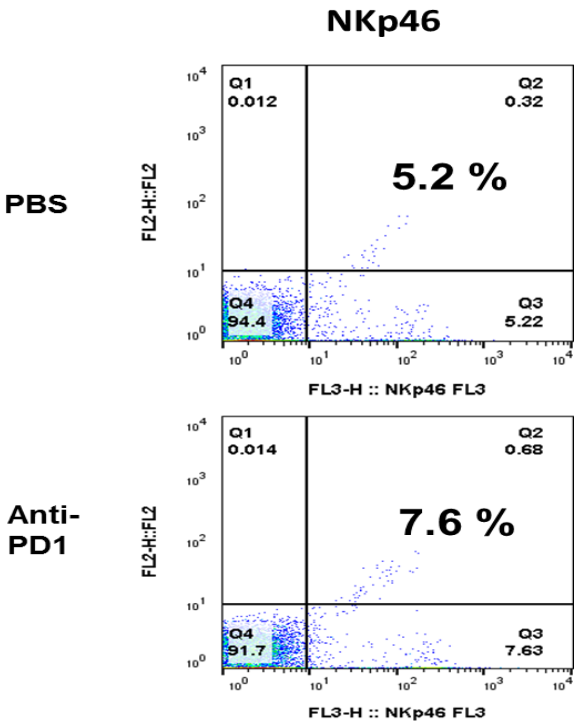

Δ (PBS):**0.62**, Δ (Anti-PD-1):**0.53**

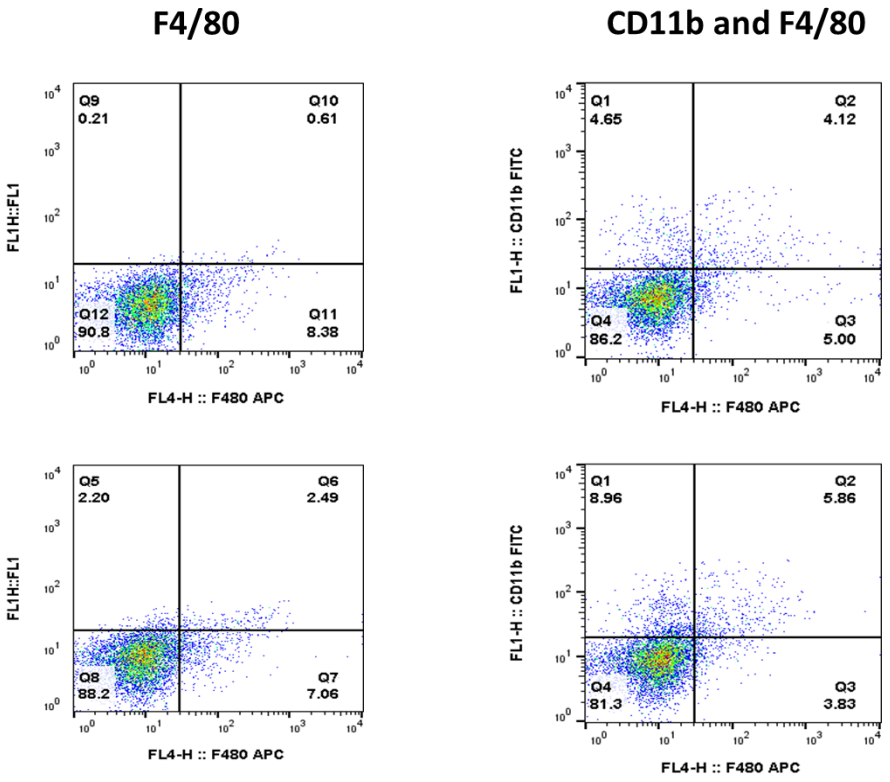

Δ (PBS):**0.21**, Δ (Anti-PD-1):**0.08**

Figure 18. The number of NK cells and macrophages were unchanged in spleens of mice after anti-PD-1 treatment.
Flow cytometry analysis was performed after obtaining single cell suspensions from spleens of mice treated with either PBS or anti-PD-1. Staining was done using anti-NKp46-PerCP, anti-F4/80-APC and/or anti-CD11b-FITC antibodies and respective isotype IgG controls.

Summary

This chapter illustrates the novel discovery that PD-1 was expressed on both NK cells and macrophages in OS lung tumors in nude mice. Current literature has widely focused on the role of PD-1 in TILs. Recently, reports have shown PD-1 expression on activated NK cells in viral infection or inflammatory conditions such as tuberculosis (152, 153). Previously, Benson D. M. *et al.* showed that anti-PD-1 antibody CT-011 enhanced the NK

cell function (cytotoxicity) against multiple myeloma cells *in vitro*. This study demonstrated that NK cells from multiple myeloma patients had PD-1 expression whereas normal healthy donors did not (154). Here, we showed that PD-1 was particularly expressed on NK cells in the OS lung tumor microenvironment following anti-PD-1 treatment as opposed to the spleen. This indicates their potential role in the therapeutic activity of anti-PD-1 therapy and the role of PDL-1 in immune-escape of OS tumor cells. Further, we showed that the number of NK cells infiltrating into the OS lung tumors was significantly increased after anti-PD-1 treatment in contrast to the spleen, where the NK cell numbers remain unchanged. It has been shown that mouse NK cells may play a role in inhibition of systemic metastasis of human glioblastoma cells in mouse models. Se Jeong Lee *et al.* studied that murine NK cell depletion induced spontaneous lung metastasis of glioblastoma cells in BALBc nu/nu mice (155). Hence, from our data, we predict that the efficacy of anti-PD-1 against OS lung metastasis and the resulting tumor cell apoptosis may be due to the mouse NK cells infiltrating the LM7 tumors.

We also demonstrated that PD-1 is expressed on mouse macrophages in OS lung tumors. Previously, PD-1 expression on macrophages has shown to be induced in inflammatory responses during infections like sepsis, thus resulting in suppression of macrophage function (156). Although studies have elucidated higher PD-1 expression on macrophages/monocytes in other immune disorders such as viremic HIV-infection, it has never been reported in the context of tumor cells to date (157, 158). Hence, our novel finding of PD-1 expression on macrophages in OS lung tumors brings to light the fact that macrophage function may be suppressed, which contributes to an immunosuppressive microenvironment in OS lung metastasis. This maybe representative of an exhausted

macrophage phenotype. Further, we also show that PD-1 on macrophages is a novel therapeutic target as anti-PD-1 treatment led to an increase in infiltration of macrophages in OS lung tumor site as opposed to the spleen. It is known that mouse macrophages play a key role in killing human tumor cells by phagocytosis (159, 160). Thus, we predict that the mouse macrophages may be exerting their function of direct cytotoxic effect on OS tumor cells upon anti-PD-1 treatment as well as maybe getting involved in phagocytosis of apoptotic cells.

In summary, our results not only highlight the importance of PD-1 expression on the innate immune cells such as NK and macrophages in OS lung metastasis but also underscore the resulting increase in infiltration of NK and macrophages as one of the potential mechanisms resulting in therapeutic efficacy of anti-PD-1.

CHAPTER 7

Increased migration of M1 macrophages and decrease in migration of M2 macrophages after PD-1 blockade

Rationale

Our data from Chapter 6 strongly implicated the involvement of macrophages in the therapeutic response of anti-PD-1 against osteosarcoma lung metastasis. Previously, we have demonstrated the efficacy of L-MTP-PE, a macrophage and monocyte activating agent, in human and canine OS (8-10). Tumor-associated macrophages (TAMs) account for about 50% of the total tumor mass and are the most abundant cells in the inflammatory infiltrate (161, 162). TAMs can be classified into two types, M1 or the 'classically activated macrophages' and M2 or the 'alternatively activated macrophages'. M1 macrophages play a tumorigenic and bactericidal role and are activated by interferon-γ (IFN-γ) and Toll-like receptor ligands such as bacterial lipopolysaccharide (LPS) (163, 164). M2 macrophages, on the contrary, promote tumor progression, wound healing and angiogenesis and are induced by IL-4, IL-10 and IL-13 (165, 166). We and others have shown that L-MTP-PE, led to the activation of M1 macrophages due to a cytokine cascade and resulted in the death of osteosarcoma cells *in vitro* (8, 167). Owing to the significance of modulation of TAMs on osteosarcoma outcomes and our discovery of increased macrophage infiltration due to anti-PD-1, we aimed to study the accumulation of sub-population of M1 macrophages versus M2 macrophages within LM7 OS lung metastases after anti-PD-1 treatment.

Here, we performed IHC analysis in frozen tissues from PBS treated and anti-PD-1 treated mice to stain for M1 macrophages using CD86 staining and paraffin-embedded tissues for M2 macrophages using CD163 staining. CD86 and CD163 are specific markers for M1 and M2 murine macrophages respectively.

Results

The infiltration of anti-tumor M1 macrophages increases in OS lung metastases after anti-PD-1 treatment

IHC analysis of M1 macrophages using CD86 staining revealed there were significantly higher number of $CD86^+$ M1 macrophages located within LM7 metastases after anti-PD-1 treatment ($p<0.05$). This is reflected by the quantification data revealing the number of $CD86^+$ cells in comparison with negative control. **(Figure 19 A and B)**

A.

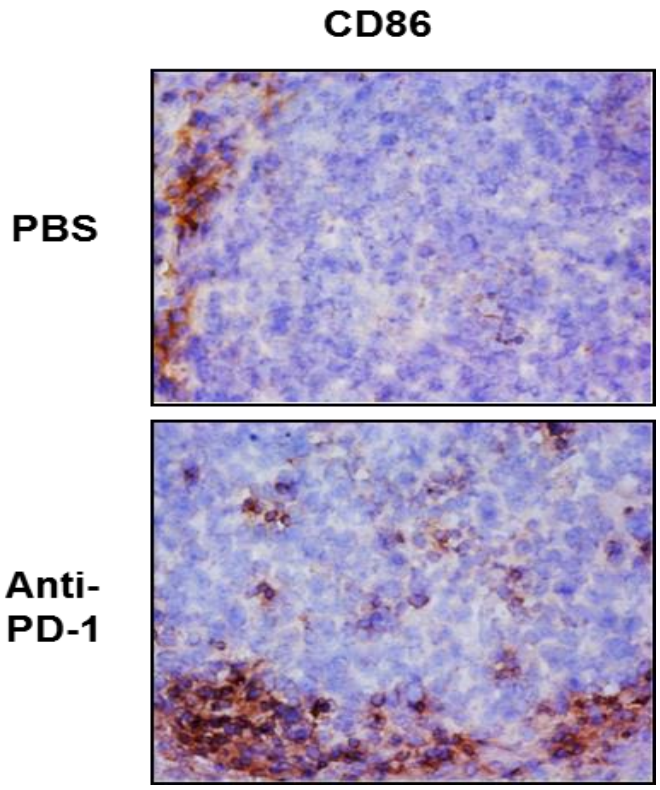

B.

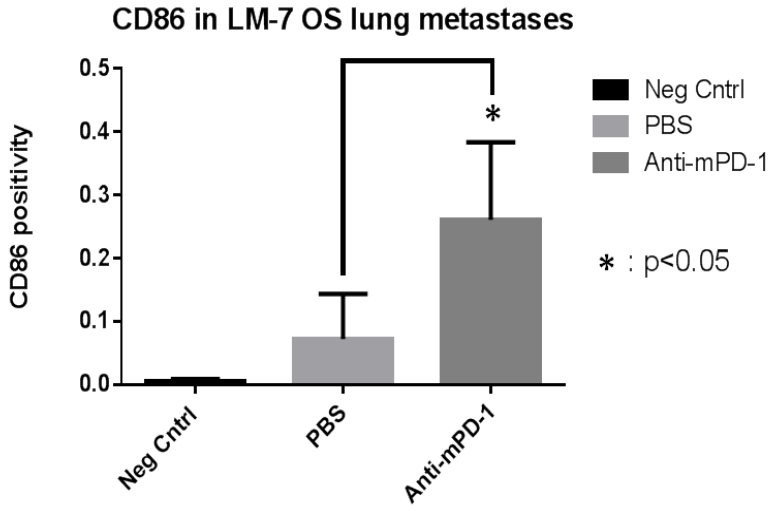

Figure 19. Anti-PD-1 treatment increases the migration of M1 macrophages in OS lung metastases.
A. CD86 staining was performed for M1 macrophage sub-population in frozen LM7 lung metastasis tissues from mice treated with PBS or anti-PD-1. Representative sections are shown (Magnification: 40X); B. Quantification for was done using Cell Quest Software and student's t-test was performed. (*$p<0.05$)

The infiltration of pro-inflammatory M2 macrophage decreases in OS lung metastases after anti-PD-1

Figure 20 A and C. reflect CD163 and CD206 staining for M2 macrophages in PBS treated mice in comparison with anti-PD-1 treated mice. We observed that there were $CD163^+$ cells towards the periphery in PBS treated mice and that they were significantly decreased in anti-PD-1 treated mice ($p< 0.05$) (**Figure 20 B)**. Similarly, we also showed using the second marker CD206 that $CD206^+$ cells were significantly decreased in anti-PD-1 treated mice ($p< 0.05$) (**Figure 20 D)**. Thus, the number of pro-tumorigenic M2 macrophages infiltrating within the OS lung metastases were reduced on treatment with anti-PD-1

A.

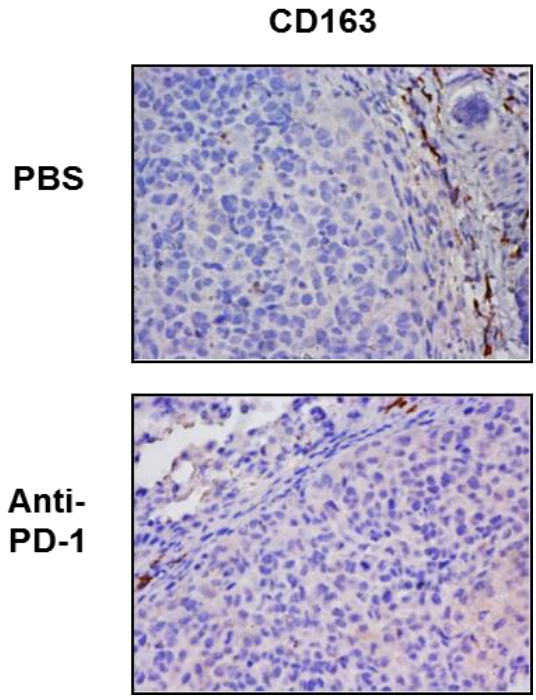

B.

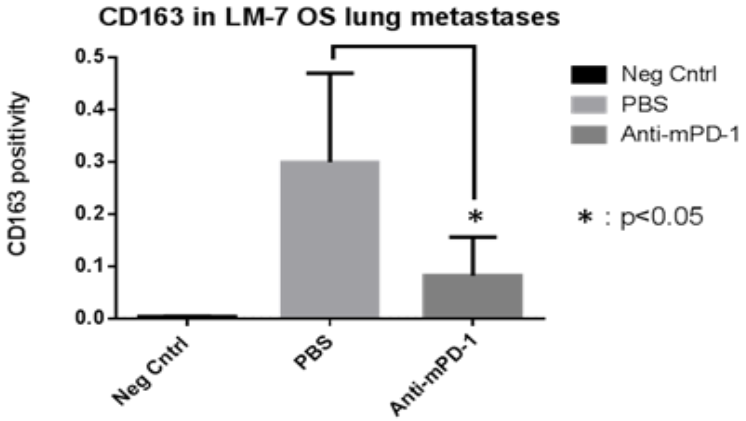

C.

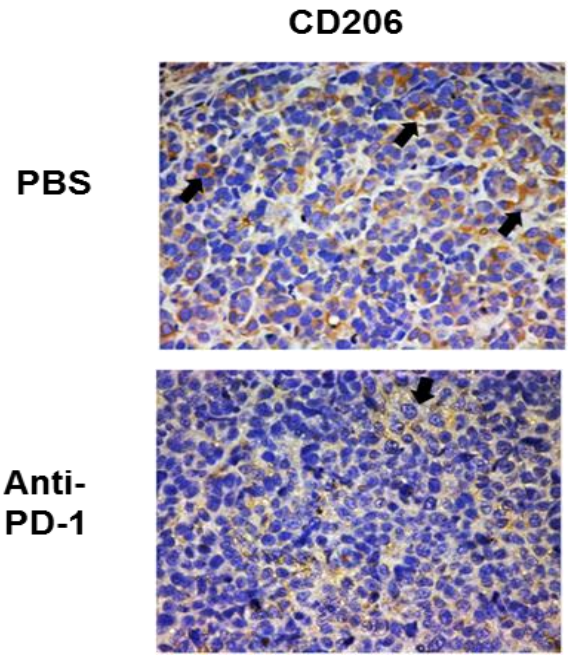

D.

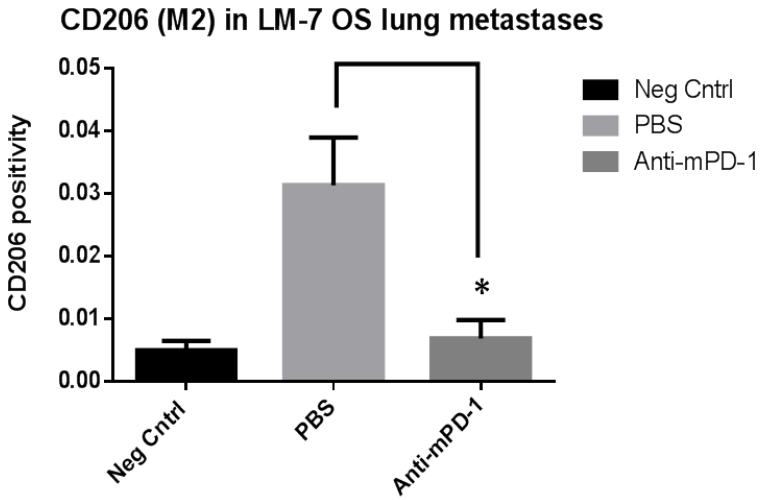

Figure 20. Anti-PD-1 treatment decreases the migration of M2 macrophages in OS lung metastases.

A. CD163 staining was performed for M2 macrophage sub-population in paraffin tissues of LM7 lung metastasis from mice treated with PBS or anti-PD-1. B. Quantification was done using Cell Quest Software and student's t-test was performed, C. CD206 staining was performed in paraffin tissues of LM7 lung metastasis from mice treated with PBS or anti-PD-

1, Representative sections are shown (Magnification: 40X); D. Quantification was done using Cell Quest Software and student's t-test was performed, (*$p<0.05$)

Summary

The role of macrophages and macrophage sub-populations in the therapeutic responses of checkpoint inhibitors is currently unknown. As our previous data showed that anti-PD-1 led to increased infiltration of macrophages, we sought to determine the changes in the macrophage sub-populations, M1 and M2, in mice after anti-PD-1 treatment.

Here, we discovered that there was a significant increase in the infiltration of M1 macrophage sub-type and a decrease in infiltration of M2 macrophage sub-type after anti-PD-1 treatment in OS lung metastases. This implies that there was an increased polarization of macrophages from pro-tumorigenic M2 to anti-tumorigenic M1 sub-type. This could be one of the mechanisms due to which there was reduced OS lung metastases observed after anti-PD-1 treatment. The role of anti-tumorigenic effect of M1 macrophages towards OS cells was demonstrated by Pahl and colleagues, when they treated M1 macrophages with L-MTP-PE and IFN-γ (167).

A previous study by Buddingh *et al*., 2011 showed that unlike other cancers, TAMs play an anti-metastatic role in OS. They found that higher numbers of infiltrating TAMs in pretreatment biopsies of OS patients correlated with better patient survival (24). However, they found a heterogeneous population of both M1 and M2 macrophage populations in the OS patient samples. Contrary to our data, a recent study showed that $CD68^+$ macrophage infiltration in primary tissue was associated with worse survival of OS patients (112). It may be possible that the contribution of macrophages may be different in primary versus metastatic OS tissues. Another point to note is that they did not differentiate M1 and M2

macrophages using specific markers, but only performed CD68 staining for total macrophage population.

From our studies, we demonstrated for the first time that PD-1 checkpoint blockade can shift the balance of M2 macrophages towards M1 macrophages, which may lead to inhibition of OS lung metastasis. Future clinical studies assessing the contribution of M1 versus M2 macrophages in the anti-tumor responses of PD-1 blocking antibodies will be needed to address this issue.

CHAPTER 8

The therapeutic efficacy of anti-PD-1 against OS lung metastases is not mediated by NK cells

Rationale

Our data from Chapter 6 revealed that treatment of anti-PD-1 antibody led to a significant increase in immune infiltration of NK cells and macrophages in the OS lung tumors grown in nude mice. These findings indicated that the anti-tumor efficacy of anti-PD-1 might be through either NK cells or macrophages. NK cells and macrophages are both part of the innate immune system and the pro-inflammatory cytokines released by activation of macrophages can lead to NK cell activation and vice versa (168-170). Because of this cross-talk between NK cells and macrophages, it is possible that the NK cells and macrophages may either be acting interdependently or they may have independent effects of the activation of immune responses upon anti-PD-1 treatment against OS lung metastases. Hence, in order to delve deeper into the detailed mechanisms of anti-PD-1, we sought to assess the individual contribution of NK cells in the therapeutic efficacy of anti-PD-1.

In order to examine if NK cells are crucial in anti-PD-1 responses, we depleted NK cells in nude mice using anti-asialo-GM1 antibody before anti-PD-1 treatment. Anti-asialo-GM1 has been widely used in *in vivo* models including *nu/nu* mice and has demonstrated success in specifically depleting NK cells, without any effect on the other immune cells (155, 171-174), Anti-asialo-GM1 binds to the cell surface glycosphingolipid GM1 without the sialic acid group, thus inhibiting NK cell activation in various mice strains (175).

Following our earlier experimental design, we intravenously injected LM7 cells to form micrometastases, and mice were randomly divided in four groups of n=5 before starting treatment. The four groups included PBS treated, anti-asialo-GM1, anti-PD-1 and anti-asialo-GM1+ anti-PD-1. Anti-asialo-GM1 (50 µl/mouse), was injected intraperitoneally twice weekly to perform NK cell depletion. In the combination group, anti-asialo-GM1 was

injected a day prior to anti-PD-1 treatment. Mice were sacrificed 5 weeks after treatment and the lungs and organs were excised for mechanistic studies. Flow cytometry and IHC analysis were used to confirm NK depletion in spleen and lung tumors respectively. The number of OS metastatic lung tumor nodules were counted.

Results

Anti-asialo-GM1 treatment causes significant depletion of NK cells in spleens of mice without any effect on macrophages

To assess the dose required for NK depletion, we conducted pilot experiments by treatment of mice with anti-asialo-GM1 (50 µl/mouse), twice a week before obtaining the spleens. Using flow cytometry analysis, we observed > 70% depletion as observed by NKp46 staining in the *nu/nu* mice **(Figure 21).** Further, there was no significant effect on the number of macrophages as the $F4/80^{+}$ cells remained constant before and after anti-asialo-GM1 treatment.

A.

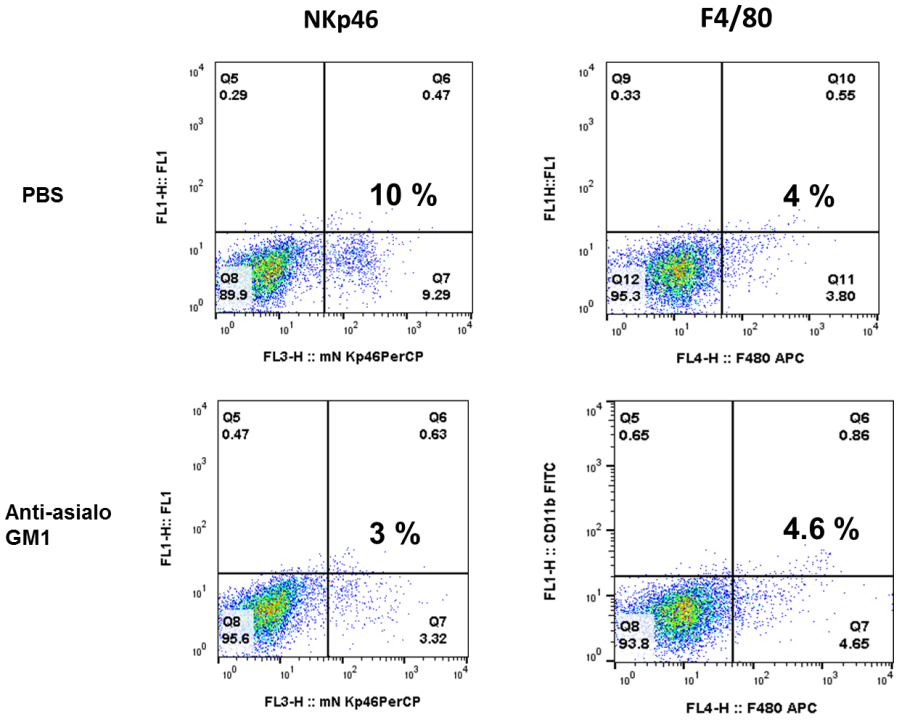

Figure 21. Anti-asialo-GM1 treatment led to a significant decrease in the number of NK cells in spleen.
Flow cytometry analysis was performed after obtaining single cell suspensions from spleens of mice treated with either PBS or anti-asialo-GM1 treatment (50 µl, twice weekly). Staining was done using anti-NKp46-PerCP or isotype IgG control antibody.

NK cell depletion using anti-asialo-GM1 reduced the number of NK cells in the mouse lung tumors

In order to confirm whether the NK depletion technique we used was effective, we performed NKp46 staining in lung tumors from mice from PBS, anti-asialo-GM1, and anti-asialo+Anti-PD-1 groups. **Figure 22 A** shows that that there was ~70% depletion of NK cells by flow cytometry in the anti-asialo-GM1 treated mice and anti-asialo+anti-PD-1 combination group compared to the PBS treated group. Similarly, IHC analysis and quantification of the images proved that $NKp46^{+}$ cells were significantly reduced in lung

metastases from anti-asialo-GM1 and anti-asialo + anti-PD-1 combination group compared to those from control PBS mice (*: $p<0.05$) (**Figure 22 B** and **C.**)

A.

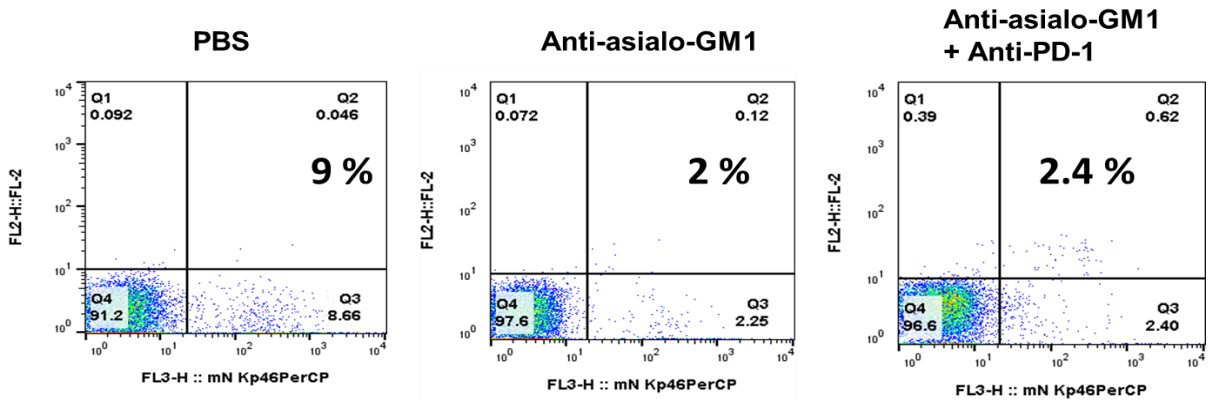

B.

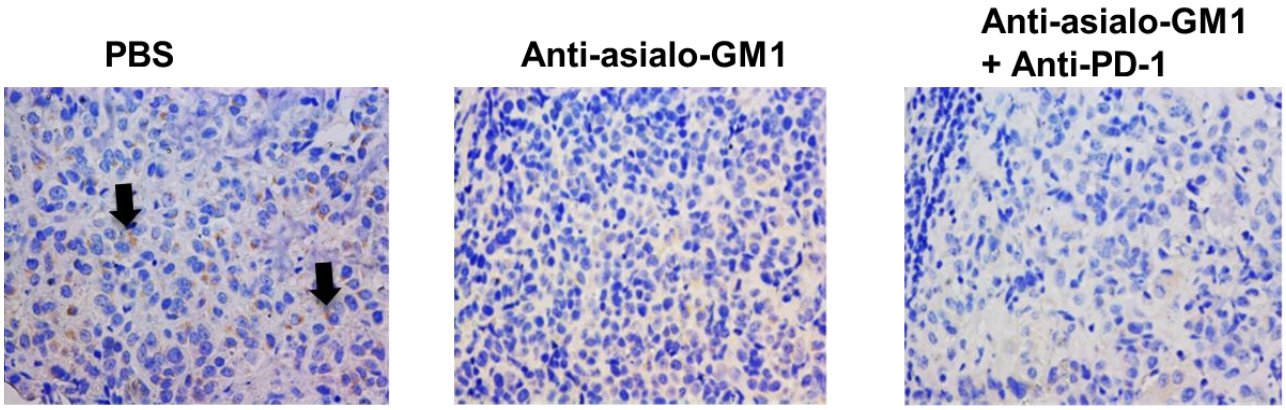

C.

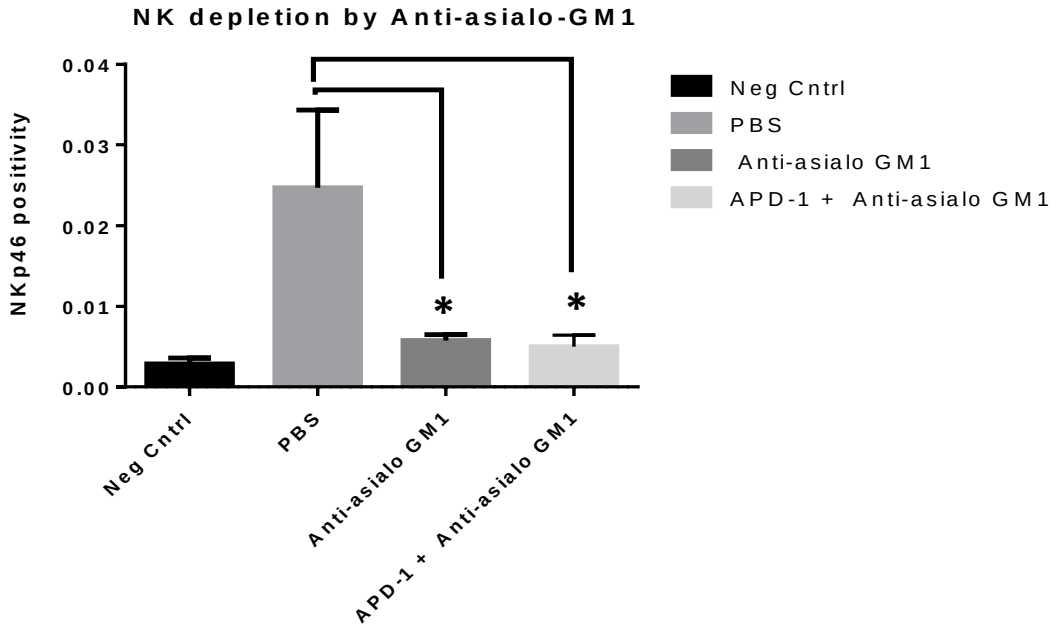

Figure 22. Anti-asialo-GM1 treatment caused a significant decrease in the number of NK cells in OS lung tumors.
A. Flow cytometry analysis was performed using anti-NKp46-PerCP or isotype IgG control antibody after obtaining single cell suspensions from lung nodules of mice treated with either PBS, anti-asialo-GM1 (50 µl, twice weekly) or combination of anti-asialo-GM1 and anti-PD-1 (200 µg/mouse), B. NKp46 staining was performed in paraffin-embedded LM7 OS lung metastases from mice treated with PBS, anti-asialo-GM1 or anti-asialo-GM1 and anti-PD-1. Representative sections are shown (Magnification: 40X); C. Quantification for was done using Cell Quest Software and student's t-test was performed, (*: $p<0.05$).

NK depletion using anti-asialo-GM1 treatment did not affect the therapeutic efficacy of anti-PD-1 against OS lung metastases

To assess if NK cells mediate the therapeutic effect of anti-PD-1, we assessed the number of macro and micrometastases formed in mice who underwent NK depletion followed by anti-PD-1 treatment. As seen in **Figure 23,** we found that anti-asialo-GM1 treatment by itself did not significantly alter the number of macro or micrometastases. Consistent with our previous data, anti-PD-1 treatment significantly decreased the number of

LM7 OS lung macro and micrometastases ($p<0.05$). The combination group of anti-asialo-GM1 and anti-PD-1 had a similar effect as anti-PD-1 alone, as there was a significant decrease in both LM7 macro and micrometastases ($p<0.05$). These results show that NK cells are not implicated in the therapeutic efficacy of anti-PD-1 against LM7 OS lung metastases.

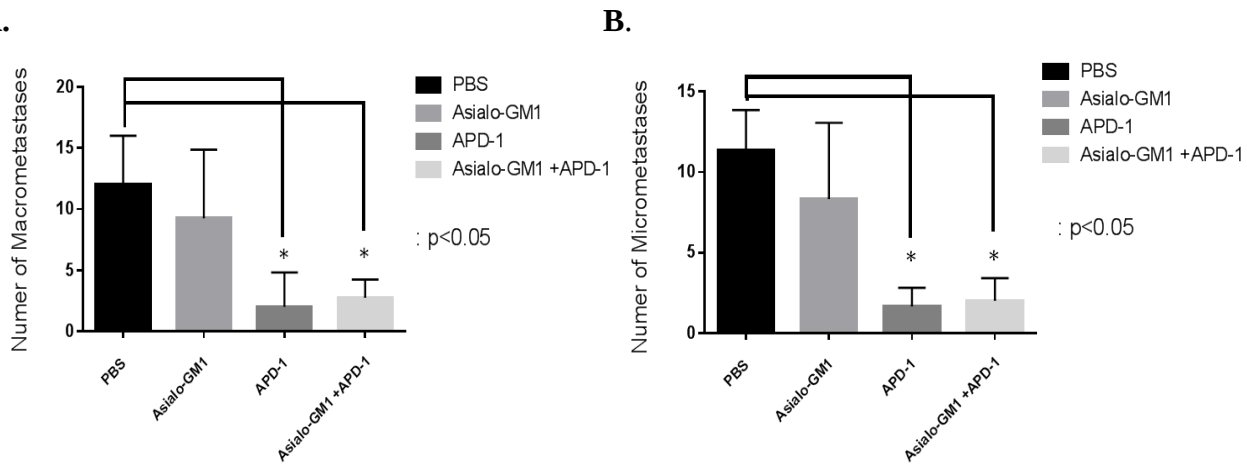

Figure 23. NK depletion did not affect the therapeutic effect of anti-PD-1 against LM7 OS lung metastases.
Mice with established micrometastases were administered either PBS, anti-asialo-GM1 (50 µl, twice weekly), anti-PD-1 (intraperitoneally 200 µg/mouse), or combination of anti-asialo-GM1 and anti-PD-1 (200 µg/mouse) for 5 weeks. Lungs were excised and the number of OS lung macrometastases **(A)** and micrometastases **(B)** were counted. Statistical analysis was performed using student's t-test (*: $p< 0.05$).

Summary

In this chapter, we investigated whether mouse NK cells are crucial in the anti-metastatic responses of anti-PD-1 in LM7 OS model. To answer this question, we transiently depleted NK cells using a widely known drug, anti-asialo-GM1, followed by treatment with anti-PD-1 to assess the number of OS lung metastases formed. We discovered that the therapeutic effect of anti-PD-1 was not compromised in NK depleted mice. The decrease in

the number of metastases formed on anti-PD-1 treatment after NK depletion remained the same as those formed on anti-PD-1 alone. Our data showed that NK cells are not the predominant cell types mediating the effects of anti-PD-1 against OS lung metastases. Additionally, anti-asialo-GM1 treatment by itself did not affect the number of metastases formed, which means that systemic NK cells did not play a role in OS lung metastases growth.

We earlier demonstrated that there was an increased infiltration of mouse NK cells in OS lung tumors after anti-PD-1 treatment. Although there was increased migration of NK cells at the lung tumor site, NK cells were not the crucial effector cells playing the role in the responses towards lung metastases. This implies that additional mechanisms such as activation of macrophages maybe involved in rejection of metastases on anti-PD-1 treatment in our model. Recent studies show that macrophages can be reprogrammed to induce cytotoxicity against tumors. Pahl *et al*. showed that L-MTP-PE activated M1 macrophages exhibited direct cytotoxicity towards OS cells through direct phagocytosis as well as through soluble factors released by activated macrophages (167). Another study using combination of IL-2 and IL-15 gene transfer in a human small-cell lung cancer model showed that tumor rejection in nude mice occurred through the direct activation of macrophages, without the involvement of NK cells (176). On the basis on our data, we predict the involvement of macrophages in the anti-tumor responses of anti-PD-1.

The cross-talk between NK cells and macrophages is complex and still being investigated. The cytokine mileu can influence the NK cell function and their killing capacity. There is a possibility that mouse NK cells may not be involved in direct cytotoxicity of human OS tumor cells, but can release cytokines such as IFN-γ, GM-CSF,

TNF-α, thus causing M1 macrophage activation and killing of M2 macrophages (170, 177). However since NK cell depletion failed to decrease the therapeutic activity of anti-PD-1, we conclude that NK cells do not play an important role in the anti-metastatic effect of anti-PD-1 against OS lung metastasis.

CHAPTER 9

The therapeutic efficacy of anti-PD-1 against OS lung metastases is mediated by macrophages

Rationale

The role of macrophages in the anti-tumor responses of PD-1 checkpoint inhibitors has not been investigated till date. In Chapter 6, we found that PD-1 was expressed in macrophages, specifically in OS lung tumors. Also, antibody-mediated PD-1 blockade led to an increased migration of macrophages, particularly classically activated M1 macrophages, which are known to have anti-tumor functionality. In addition, we discovered that mouse NK cells did not directly contribute to the efficacy of anti-PD-1 in our OS nude mouse model. This led us to investigate if macrophages may be independently involved in the therapeutic response of anti-PD-1 against OS lung metastases.

To examine if macrophages play a crucial role in anti-metastatic efficacy of anti-PD-1, macrophage depletion was performed using Clodronate liposomes. Clodrosome has been used as a standard agent for depleting macrophages in various mouse models (178-180). As per our experimental design, we intravenously injected LM7 cells to form micrometastases, and mice were randomly divided in four groups of n=5. The four groups included PBS, Clodrosome (200 µl/mouse., anti-PD-1 (200 µg/mouse) and Clodrosome (200 µl/mouse)+anti-PD-1 (200 µg/mouse). Anti-PD-1 and Clodrosome were both injected intraperitoneally twice weekly. In the combination group, Clodrosome was injected a day prior to anti-PD-1 treatment. Mice were sacrificed 5 weeks after treatment and the lungs and organs were obtained. Flow cytometry and IHC analysis were used to confirm macrophage depletion in spleen and lung tumors respectively. The numbers of OS metastatic lung tumor nodules were counted to assess therapeutic efficacy.

Results

Macrophage depletion using Clodrosome reduces the number of macrophages in the mouse spleen and lungs, with no effect on NK cells

In order to ensure that the macrophage depletion is successful, we injected mice with Clodrosome (200 µl/mouse), twice a week before obtaining the spleen and lungs. Using flow cytometry analysis, we observed a significant decrease in macrophage population ($CD11b^{+}F480^{+}$) as observed by CD11b and F4/80 staining in mice **(Figure 24 A).** Further, Clodrosome treatment had no effect on the number of NK cells, thus ensuring that the depletion was specific to macrophages **(Figure 24 B).**

A.

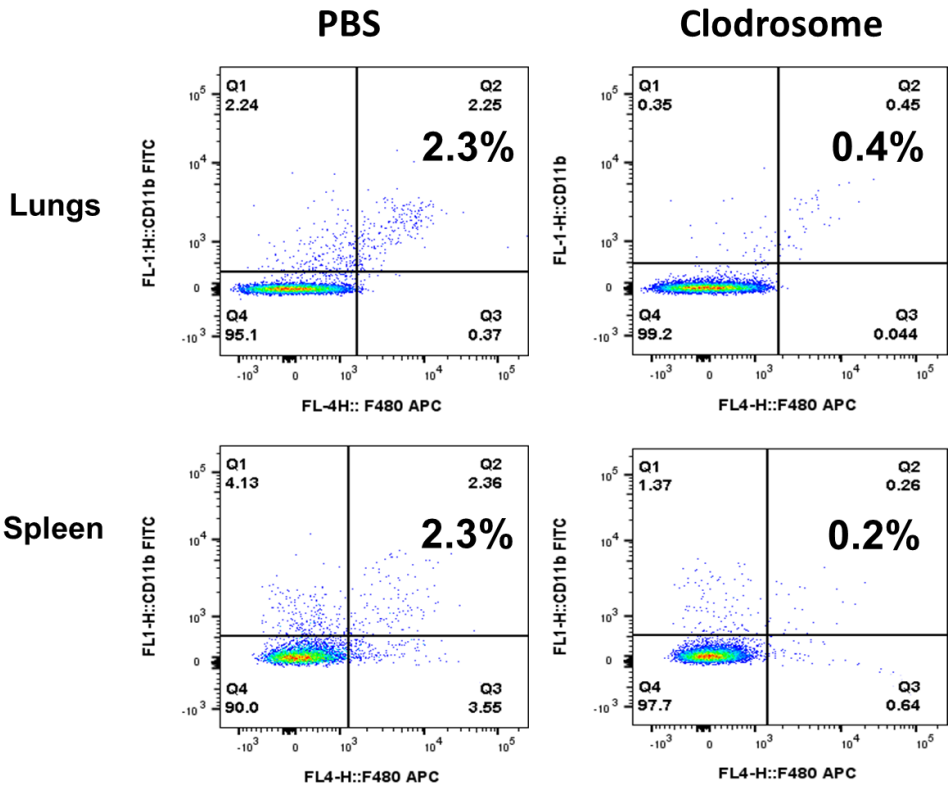

B.

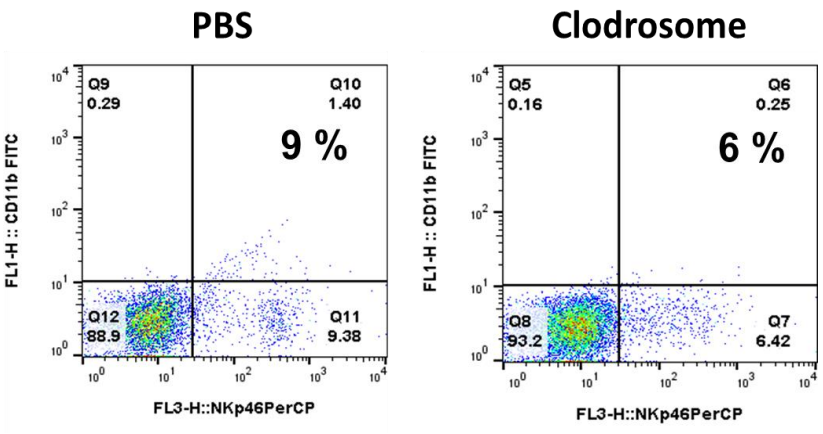

Figure 24. Clodrosome treatment led to a significant decrease in the number of macrophages in spleens and lungs of mice
A. Flow cytometry analysis was performed after obtaining single cell suspensions from spleens and lungs of mice treated with either PBS or Clodrosome (200 µl, twice weekly). Double staining was done using anti-CD11b-FITC and anti-F4/80-APC antibodies; B. NK cells were identified in spleen from mice with or without Clodrosome treatment using anti-NKp46-PerCP or isotype IgG control antibody

Clodrosome treatment before anti-PD-1 impairs the therapeutic efficacy of anti-PD-1 against OS lung metastases

We hypothesized that macrophages may be involved in efficacy of anti-PD-1 in terms of regression of OS lung metastasis. Mice having micro-metastases were depleted of macrophages with Clodrosome followed by anti-PD-1 treatment after 24 hours for 5 weeks. We assessed the effect on the lung metastases by counting the number of macro and micrometastases formed. As shown in **Figure 25**, Clodrosome treatment by itself had no effect on the number of metastases. Anti-PD-1 by itself caused significant decrease in both LM7 macro and micrometastases ($p<0.05$). However, the therapeutic effect of anti-PD-1 as determined by the number of metastases formed was significantly compromised in mice

following macrophage depletion by Clodrosome. These results indicate that macrophages play an important role in anti-metastatic effect of anti-PD-1 in OS lung metastasis.

A. **B.**

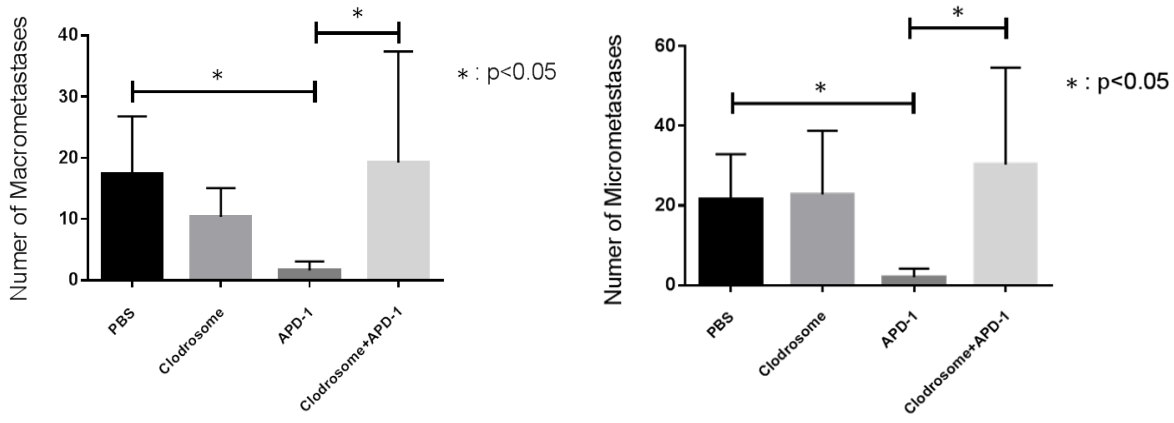

Figure 25. Macrophage depletion using Clodrosome impairs the therapeutic effect of anti-PD-1 against LM7 OS lung metastases.
Mice with established micrometastases were administered either PBS, Clodrosome (200 µl/mouse), anti-PD-1 (intraperitoneally, 200 µg/mouse), or combination of Clodrosome (200 µl/mouse) and anti-PD-1 (200 µg/mouse) for 5 weeks. Lungs were excised and the number of OS lung macrometastases and micrometastases were counted. Statistical analysis was performed using student's t-test (*: $p < 0.05$).

Summary

In this chapter, we investigated if macrophages are important in the anti-tumor response of anti-PD-1 against LM7 OS lung metastasis. We discovered that macrophage depletion using Clodrosome significantly compromised the efficacy of anti-PD-1 against OS lung metastasis. Our findings imply that macrophages are predominantly involved as the effector cells in the anti-tumor responses of anti-PD-1. Further, Clodrosome by itself did not affect the number of metastases, which indicated that systemic macrophages did not play a role in OS lung metastases growth.

Our data correlated with the increased infiltration of macrophages, including M1 macrophage sub-types, in OS lung tumors after anti-PD-1 treatment which we discovered earlier. Previous studies have shown that activated macrophages exhibit cytotoxicity towards OS cells through direct phagocytosis following treatment with agents such as L-MTP-PE (167). In addition, contrary to other cancers, TAMs play an anti-metastatic role in OS, as higher numbers of infiltrating TAMs in pretreatment biopsies of OS patients were found to correlate with better patient survival (24). As TAMs are the immune cells accounting for about 50% of the total solid tumor mass including OS, our results are particularly significant (161, 162). Our human LM7 lung metastasis model is in nude mice that are T-cell deficient. Thus, we can conclude that amongst the immune cell types, macrophages contributed to the anti-metastatic efficacy of anti-PD-1 in our LM7 OS lung metastasis model. Hence, future studies evaluating the role of macrophages in anti-tumor responses to the PD-1 blockade antibodies in the clinical settings are warranted.

CHAPTER 10

PD-1 expression in human OS cell lines

Rationale

Our data revealed that PD-1 was expressed in NK cells and macrophages in nude mice in the OS lung tumors. Although PD-1 was discovered as an inhibitory receptor on immune cells, recent evidence demonstrated PD-1 expression on melanoma cancer cells and its novel implication in melanoma tumorigenesis (181). Since we are using a PD-1 blocking antibody, we investigated if PD-1 receptor is expressed in our OS cell lines. We hypothesize that if PD-1 is expressed on OS cells, anti-PD-1 treatment may have a direct cytotoxic effect causing decreased cell viability.

Hence, we conducted flow cytometry analysis in a panel of OS cell lines such as LM7, KRIB, U2OS, 143B, SAOS-2, C-CH-OSD, CCH-OS-O and MG63.2 for obtaining PD-1 expression. For determining hPD-1 expression on LM7 tumors *in vivo*, single cell suspensions of LM7 lung tumors were obtained and double staining was performed using anti-mCD45 (a pan-lymphocyte marker) and anti-hPD-1 before performing flow cytometry.

Results

Variable levels of PD-1 are expressed in OS cells

To study if PD-1 receptor itself has any potential role in OS, we examined PD-1 expression in OS cell lines. Freshly isolated human PBMCs (peripheral blood mononuclear cells) stimulated by PHA (Phytohaemagglutinin) (20 μg/ml) for 48 hours were used as a positive control. We found a variable expression of PD-1 from 1-15 % **(Figure 26 A and B)**. KRIB, U2OS, 143 B and LM7 cells had the highest PD-1 expression levels within the panel. Our data implicated that PD-1 on the tumor cells may also have a potential role in OS.

A.

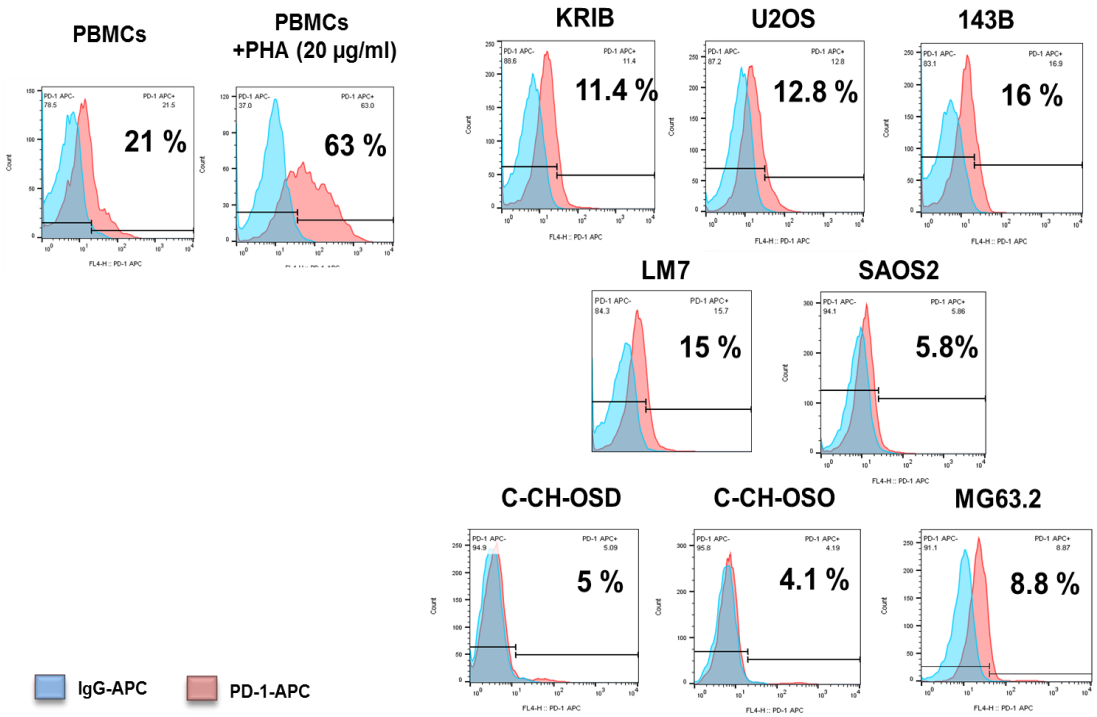

B.

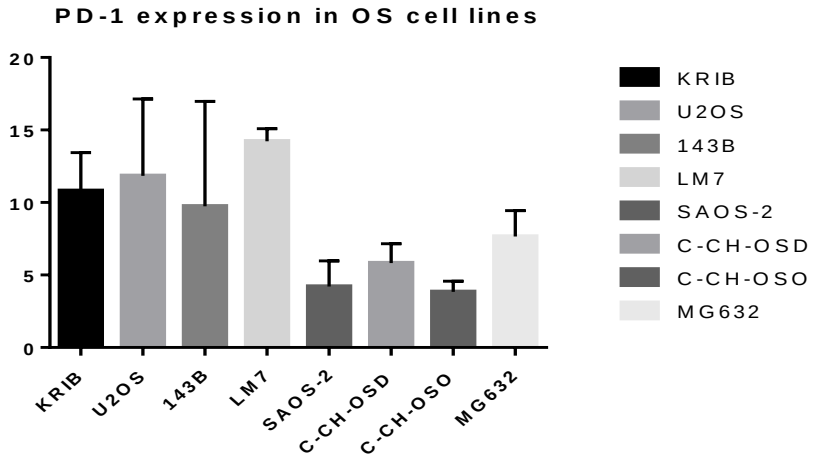

Figure 26. Variable levels of PD-1 are expressed in OS cell lines.
A. Flow cytometry analysis was performed to assess surface PD-1 expression in a panel of OS cell lines including PHA-stimulated PBMCs as a positive control. Staining was performed using either IgG-APC or PD-1-APC antibody for 30 min. Representative flow charts are shown; B. Mean and standard deviation of PD-1 positivity compared to IgG controls as determined by flow cytometry from three independent experiments

PD-1 is expressed in tumor cells from LM7 OS lung metastases and lung tumors

Figure 27 shows that ~4% cells were $CD45^+$ in LM7 OS lung tumors, which are mouse immune cells and were used to exclude the human tumor cells. Total $PD\text{-}1^+$ population was ~9%. $CD45^-PD^+$ population represented LM7 cells tumor cells and 9%-15% PD-1 positivity was observed. Thus, our results showed that there were cells within the LM7 OS lung tumors that expressed PD-1, similar to our *in vitro* findings.

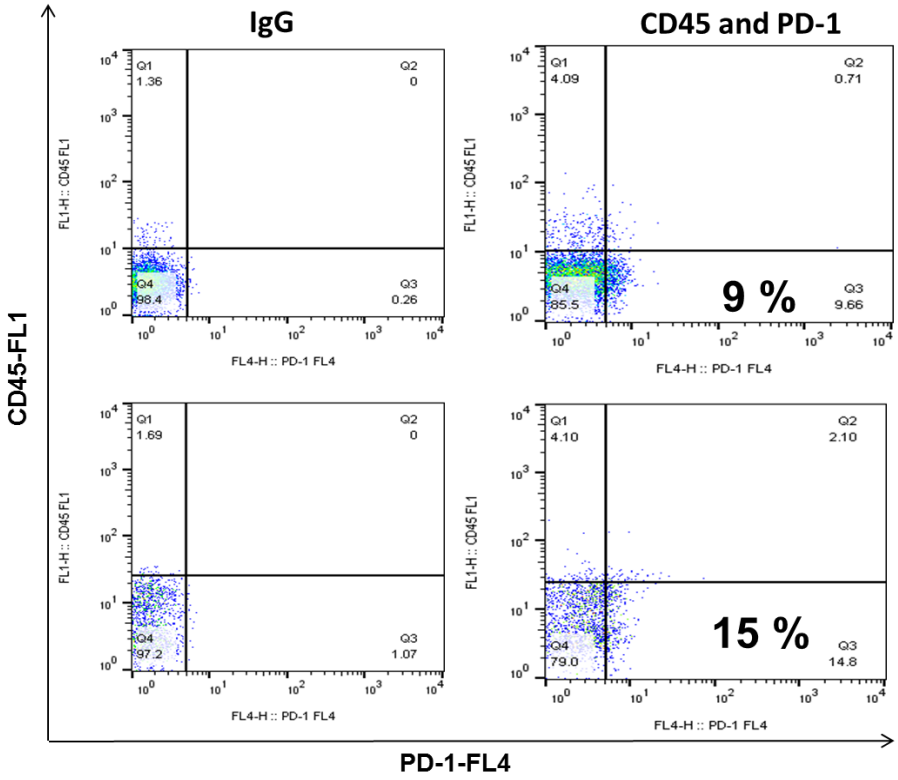

Figure 27. PD-1 is expressed in LM7 OS lung tumor cells.
Flow cytometry analysis was performed after obtaining single cell suspensions from lung tumor nodules of mice. Double staining was done using anti-mCD45-FITC and anti-hPD-1-APC antibodies. Representative flow charts are shown

Summary

We discovered for the first time that PD-1 expression was detected in OS cell lines *in vitro* and OS lung tumors *in vivo*. This is a novel finding as the role of PD-1 receptor in OS cancer cells has not been studied before. It shows that PD-1 is not only an immune-receptor but it may also play a potential tumorigenic role in OS cancer cells. In this context, PDL-1 may bind with PD-1 on cancer cells to activate downstream cancer signaling, thus promoting cancer progression. Previously, PD-1 expressing tumor sub-populations have been described in melanoma cells (11.3-29.5%) as well as melanoma tumors (8.7 %) (181). Similarly, our data showed ~15 % PD-1 positivity in LM7 OS cells and 9-15 % in LM7 lung tumors. Hence, the therapeutic effect of anti-PD-1 as we demonstrated in our *in vivo* LM7 model may be in part due to the PD-1 expression on LM7 OS cells. This highlights the importance of PD-1 receptor on OS cancer cells as potentially interesting independent target for evaluation.

CHAPTER 11

p-Stat3/p-Erk1/2/PDL-1 pathway as a molecular mechanism involved in anti-PD-1 efficacy against OS lung metastasis

Rationale

In Chapter 10, we showed that PD-1 is expressed in the panel of OS cell lines *in vitro.* As we observed an inhibitory effect on LM7 tumor cell proliferation, we hypothesized that anti-PD-1 may exert an effect on by inhibiting signaling in LM7 OS tumor cells. Here, we investigate the signaling pathways that are altered after anti-PD-1 in LM7 tumors *in vivo*. We primarily evaluated PDL-1 expression as well as its key regulators, p-Stat3-703 and p-Erk1/2 (extracellular signal-regulated kinase ½). In addition, p-Stat1, levels were also determined. We also evaluated cleaved caspase-3 protein expression to assess apoptosis.

We assessed PDL-1 expression on LM7 OS lung metastases with or without anti-PD-1 treatment by IHC staining. For *in vivo* experiments, we obtained lysates from tumor nodules of mice treated with anti-PD-1 for 5 weeks to perform western blotting.

Results

PDL-1 expression decreases in OS lung metastases after anti-PD-1 treatment

Figures 28 A and B depict representative images and quantification of PDL-1 staining from LM7 OS metastases of PBS treated mice compared to anti-PD-1 treated mice. We used the antibody against human PDL-1 for staining. We observed that there was a significant decrease in PDL-1 expression on LM7 lung metastases after anti-PD-1 treatment with respect to the PBS controls ($p<0.05$). This implies that blocking PD-1/PDL-1 interaction due to anti-PD-1 could be causing the PDL-1^{+} LM7 cells to die over 5 week treatment, resulting in an overall decrease in PDL-1 positivity.

A.

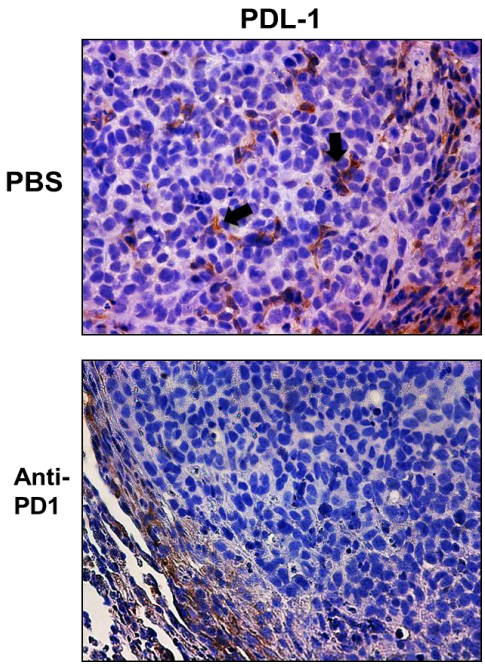

B.

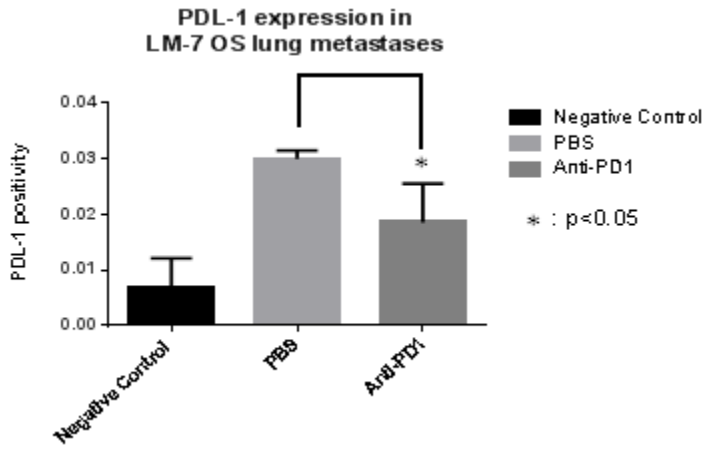

Figure 28. Anti-PD-1 decreased PDL-1 expression in LM7 OS lung metastases.
A. PDL-1staining was performed for in paraffin tissues of LM7 lung metastasis from mice treated with PBS or anti-PD-1 using anti-hPDL-1 antibody. B. Quantification was done using Cell Quest Software and student's t-test was performed, *p<0.05.

PDL-1 and phosphorylation of Erk1/2 and Stat3-705 decreases in lung tumors after anti-PD-1

Figure 29 A and B. depicts that PDL-1 levels were significantly decreased by about 50% on anti-PD-1 treatment in lung tumor nodules compared to PBS controls as determined by western blotting and Image J analysis. This correlated with the IHC data shown above. Since we were interested in delineating the mechanism by which PDL-1 was reduced on anti-PD-1 treatment, we evaluated p-Stat3-705 and p-Erk1/2 levels. We observed that there was a significant decrease in p-Stat3-705 levels (~80%) as well as total Stat3 levels in lung tumors after anti-PD-1 treatment. However, p-Stat1-705 as well as total Stat-1 levels remained unchanged. Further, there was also a significant reduction in p-Erk1/2 levels (~60%) after anti-PD-1 treatment. p-Erk1/2 is an indicator of cell proliferation and p-Stat3-705 is implicated in tumor metastasis and OS cell proliferation (182, 183). This may be an effect of immune cells inducing cell death. Hence, our data implies that the therapeutic efficacy of anti-PD-1 against OS lung metastasis *in vivo* may be due to inhibition of tumor cell proliferation by blocking p-Stat3/p-Erk1/2 and PDL-1 signaling pathways.

A.

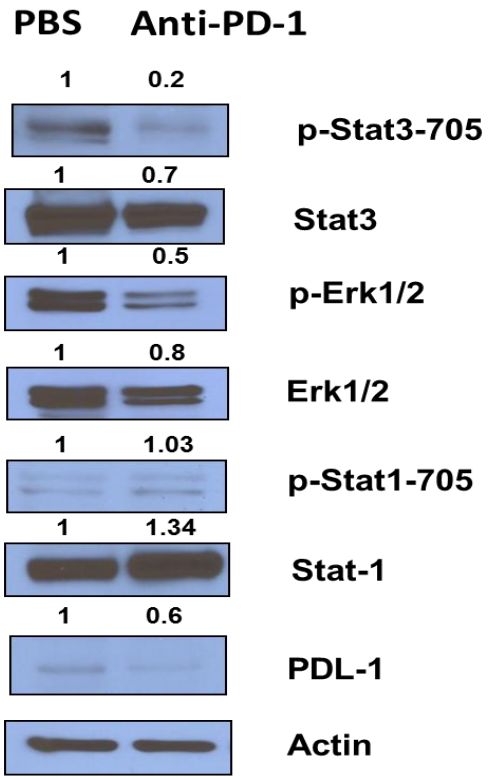

B.

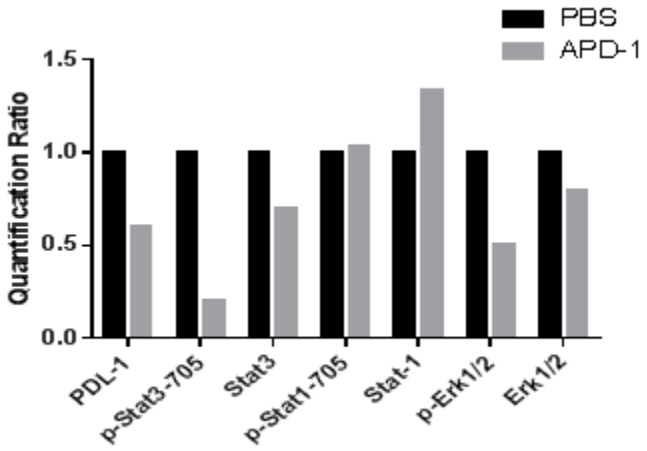

Figure 29. PDL-1, p-Stat3, p-Erk1/2 were decreased in lung tumor lysates after anti-PD-1 treatment *in vivo*.

Lysates were obtained from LM7 lung tumor nodules of mice treated with PBS or anti-PD-1 (200 μg/mouse) for 5 weeks, using RIPA buffer followed by sonication. Western blotting was performed to probe for p-Stat3-705, Stat3, p-Stat1, Stat-1, PDL-1, p-Erk1//2 and Erk1/2 proteins. Actin as a loading control.

Summary

Earlier, we showed that anti-PD-1 treatment resulted in increased infiltration of macrophages and NK cells, possibly leading to increased apoptosis and decreased tumor cell proliferation. In this chapter, we investigated the signaling mechanisms affected by anti-PD-1 antibody *in vivo*. We demonstrated that PDL-1 expression is downregulated on LM7 lung metastases as well as lung tumors after-anti-PD-1 treatment. Since PDL-1 is involved in immune evasion response by binding to PD-1, our data hints to the possibility that anti-PD-1 may be resulting in immune cell activation to cause elimination of PDL-1^{+} LM7 cells and decrease in PDL-1 expression on LM7 tumor cells. PDL-1 expression has been known to be regulated by multiple signaling pathways. Previously, a study showed that PDL-1 expression was significantly upregulated in B-raf inhibitor resistant melanoma cells, due to the increased p-Stat3 as well as p-Erk1/2 levels (184). Here, we discovered that anti-PD-1 blocks p-Stat3 and p-Erk1/2 pathways after *in vivo* anti-PD-1 treatment. Thus, the decrease in PDL-1 expression observed *in vivo* may be likely due to both decreased p-Stat3 and p-Erk1/2.

It is known that p-Stat3 is involved in OS cell proliferation and its overexpression correlates with poor prognosis (183, 185). p-Stat3 and p-Erk1/2 are the markers of poor chemotherapeutic responses in OS patients (182). In addition, p-Stat3 is involved in a number of cellular responses including cell survival, apoptosis, migration, immune cell evasion as well as metastasis (186). Our data demonstrated that anti-PD-1 promoted tumor cell apoptosis *in vivo.* Thus, the enhancement of LM7 tumor cell apoptosis and inhibition of lung metastasis due to anti-PD-1 could be attributed to inhibition of p-Stat3-705 signaling. In addition, the reduced p-Erk1/2 expression corroborates our data of decreased Ki-67 staining

observed in anti-PD-1 treated LM7 lung metastases, indicating decreased tumor cell proliferation.

Our data showed that anti-PD-1 exerted an effect on OS tumor cell signaling *in vivo*. Here, we uncover the novel finding that anti-PD-1 inhibited the p-Stat3/p-Erk1/2 signaling in LM7 OS tumor cells.

CHAPTER 12

Discussion

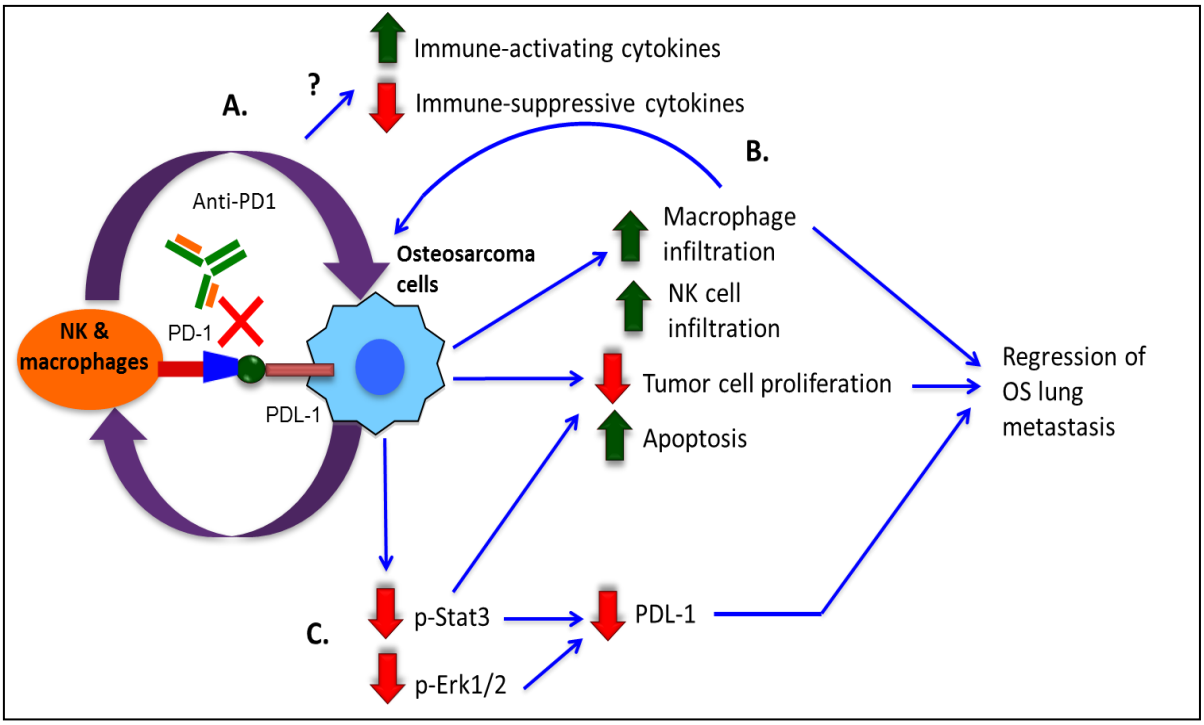

Figure 30. Proposed model of mechanisms leading to regression of OS lung metastasis after PD-1 blockade
A. PDL-1 is upregulated in OS cells. Anti-PD-1 treatment blocks interaction of tumor PDL-1 with PD-1 on NK cells and macrophages in LM7 OS lung tumors**; B.** Anti-PD-1 treatment leads to increased migration of NK cells and macrophages in OS lung tumors. The resulting effect is inhibition of tumor cell proliferation and enhanced tumor apoptosis. Macrophages, but not NK cells are implicated in the anti-metastatic effect of anti-PD-1 in OS; **C.** Anti-PD-1 also led to blockade of the p-Stat3/p-Erk1/2 and PDL-1 pathway, which is involved in proliferation and apoptosis. Anti-PD-1 treatment ultimately leads to regression of OS lung metastasis.

OS presents in about 20% of new patients with aggressive lung metastasis. These patients have a 5-year survival of only 25-30%. (2, 4). The major organ of metastatic spread is the lung and the survival of patients with relapsed OS is also significantly low, as less than 20% of the patients survive (187). Due to the limited therapeutic options, novel targeting therapies need to be investigated for the treatment of OS lung metastasis. Immunotherapeutic approaches have recently shown promise in the treatment of a wide variety of cancers. L-MTP-PE, an activator of macrophages and monocytes, has been the only novel agent that has

demonstrated clinical efficacy in the past two decades. L-MTP-PE resulted in 8% improvement in overall survival of OS patients when combined with standard chemotherapy (12-14).

Previous data from our lab showed that aerosol IL-2 in combination with NK cell therapy showed a higher efficacy against OS lung metastasis than either therapy alone. (34). However, complete elimination was not observed and metastasis disease relapse was seen as mice continued to die after combination therapy (35). Hence, we hypothesize that resistance to the therapy may be due to the immunosuppressive responses in the OS lung microenvironment. OS is a cancer characterized by high genomic instability, with several known high-frequency mutations like Tp53, Rb1, as well as ATRX , DLG2, PTEN and mTOR (188). In addition, it was recently discovered that OS tumors exhibit multiple re-arrangements, kataegis (hypermutations associated with structural variations) and Chromothripsis (chromosomal shattering) in certain cases (188-190). Owing to this, OS can be classified as an immunogenic tumor type. Overexpression of PDL-1 on the tumors has been known as one of the mechanisms resulting in immune escape by binding to the immune-inhibitory receptor, PD-1 present on immune cells.

Our study revealed that PDL-1 is expressed in OS cell lines and OS lung metastases from patient samples, validating its importance in OS. The findings presented in this study showed that blocking PD-1-PDL-1 interactions using PD-1 checkpoint inhibitor resulted in inhibition of OS lung metastasis. Although PD-1 blockade has shown efficacy in various tumor types, our study is the first to demonstrate the efficacy of anti-PD-1 against OS lung metastasis. Most of the previous studies have focused on the role of T-cell immune activation after blockade of PD-1 pathway showing T-cells to be important in anti-tumor responses. Our

findings demonstrate for the first time that anti-PD-1 led to increased macrophage infiltration as well as activation of anti-tumor M1 macrophage sub-types. Our data showing PD-1 expression on macrophages and NK cells in OS lung tumors is novel and underlines the role of PD-1 as a therapeutic target in OS lung metastasis. In our model, the PD-1 regulatory signal is shut-off on the immune cells at the tumor site, thus potentially triggering a cytokine cascade within the tumor-immune cell microenvironment. The resident NK cells immune cells may secrete immune-activating cytokines like IL-2, IFN-γ, and macrophage inflammatory protein (MIP)-1α, resulting in macrophage activation (168). This may lead to release of cytokines from activated macrophages like TNF-α and IL-6 (8). Activated NK cells may lead to increase in the number of M1 macrophages, and spare the M2 macrophages (177). On the contrary, immunosuppressive cytokines secreted by the OS tumor cells such as TGF-β and IL-10 may be decreased, thus shifting the balance towards an activated immune response. This may attract more infiltrative NK and macrophages at the localized tumor site, thus increasing their migration and proliferation, and enhanced anti-tumor function.

In addition, we demonstrate that PD-1 is also expressed in OS cell lines, which is an innovative finding implying that PD-1 can be considered as a potential target not only with respect to immune cells but also tumor cells by themselves. We also found a unique mechanism that anti-PD-1 directly affected the p-Stat3/p-Erk1/2 signaling pathway on OS tumor cells, resulting in increased apoptosis and decreased cell proliferation. Overall, our results indicate that PD-1/PDL-1 signaling axis is a promising potential therapeutic target for OS lung metastasis.

PDL-1 expression in OS

A large body of evidence shows that PDL-1 is overexpressed in a number of different cancers like melanomas, renal, pancreatic and non-small cell lung cancer (72-76). PDL-1 upregulation has been described at the transcript level in OS and PDL-1 expression has been described in OS metastasis using immunofluorescence (103, 111). Here, we investigated the expression of PDL-1 at the protein level in OS cell lines and OS lung metastases from patients using DAB staining method for paraffin-embedded tissues and a specific anti-human PDL-1 antibody.

Our *in vitro* findings revealed that > 90% PDL-1 positivity was seen in 3 out of 8 cell lines, > 50% PDL-1 positivity was seen in 2 out of 8 cell lines and 3 out of 8 cell lines showed < 25% positivity. Thus, PDL-1 expression was variable in our OS cell line panel. Further, our data for total PDL-1 protein levels goes along with the flow cytometry data, indicating that equivalent levels of intracellular PDL-1 are cycled back to the cell surface in different OS cell lines. Thus, the variability in PDL-1 expression is not due to differences in protein localization at the membrane versus cytoplasm in OS cell lines. A recent study also showed variable PDL-1 expression in a large set of melanoma cell lines, but did not find any association of PDL-1 expression with the oncogene-driver mutations (117).

The variability in PDL-1 expression in between the various cell lines could be possibly due to complex genomic variations in the OS cell lines. Recent evidence using whole-genome sequencing showed that 56% OS patients had mutations in Rb and Tp53 pathway and 24% possessed alterations in PI3-K/mTOR pathway, including PTEN mutations (191). Since PDL-1 expression has been known to be upregulated by PI3-K-Akt-mTOR pathway alterations as well as PTEN deletions in non-small cell lung cancer and

glioblastoma, it is a possibility that differences in PDL-1 expression could be co-related with mutations in these pathways (67, 192, 193).

Since PDL-1 expression was variable in OS cell lines, it would be interesting to compare the *in vivo* therapeutic responses of anti-PD-1 in LM7 model (intermediate-high PDL-1 expression) using another cell line model such as C-CH-OSD, which showed low PDL-1 expression. However, as shown in earlier studies, there is a possibility that there may be no correlation as the efficacy of anti-PD-1 antibodies was found to be independent of PDL-1 expression (86, 87). In addition, *in vivo* PDL-1 expression levels could be modulated by the tumor microenvironment. We also showed for the first time that PDL-1 was overexpressed in lung metastases from OS patients with IHC staining using paraffin-embedded tissues. PDL-1 positivity was observed in (~80 %) in 8 out of 10 patients. Our data are almost similar to those from another group where they demonstrated PDL-1 expression in in 75% of OS metastatic patients using immunofluorescence assays (103). The staining with the PDL-1 antibody we used was superior to this study as we could detect PDL-1 in OS primary tumors as well. PDL-1 expression levels and pattern was variable amongst the different OS patient tissues and an average of ~30 % PDL-1 positivity was observed. Since OS tumors are highly heterogeneous and have numerous sub-types, it can be anticipated that PDL-1 expression levels are variable. Our data of variable PDL-1 expression go along with those from several studies in other cancers like squamous cell carcinoma (5-60%), non-small cell lung cancer (35- 95%) and melanoma (40-100%), where similar ranges were observed in paraffin tissue samples (71, 74, 194-197). Our results are also similar to those discovered recently in primary OS tumor samples, where a variable range of PDL-1 expression was

observed, with majority of tumors showing <25% staining (112). Here, they analyzed only primary tumors and not metastases.

Future studies entailing staining for a larger set of OS lung metastases will enable the co-relation of PDL-1 expression with OS sub-types and patient parameters like stage, overall survival and metastasis-free survival. Since we also observed PDL-1 expression in OS primary bone samples, it would be interesting to look at PDL-1 expression from matched patient samples from primary and lung metastases to examine the differences in PDL-1 expression. Currently, patients with as low as >1% PDL-1 positivity have shown better clinical responses towards anti-PD-1 antibodies in non-small cell lung cancer (126). Thus, our data of PDL-1 expression in OS is of translational significance as it will provide the basis for the design of clinical trials to pre-select the potential patients that may respond to PD-1/PDL-1 targeting agents.

Therapeutic efficacy of anti-PD-1 against OS lung metastases

Recent investigations show that PD-1/PDL-1 checkpoint inhibitors induce tumor regression in pre-clinical models such as melanoma, colon cancer and pancreatic cancer when used alone or augment the effect of other immunotherapies such as adoptive T-cell therapy or CTLA-4 antibodies when used in combination (60, 76, 127-130). Most of these studies evaluating PD-1 targeting agents have focused on the activation of T-cell function and infiltration as a mechanism resulting in anti-tumor responses. Here, we discovered that anti-PD-1 caused regression of OS lung metastases, tumor cell apoptosis and decreased tumor cell proliferation, using a human OS xenograft *nude* mouse model **(Figure 7, 8 and 9).** We observed that the number of LM7 OS lung macro-metastases (visual) and micro-metastases (microscopic) was significant decreased in the anti-PD-1 treatment mice group as

compared to the PBS treated controls ($p < 0.05$) **(Figure 7).** The dose of anti-PD-1 which was administered was comparable to that used for tumor models in other studies (60, 108, 109). Another crucial finding from our studies was that the *in vivo* dose of anti-PD-1 administered did not cause any significant toxicity in nude mice. **(Figure 11, 12, 13).**

Due to the significant homology between mPD-1 and hPD-1 receptor (66%) as well as mPDL-1 and hPDL-1 (77%), the binding affinities of mPD-1 to mPDL-1 and mPD-1 to hPDL-1 are equivalent (52, 131, 132). Hence, in our model, anti-murine PD-1 antibody likely exerts therapeutic efficacy due to blockade of binding of mPD-1 on endogenous mouse NK cells and macrophages with hPDL-1 on LM7 tumor cells. In addition, anti-murine PD-1 antibody may also bind to hPD-1 on LM7 cells and exert a direct effect by preventing the binding to hPDL-1 on the tumor cells. Our data are in congruence with a recent study, which showed that PDL-1 blockade resulted in fewer metastases in a metastatic osteosarcoma mouse model, thus reiterating the importance of PD-1/PDL-1 signaling in OS (103).

In addition, we demonstrate that anti-PD-1 led to enhanced apoptosis, decreased tumor cell proliferation and decrease in PDL-1 expression on tumors. Consistent with our data, studies by Akbay E. A. *et al*. and Chen Y. *et al*. have also previously reported that anti-PD-1 decreased lung tumor growth through increased apoptosis (198, 199). Here, in addition to induction of apoptosis, we also show an inhibitory effect on tumor cell proliferation. It has also been shown that PDL-1 correlates with proliferative potential or Ki-67 expression of tumor cells (124). Thus, the decrease in tumor PDL-1 expression along with Ki-67 staining is likely due to an increase in death of tumor cells expressing PDL-1 after anti-PD-1 treatment. We also elucidated that inhibition of tumor cell proliferation and apoptosis induction were mechanisms involved in the therapeutic efficacy of anti-PD-1. Here, we used a PD-1

blocking antibody for our study. However, anti-PD-1 antibodies like Nivolumab and Pembrolizumab are currently showing promising results clinically in other cancers (101, 102). Our findings are clinically relevant and they indicate that anti-PD-1 antibodies may show promise in the treatment of patients with OS lung metastases.

Anti-PD-1 enhances NK and macrophage infiltration in OS lung tumors

Most of the studies evaluating PD-1 blocking agents have focused on the role of T cells in the anti-tumor efficacy of anti-PD-1. PD-1 has been known to be upregulated on T cells in the tumors, which is responsible for T-cell dysfunction and immunosuppression (60, 103, 151). PD-1 upregulation on NK cells and macrophages has been shown in certain inflammatory conditions like viral infection and sepsis (152, 153, 156).

Our data provide the first evidence that PD-1 is expressed on macrophages and NK cells in the metastatic tumors. We found that PD-1 is upregulated on NK and macrophages in OS lung tumor metastatic sites as opposed to those in the spleen **(Figure 14).** This implies that the function of NK cells and macrophages is suppressed in the OS lung metastasis tumor microenvironment. Since we have demonstrated that PDL-1 is overexpressed on OS tumor cells, PD-1 on NK cells and macrophages may be binding to the PDL-1 on the tumor cells resulting in suppression of anti-immune response in this model. We further show that PD-1 blockade caused an increase in both NK and macrophage infiltration in the OS lung tumors in contrast with peripheral immune organ like spleen **(Figure 16 and 17).** Our data are novel as we are the first to uncover that anti-PD-1 can lead to an increase in the number of NK cells and macrophages in the OS lung tumors, which ultimately result in apoptosis and reduced number of OS metastases. It has been found that extrathymic T cell-subset population increases in nude mice after 3-4 months of age (200). However, since we used young (4-

week old) nude mice in our study, the contribution of T cells in anti-PD-1 responses can be regarded as insignificant. In addition, we also demonstrated that anti-PD-1 induces the polarization of pro-tumorigenic M2 to anti-tumor M1 macrophages. Previously, Pahl, J. H. *et al.* has illustrated the role of anti-tumorigenic effect of M1 macrophages towards osteosarcoma cells after the treatment of M1 macrophages with L-MTP-PE and IFN-γ (167). The potential cytokines that may lead to increase in the ratio of M1 to M2 include increased levels of IFN-γ, TNF-α, MIP-1α and GM-CSF (increase in M1 macrophages) and decrease in the levels of CSF-1, IL-4, IL-13, IL-10 and TGF-β (decrease of M2 macrophages) (201).

Similar to TAMs, anti-tumor N1 neutrophil sub-types and pro-tumorigenic N2 sub-types have been described (202). PD-1 expression on neutrophils as well neutrophil sub-types has not yet been investigated in tumor types. Since we are using the nude mouse model, it will be interesting to assess PD-1 expression on neutrophils in OS lung tumors and the role of neutrophils in anti-PD-1 responses. PDL-1 is expressed on neutrophils in conditions like hepatocellular carcinoma and sepsis, which causing T-cell suppression and PD-1 targeting agents have been shown to enhance the anti-tumor neutrophil function (203, 204). PDL-1 expression on neutrophils in OS lung metastases and the effect of anti-PD-1 antibody maybe evaluated in the future.

Recently, another group showed that PDL-1 blockade can lead to restoration of T cell function in a metastatic OS mouse model. However, the mice died due to incomplete T-cell response because of other inhibitory checkpoints like CTLA-4 (103). Our data is unique as this would entail targeting the PD-1 receptor expressed on immune cells, thus inducing the immune responses from both innate and adaptive immune system, which may result in better responses as opposed to targeting PDL-1 on the tumors. However, in this regard, it will be

crucial to study the effect of anti-PD-1 in an immunocompetent mouse model to understand the role of NK and macrophages in the presence of T cells.

Although anti-PD-1 increased the number of NK cells and macrophages at the OS lung tumor sites, we determined that mouse NK cells did not play a major role in the therapeutic efficacy of anti-PD-1. Depletion of NK cells using anti-asialo-GM1 in presence of anti-PD-1 showed similar efficacy as anti-PD-1 by itself (**Figure 22)**. Thus, additional mechanisms such as activation of macrophages maybe involved in the rejection of metastases on anti-PD-1 treatment. Studies using immunotherapeutic agents like L-MTP-PE and IL-2/IL-15 have revealed that macrophages can be directly activated independent of NK cells, resulting in phagocytosis of cancer cells (167, 176). Thus, NK cells do not independently have anti-tumor functions and are not involved in the therapeutic response of anti-PD-1 towards OS lung metastasis.

Macrophages may play anti-tumor functions through a variety of downstream effector mechanisms. A previous study by Buddingh *et al*., 2011 revealed that TAMs play an anti-metastatic role in OS, as higher numbers of infiltrating TAMs in pretreatment biopsies of OS patients correlated with better patient survival (24). It has also been shown that L-MTP-PE treatment resulted in activation of M1 macrophages, which released soluble factors such as tumor necrosis factor (TNF-α), IL-6 and IL-1β, resulting in anti-tumor effects against OS cells (167). Certain chemokines such as Macrophage-inflammatory protein-1α (MIP-1α), Monocyte chemoattractant protein-1 (MCP-1) may also be released by macrophages as observed in IL-12/IL-15 gene transfer study (176). Activated macrophages may result in killing of cancer cells ultimately through phagocytosis. Phagocytosis-mediated killing by macrophages may be due to the toxic reactive oxygen species or the induction of enzyme

inducible NO synthase (iNOS), which results in NO (Nitric Oxide) production (163). Macrophages exert their cytotoxic functions against tumor cells through the effector molecule, NO (205). Increased iNOS and NO has been associated with decreased tumor growth and metastasis in mouse tumor models (176, 206).

PD-1 expression in OS

PD-1 has been primarily studied as an inhibitory receptor expressed on immune cells like T cells, B cells, natural killer cells, monocytes on activation (44). As we were exploring the therapeutic effect of a PD-1 blocking antibody in this study, we also investigated whether PD-1 is expressed on OS cell lines. Interestingly, we discovered that PD-1 is expressed on all OS cell lines and that variable levels of PD-1 expression were observed **(Figure 26).** We also found expression of PD-1 in a sub-population of LM7 tumor cells *in vivo* **(Figure 27).** In support of our results, recent evidence shows that PD-1 is expressed by melanoma cell lines (181). Our data implies that besides the PDL-1 expression on OS cells, PD-1 expression by itself on OS cells can also be a potential druggable target.

Our findings of PD-1 expression led us to investigate if PD-1 has any role in proliferation and viability of LM7 OS cells. Treatment of anti-PD-1 resulted in a significant decrease in cell viability after 48 and 72 hours **(Appendix Fig A1).** Our data indicated that in addition to its effect on immune responses, the therapeutic activity of anti-PD-1 maybe mediated by directly binding to PD-1 on LM7 cells, thus preventing the ligation with PDL-1 on OS tumor cells themselves. Considering that PD-1 is expressed in *in vivo* tumors, the therapeutic effect of anti-PD-1 in our *in vivo* model could be due to the dual effects of immune cell (macrophage) infiltration as well as the direct cytotoxic effect on the LM7

tumor cells. Here, anti-PD-1 may prevent the ligation of tumor PD-1 with PDL-1 on tumor cells as well PDL-1 on host immune cells, which remains to be distinguished.

Our results are novel and provide a new mechanism of PD-1 targeting agents in OS. Considering PD-1 expression in OS cell lines, the assessment of PD-1 expression on tumor cells in OS patient lung metastases is also warranted. PD-1 expression on tumors, in addition to PDL-1 expression may provide relevant information for selection of patients who may respond to PD-1 targeted therapies.

Anti-PD-1 blocks p-Stat3/p-Erk/PDL-1 pathway in OS

Based on PD-1 expression in LM7 cells and tumors, we explored the effects of anti-PD-1 on downstream signaling pathways in LM7 cells *in vitro* and LM7 tumors *in vivo*. We found that anti-PD-1 treatment downregulated p-Stat3-705, p-Erk1/2 and PDL-1 protein levels in the *in vivo* LM7 tumors **(Figure 29)**. In addition, to complement our *in vivo* data, we also found that anti-PD-1 led to decreased expression of p-Stat3-705 and p-Erk1/2 following *in vitro* anti-PD-1 treatment **(Appendix Figure A2)**. As PDL-1 has shown to be regulated by p-Stat3 and p-Erk1/2, which are upstream of PDL-1 in B-raf inhibitor resistant melanoma cells, the decrease in *in vivo* PDL-1 expression may be due to blockade of both p-Stat3 and p-Erk1/2 (184). However, contrary to the *in vivo* setting, PDL-1 levels increased following *in vitro* treatment with anti-PD-1, which may be due to the lack of immune cell interactions or alternative feedback mechanisms controlling PDL-1 expression. p-Stat3 has been shown to be involved in OS cell proliferation and other functions like prevention of apoptosis, migration, immune cell evasion and metastasis (183, 185, 186, 207). Also, p-Stat3 overexpression has been reported to be co-related with poor prognosis and p-Stat3 and p-Erk1/2 have been associated with poor chemotherapeutic responses in OS patients (182,

183). Hence, our data implies that the therapeutic efficacy of anti-PD-1 against OS lung metastasis as well as increased tumor cell apoptosis could be attributed to the inhibition of p-Stat3-705 signaling.

We interpret our data to mean that anti-PD-1 caused inhibition of downstream p-Stat3 and p-Erk1/2 signaling pathways on LM7 cells. A recent study by Kleffel S *et al*. reported that PD-1 is expressed on melanoma cells and that PD-1 blockade led to reduced tumor growth by targeting mTOR pathway in melanoma cells in addition to its effect on activating immune cell responses (181). Our findings provide a new mechanism of PD-1 targeting agents with respect to the blockade of p-Stat3/p-Erk1/2 signaling in OS both *in vitro* an *in vivo* and the resulting inhibitory effect on proliferation and induction of apoptosis.

CHAPTER 13

Future Directions

Mechanism/s of PDL-1 regulation in OS

PDL-1 has been known to be regulated by both intrinsic and adaptive mechanisms (66) Our results indicate that PDL-1 is variably expressed in OS cell lines and OS metastatic lung patient samples. This implies that PDL-1 is constitutively expressed, due to intrinsic mutations, in addition to the adaptive mechanisms existing in the patient tumor microenvironment. It was previously demonstrated that PDL-1 expression has been associated with PTEN deletion and activated PI3-K/Akt pathway in glioblastoma (67, 192, 193). To study the mechanism of regulation of PDL-1 in OS, further experimentation is necessary. Since OS is a cancer with high mutational load, the correlation of PDL-1 with frequently occurring mutations such as mutations in p53, Rb, PTEN, PI3-K/Akt, mTOR pathway can be assessed. In cell lines, mutational analysis could be performed by Sanger sequencing for OS cell line panel and then PDL-1 expression may be compared in different cell lines to evaluate if any co-relation exists with any of the mutations. Also, RNA expression from OS TCGA (The Cancer Genome Atlas) database can be obtained to assess the correlation of these genes or other pathway aberrations to PDL-1 positivity in tumors. In our study, LM7 cells are p53 null, but showed PDL-1 positivity. Hence, as shown in **Table 4**, PDL-1 expression in the available OS cell line panel did not correlate with p53 status in OS cell lines.

PDL-1 expression has been shown to be upregulated by cytokines like IFN-γ, which then suppresses the activation of T cells (70, 71). In order to assess such adaptive mechanisms that may regulate PDL-1 overexpression in patient samples, IHC staining may be performed for PDL-1 tumor expression and macrophage (CD68) or NK cell (CD56) infiltration markers in a large OS lung metastases patient TMA followed by statistical co-

relation analysis. This will provide an insight if PDL-1 expression on tumors can be correlated with increased immune cell infiltration in patients with OS lung metastases.

Our data showed that PD-1 blockade resulted in downregulation of p-Stat3 and PDL-1 expression in our *in vivo* OS model. To assess the translational significance of these findings, staining of p-Stat3-705 may be performed in OS lung metastases, from pre-treatment and post-treatment biopsies of patients receiving anti-PD-1. Correlation studies maybe performed for p-Stat3 expression and clinical outcomes in response to anti-PD-1 treatment in metastatic OS patients. This can futuristically help to select patients with that may be likely to respond to the treatment with PD-1/PDL-1 blockade, which is an unanswered question till date.

Table 4. p53 status in OS cell lines

Cell Line	p53 status	PDL-1 Status
KRIB	Kras mutant, p53 wild-type	High
143 B	p53 wild-type	High
U2OS	p53 wild-type	High
LM7	p53 null	Intermediate
SAOS-2	p53 null	Intermediate
C-CH-OSD	p53 Mutant	Low
C-CH-OSO	p53 Mutant	Low
MG63	p53 wild-type	Low

Therapeutic Efficacy of PD-1 blockade in immunocompetent, immunocompromised and PD-1 knockout mouse models

Our work demonstrated that anti-PD-1 caused regression of OS lung metastases in mice in a human OS xenograft nude mouse model. We also observed that there was increased infiltration of mouse NK cells and macrophages in OS lung tumors, although the efficacy could not be attributed to the NK cells by themselves. However, the limitations of this model are that we cannot study the contribution of macrophages and NK cells to the therapeutic efficacy in presence of T cells. Recently, a study investigated the effects of blocking PDL-1 using a mouse OS metastatic model, and showed decreased tumor burden due to increased infiltration and activation of CTLs (103). However, no investigations were performed to see whether NK cells and/or macrophages also contributed to the therapy responses. Thus, it will be interesting to study the effect of anti-PD-1 antibody using a BALB/c OS lung metastasis mouse model. For this purpose, a mouse metastatic osteosarcoma cell line K7M3 would be injected to establish micro-metastases (5-10 days), followed by treatment with anti-PD-1 (intraperitoneally 200 μg per mouse) or PBS for 5 weeks. After sacrificing the mice and extracting the lungs, the number of lung metastases formed will be counted, in addition to tumor cell apoptosis, to ascertain the therapeutic efficacy in this model. Also, T cell, macrophage and NK infiltration will be assessed to compare the individual contribution of immune cells.

Our results demonstrated a unique finding of PD-1 expression on the LM7 cells. Thus, in order to assess the contribution of therapeutic efficacy of anti-PD-1 by PD-1 blockade of tumor cells, independent of that attributed due to PD-1 blockade of macrophages or NK cells, immunocompromised NSG mice could be used. NSG mice are NK cell, T cell

deficient and also have inactivated macrophages. Similar schema for LM7 injection and anti-PD-1 treatment will be followed. Thus, if PD-1 on OS cells is involved in proliferation and metastasis, anti-PD-1 treatment would show a significant therapeutic effect in NSG mice, independent of effects of immune system activation. Similarly, to eliminate the contribution of host PD-1, PD-1 (-/-) mice which have been crossed with BALB/c background could be utilized (208). Efficacy of anti-PD-1 in PD-1 (-/-) mice compared to PD-1 wild-type animals will provide information of the effective contribution of PD-1 expression on LM7 OS tumor cells.

To prove that PD-1 by itself induces metastasis, stable PD-1 overexpression may be conducted in LM7 cells using lentiviral vector constructs followed by administration in NSG mice to examine if there is accelerated metastasis due to PD-1 on OS tumor cells. Further, treatment with anti-PD-1 may be performed to assess if there is reduced metastasis formation in PD-1-overexpressing LM7 group versus vector control group in NSG mice.

PD-1 in peripheral blood of OS patients

In our study, we found that PD-1 is expressed on NK cells and macrophages in the OS lung tumors in mice. These findings support our hypothesis that PD-1 on the immune cells of innate system plays an important role in immunosuppression in OS lung metastasis. Recently, it was shown that there were more PD-1^+ immune cells in PDL-1 positive OS primary tumors than those without PDL-1 expression (112). Thus, in order to provide the translational context of our findings, PD-1 expression on NK cells and macrophages in OS lung metastases from patients may be explored. For this purpose, double immunofluorescence staining for PD-1 and CD56 as well as PD-1 and CD68 may be performed using paraffin-embedded OS lung metastases samples.

Our results also lead us to explore PD-1 expression on NK cells and macrophages in the peripheral blood from OS lung metastases patients. A study by Zheng W *et al*. showed that PD-1 is important in progression of OS and that higher PD-1 levels on $CD4^+$ T cells in blood were found with patients with OS metastasis (209). Earlier studies in renal cancer as well as multiple myeloma have also found peripheral PD-1 expression to be elevated in immune cells like monocytes, NK cells as well as T cells and that the PD-1 expression co-related with the stage of the disease (154, 210). Hence, in order to assess PD-1 expression in immune-cell subsets, blood samples will be obtained from multiple healthy donors as well as from OS patients with lung metastases and primary tumors. Purified peripheral blood mononuclear cells (PBMCs) will be isolated by Ficoll-plaque separation followed by staining with NK cell marker (CD56) and macrophage marker (CD68) and M1 (CD86) or M2 (CD163) markers. Statistical analysis will be performed to assess the co-relation of PD-1 expression with the stage of disease.

Role of PD-1 expression in OS cells

Our data of PD-1 expression in OS cell lines, and the effects on p-Stat3/p-Erk1/2 downstream signaling implicate a potential tumorigenic role of PD-1 in OS cells. Since we used anti-murine blocking PD-1 antibody, we may use anti-human PD-1 blocking antibody to evaluate cytotoxicity. These findings can be confirmed using genetic knockdown by PD-1 shRNA's to observe the effects on cytotoxicity, apoptosis and downstream signaling. Stable shRNA knockdown LM7 cells will be generated using lentivirus and maintained in appropriate antibiotic. MTT assays for cytotoxicity and Annexin-V staining assays for apoptosis will be performed. Also, in the context of PD-1 downstream signaling, it will be crucial to further address the mechanism by which PD-1 blockade inhibits the p-Stat3 and p-Erk1/2 downstream signaling pathways. Since, PD-1 is a transmembrane receptor and functions through phosphorylation of ITIM and ITSM motifs present within the cytoplasmic domain, site directed mutagenesis could be used to create constructs with inactivating point mutations in tyrosine sites (Y225F/Y248F) followed by transduction in OS cells. Thus, we could assess the p-Stat3 and p-Erk1/2 protein levels, proliferation and cell growth in Y225F/Y248F mutant LM7 cells as compared to vector controls to see if intrinsic signaling and function of PD-1 receptor is abrogated.

Effect of PD-1 blockade on primary OS tumors

Our studies reflected the efficacy of anti-PD-1 against the formation of OS lung metastasis. However, since we observed PDL-1 expression in primary tumors from patients, it is also possible that PDL-1/PD-1 interaction may play a role in the growth of primary OS bone tumors. Since the OS bone tumor physiology may differ from lung tumor

microenvironment, it will be crucial to study the role of macrophages in the context of regression of primary tumors as well as assess the time required for development of lung metastases. For this purpose, intra-osseous injection of K7M3 cells in proximal tibia may be performed in BALB/c mice to form primary tumors (211). After the confirmation of primary tumor mass by palpation, treatment will be performed using anti-PD-1 for 5 weeks. If the tumors outgrow, the legs will be amputated and treatment will be continued to evaluate the effect on pulmonary metastases. The end-points to be assessed will include the size of primary tumors, time required for formation of metastases and infiltration of macrophages, NK and T cells in the tumors.

Combination with other therapies

Combination of anti-PD-1 and L-MTP-PE

Our data showed dramatic effects of anti-PD-1 by itself on the number of OS lung metastases. However, the impact on survival of the mice remains to be answered. Anti-PD-1 treatment alone may increase survival in mice, but it is also a possibility that resistance may develop to single agent alone. Currently, a number of clinical trials and preclinical studies of anti-PD-1 antibodies are being conducted alone or in conjunction with other therapies **(Table 1 and 2)**. Although the anti-PD-1 antibody we used is a blocking antibody and not of clinical grade, novel combination treatment strategies may be utilized based on our results to provide pre-clinical information for design of future clinical trials.

In our study, we discovered a novel finding that one of the mechanisms of therapeutic efficacy of anti-PD-1 against OS lung metastasis is through increased macrophage infiltration. In contrast to other cancer types, TAMS have shown to play an anti-metastatic

role in OS. It was shown that the macrophage infiltration in pretreatment biopsies of OS patients correlated with better patient survival (24). Our lab has previously discovered the efficacy of L-MTP-PE, a macrophage and monocyte activating agent, in human and canine OS (8-10). L-MTP-PE in combination with standard adjuvant chemotherapy led to 8 % improvement in the overall survival of patients. Currently, this agent has been approved by European Medical Agency and in other countries for the treatment of surgically resectable non-metastatic OS in combination with chemotherapy as (12-14). Thus, it will be interesting to study the synergy between anti-PD-1 and L-MTP-PE in our *in vivo* OS mouse model. Treatments will be done with single agents alone and combination of both after the establishment of micrometastases. Therapeutic efficacy may be measured using number of tumor nodules formed, lung weights as well TUNEL assay for apoptosis. Also, the infiltration of M1 macrophages versus M2 macrophages may be studied using IHC staining to assess macrophage polarization.

Combination of anti-PD-1 and IL-2 muteins

Other immune activating agents such as IL-2 are known to induce NK and T-cell activation. (26, 27) Our laboratory has shown the efficacy of single agent aerosol IL-2 in a human OS pulmonary metastasis model. Aerosol IL-2 increased the number of NK cells in the lung tumors (34). However, relapse is seen when single agent treatment is given as mice succumb to the disease. It will be interesting to utilize either Aerosol IL-2 or IL-2 muteins such as the no-α mutein in combination with anti-PD-1 to assess if synergy may exist. These are IL-2 variants created to preferentially bind to the IL-2 receptor chains responsible for cytotoxic T-cells proliferation. No-α mutein has reduced affinity to CD25, the IL-2 receptor responsible for Treg proliferation, and maintain normal binding with IL-2Rβγ. No-α mutein

has been shown to inhibit the metastasis of B16 melanoma-variant and 3LL-D122 Lewis lung carcinoma in mice (212). Combination treatment of no-α mutein with anti-PD-1 may be done using either human (LM7) or mouse (K7M3) OS model. The end-point will be to assess the effect on number of metastatic nodules, infiltration of immune cell subsets and tumor cell apoptosis.

Combination of anti-PD-1 and anti-GD2 antibodies

Targeted antibodies specific to antigens overexpressed in OS maybe combined with anti-PD-1 antibodies. GD2 is a glycosphingolipid derivative, involved in attachment of tumor cells to extracellular matrix. GD2 is known to be overexpressed in OS patients at the cell surface (213, 214). Anti-GD2 antibodies such as ch14.18 have shown responses in the past in OS patients, primarily due through augmentation of immune responses against the antibody bound tumor cells though antibody-dependent cellular cytotoxicity (ADCC) (215, 216). Currently, clinical trials of humanized anti-GD2 antibodies such as 3F8 (Hu3F8) are being tested for recurrent OS (NCT02502786). Macrophages are one of the effector cells that can mediate ADCC function to eliminate the tumor cells after monoclonal antibody treatment (217). Hence, anti-PD-1 agents can be used as a potential strategy to enhance macrophage activation and subsequent ADCC when combined with anti-GD2 antibodies for the treatment of OS.

Anti-PD-1 treatment in transplant patients

In certain tumors such as advanced neuroblastoma, hematopoietic stem cell transplantation (HSCT) is performed following high-dose chemotherapy. However, most patients show relapse seen as minimal residual disease and resulting in poor clinical

outcomes. After HSCT, immune deficiency is observed in tumors due to defective T-cell signaling, impaired lymphocyte function and reduced effector cell numbers (218, 219). As our data elucidated the activation of macrophages using PD-1 blockade, PD-1 checkpoint inhibitors may have potential application in post-transplant patients undergoing chemotherapy, to boost anti-tumor responses

Thus, novel combination strategies with PD-1 checkpoint inhibitors can be utilized and may show promise for the effective treatment of OS lung metastases in the future.

APPENDIX A

Anti-PD-1 treatment *in vitro* induces cytotoxicity in LM7 cells

Since we observed PD-1 expression on LM7 cells, we determined the *in vitro* effect of anti-PD-1 treatment in LM7 cells. To determine the *in vitro* sensitivity of LM7 cells to anti-PD-1, LM7 cells were treated with anti-mPD-1 in increasing concentrations from 1 to 20 µg/ml for 24, 48 and 72 hours. As shown in **Figure A1 a)**, there were no significant changes in proliferation after anti-PD-1 at 24 hours at all doses from 1-20 µg/ml. However, after 48 hours, there was a dose-dependent decrease in cell proliferation, with a significant decrease observed with 10 µg/ml (69.1%) and 20 µg/ml (58.5%), ($p<0.05$). At 72 hours, further decrease in cell proliferation was observed at all doses from 1 to 20 µg/ml. [1 µg/ml (48.8%), 2 µg/ml (35.7%), 5 µg/ml (35.99%), 10 µg/ml (30.9 %), 20 µg/ml (26.4 %). A significant decrease in proliferation was seen at all doses at 72 hours ($p<0.05$).

Figure A1 b) depicts the changes in cell viability of LM7 cells after anti-PD-1 treatment at 24, 48 and 72 hours at three doses of 1, 10 and 20 µg/ml. At 24 hours, there were no significant changes in cell viability. However, at 48 hours, a significant decrease in cell proliferation was noted at doses of 10 µg/ml (50.6%) and 20 µg/ml (46.7%), similar to the MTT data. Also, at 72 hours, a significant decrease in cell proliferation was observed at 10 µg/ml (36.5%) and 20 µg/ml (33.3%). These results implied that anti-PD-1 had a direct cytotoxic effect on LM7 cells. Our *in vitro* cytotoxicity data showed that anti-PD-1 treatment led to a significant reduction in cell proliferation and cell viability, most likely due to the PD-1 expression on LM7 cells. Kleffel S *et al.* have shown that anti-PD-1 caused decrease in three-dimensional melanoma cell growth *in vitro*, but had no effect on cell death (181). Our *in vitro* results not only support the fact that PD-1 blockade by anti-PD-1 causes inhibition of

OS cell proliferation, but also delineate the mechanism of an induction of apoptosis in LM7 cells.

A.

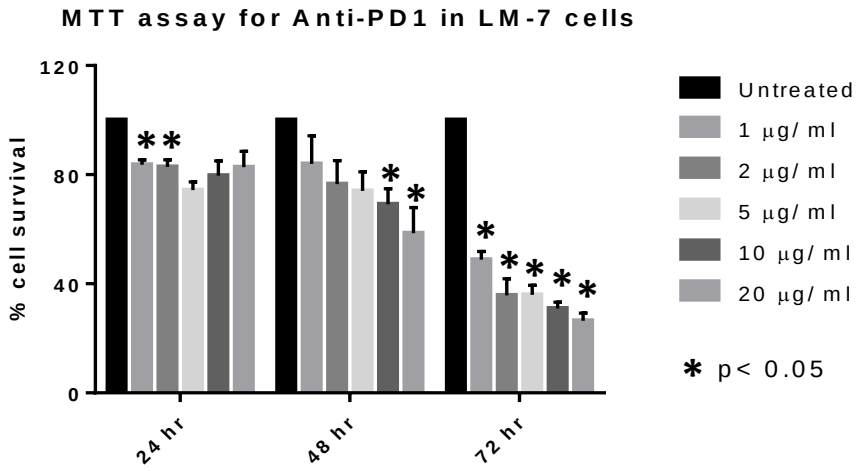

B.

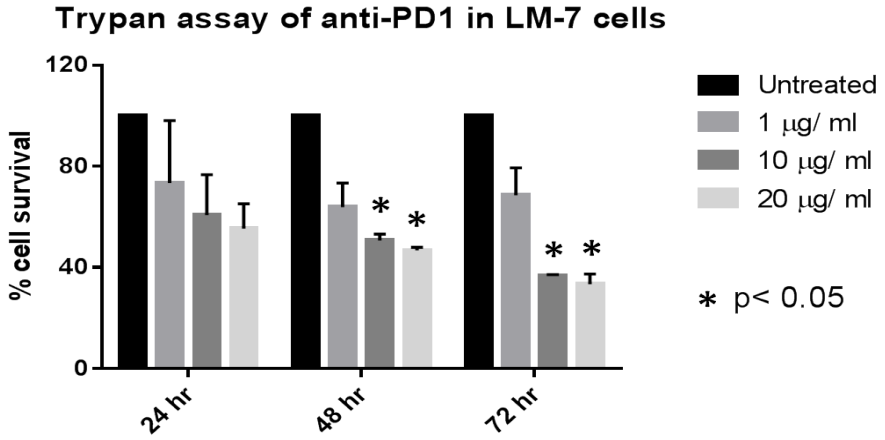

Figure A1. Anti-PD-1 antibody decreases cell viability of LM7 cells.
a) LM7 cells were treated with anti-PD-1 (1 to 20 µg/ml) for 24, 48 and 72 hours. MTT was added to detect the effect on cell proliferation, b) Trypan blue assays were conducted at the doses 1, 10 and 20 µg/ml for 24, 48 and 72 hours. Typan blue was added and cell counts were computed for determining cell viability.

Anti-PD-1 treatment causes an increase in cleaved caspase-3 and cleaved-PARP expression *in vitro* in LM7 cells

We demonstrated that anti-PD-1 treatment significantly decreased cell viability of LM7 cells *in vitro*. Recently, Kleffel S *et al*. discovered for the first time that PD-1 receptor is present on melanoma cells and plays a role in tumorigenesis through intrinsic downstream signaling. They showed that binding of the ligand PDL-1 expressed on melanoma cells or host cells to PD-1 on melanoma cells activates downstream mTOR (mammalian target of rapamycin) pathway (181). Thus, this study showed that PD-1 blocking antibody, in addition to augmenting the immune response against tumor cells through immune cell activation, can also exert a direct therapeutic effect by blocking the PD-1 downstream signaling on melanoma cells. In order to assess the effect on apoptosis, LM7 cells were treated with anti-PD-1 (10 μg/ml) for 72 hours. We selected this dose as it was the lowest dose that caused a significant reduction in both cell proliferation and viability as seen above. This was followed by western blotting. As shown in **Figure A2**, anti-PD-1 treatment led to an increase in both cleaved caspase-3 and cleaved-PARP expression, which implies an induction of apoptosis. Hence, we conclude that anti-PD-1 not only inhibited cell proliferation, but also promoted cell death through apoptosis.

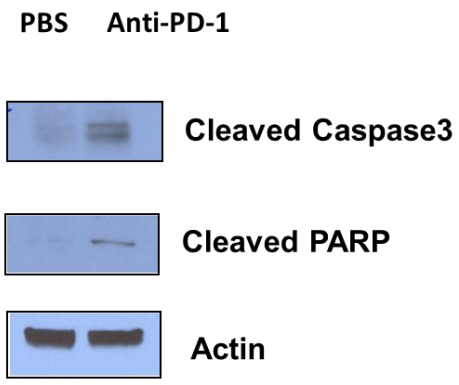

Figure A2. Anti-PD-1 treatment induced apoptosis in LM7 cells *in vitro*.
LM7 cells were treated with anti-PD-1 (10 μg/ml) for 72 hours before obtaining lysates. Western blotting using anti-cleaved caspase-3 and anti-cleaved-PARP antibodies was performed to assess the effect on apoptosis using Actin as a loading control.

p-Stat3-705 and pErk1/2 protein levels are significantly decreased following anti-PD-1 treatment in LM7 cells *in vitro*

Since anti-PD-1 significantly affected cell viability of LM7 cells *in vitro*, we assessed the downstream signaling pathways affected after anti-PD-1 (10 μg/ml) for 72 hours. We observed that there was a significant decrease in p-Stat3-705 levels as seen by western blotting **(Figure A3)**. Also, p-Erk1/2 expression was significantly reduced. p-Akt levels were not affected in LM7 cells after anti-PD-1 treatment demonstrating that this was not the primary pathway that was involved in the treatment response. Contrary to our *in vivo* findings, PDL-1 was increased in LM7 cells on anti-PD-1 treatment. This may be due to the absence of PD-1/PDL-1 immune interactions present *in vitro* or alternative feedback mechanisms controlling PDL-1 expression apart from p-Stat3 and p-Erk1/2. Hence, our data

indicates that anti-PD-1 results in inhibition of p-Stat3 and p-Erk1/2 pathways, which are involved in tumor cell proliferation and apoptosis.

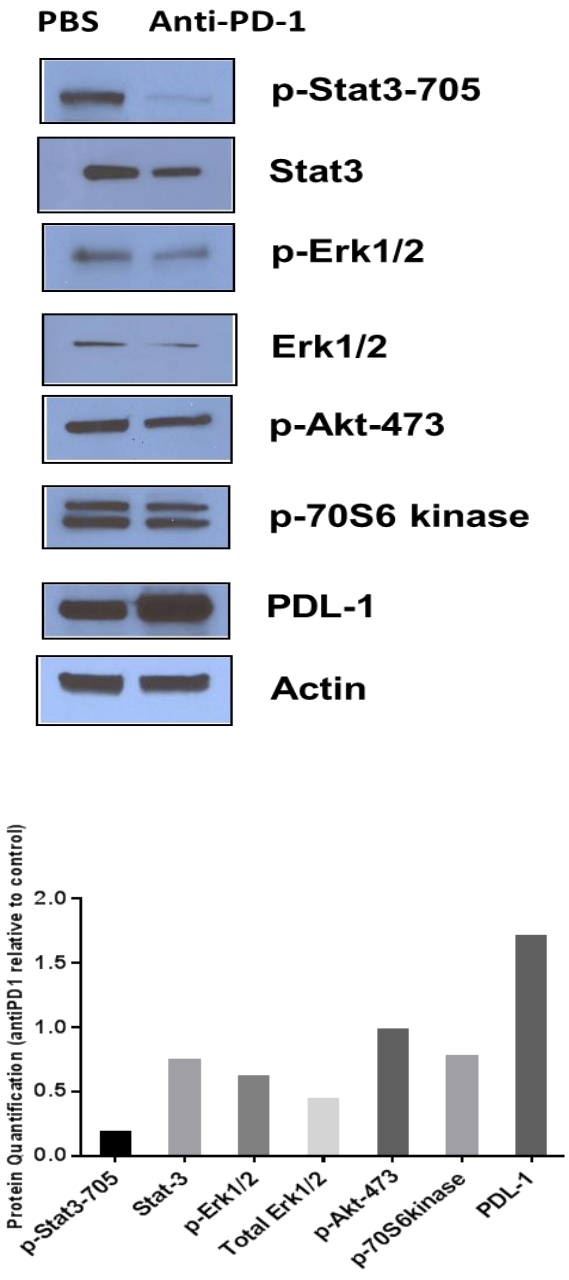

Figure A3. *In vitro* anti-mPD-1 treatment in LM7 cells caused decreased p-Stat3, p-Erk1/2 protein levels.
LM7 cells were treated with anti-PD-1 (10 μg/ml) for 72 hours before obtaining lysates using RIPA buffer. Western blotting was performed to assess antibodies was performed to assess p-Stat3-705, Stat3, PDL-1, p-Erk1//2, Erk1/2, p-Akt, p-70S6 Kinase protein levels. Actin was used as a loading control.

BIBLIOGRAPHY

1. Ottaviani, G., and N. Jaffe. 2009. The epidemiology of osteosarcoma. *Cancer Treat Res* 152: 3-13.
2. Gill, J., M. K. Ahluwalia, D. Geller, and R. Gorlick. 2013. New targets and approaches in osteosarcoma. *Pharmacol Ther* 137: 89-99.
3. Isakoff, M. S., S. S. Bielack, P. Meltzer, and R. Gorlick. 2015. Osteosarcoma: Current Treatment and a Collaborative Pathway to Success. *J Clin Oncol* 33: 3029-3035.
4. Anderson, M. E. 2016. Update on Survival in Osteosarcoma. *Orthop Clin North Am* 47: 283-292.
5. Geller, D. S., and R. Gorlick. 2010. Osteosarcoma: a review of diagnosis, management, and treatment strategies. *Clin Adv Hematol Oncol* 8: 705-718.
6. Duchman, K. R., Y. Gao, and B. J. Miller. 2015. Prognostic factors for survival in patients with high-grade osteosarcoma using the Surveillance, Epidemiology, and End Results (SEER) Program database. *Cancer Epidemiol* 39: 593-599.
7. Bruland, O. S., H. Hoifodt, G. Saeter, S. Smeland, and O. Fodstad. 2005. Hematogenous micrometastases in osteosarcoma patients. *Clin Cancer Res* 11: 4666-4673.
8. Kleinerman, E. S., S. F. Jia, J. Griffin, N. L. Seibel, R. S. Benjamin, and N. Jaffe. 1992. Phase II study of liposomal muramyl tripeptide in osteosarcoma: the cytokine cascade and monocyte activation following administration. *J Clin Oncol* 10: 1310-1316.

9. MacEwen, E. G., I. D. Kurzman, R. C. Rosenthal, B. W. Smith, P. A. Manley, J. K. Roush, and P. E. Howard. 1989. Therapy for osteosarcoma in dogs with intravenous injection of liposome-encapsulated muramyl tripeptide. *J Natl Cancer Inst* 81: 935-938.

10. Fidler, I. J., S. Sone, W. E. Fogler, and Z. L. Barnes. 1981. Eradication of spontaneous metastases and activation of alveolar macrophages by intravenous injection of liposomes containing muramyl dipeptide. *Proc Natl Acad Sci U S A* 78: 1680-1684.

11. Meyers, P. A. 2009. Muramyl tripeptide (mifamurtide) for the treatment of osteosarcoma. *Expert Rev Anticancer Ther* 9: 1035-1049.

12. Meyers, P. A., C. L. Schwartz, M. D. Krailo, J. H. Healey, M. L. Bernstein, D. Betcher, W. S. Ferguson, M. C. Gebhardt, A. M. Goorin, M. Harris, E. Kleinerman, M. P. Link, H. Nadel, M. Nieder, G. P. Siegal, M. A. Weiner, R. J. Wells, R. B. Womer, and H. E. Grier. 2008. Osteosarcoma: the addition of muramyl tripeptide to chemotherapy improves overall survival--a report from the Children's Oncology Group. *J Clin Oncol* 26: 633-638.

13. Kleinerman, E. S., J. B. Gano, D. A. Johnston, R. S. Benjamin, and N. Jaffe. 1995. Efficacy of liposomal muramyl tripeptide (CGP 19835A) in the treatment of relapsed osteosarcoma. *Am J Clin Oncol* 18: 93-99.

14. Nardin, A., M. L. Lefebvre, K. Labroquere, O. Faure, and J. P. Abastado. 2006. Liposomal muramyl tripeptide phosphatidylethanolamine: Targeting and activating macrophages for adjuvant treatment of osteosarcoma. *Curr Cancer Drug Targets* 6: 123-133.

15. Tarek, N., and D. A. Lee. 2014. Natural killer cells for osteosarcoma. *Adv Exp Med Biol* 804: 341-353.

16. Ljunggren, H. G., and K. Karre. 1990. In search of the 'missing self': MHC molecules and NK cell recognition. *Immunol Today* 11: 237-244.

17. Ruggeri, L., M. Capanni, E. Urbani, K. Perruccio, W. D. Shlomchik, A. Tosti, S. Posati, D. Rogaia, F. Frassoni, F. Aversa, M. F. Martelli, and A. Velardi. 2002. Effectiveness of donor natural killer cell alloreactivity in mismatched hematopoietic transplants. *Science* 295: 2097-2100.

18. Miller, J. S., Y. Soignier, A. Panoskaltsis-Mortari, S. A. McNearney, G. H. Yun, S. K. Fautsch, D. McKenna, C. Le, T. E. Defor, L. J. Burns, P. J. Orchard, B. R. Blazar, J. E. Wagner, A. Slungaard, D. J. Weisdorf, I. J. Okazaki, and P. B. McGlave. 2005. Successful adoptive transfer and in vivo expansion of human haploidentical NK cells in patients with cancer. *Blood* 105: 3051-3057.

19. Curti, A., L. Ruggeri, A. D'Addio, A. Bontadini, E. Dan, M. R. Motta, S. Trabanelli, V. Giudice, E. Urbani, G. Martinelli, S. Paolini, F. Fruet, A. Isidori, S. Parisi, G. Bandini, M. Baccarani, A. Velardi, and R. M. Lemoli. 2011. Successful transfer of alloreactive haploidentical KIR ligand-mismatched natural killer cells after infusion in elderly high risk acute myeloid leukemia patients. *Blood* 118: 3273-3279.

20. Denman, C. J., V. V. Senyukov, S. S. Somanchi, P. V. Phatarpekar, L. M. Kopp, J. L. Johnson, H. Singh, L. Hurton, S. N. Maiti, M. H. Huls, R. E. Champlin, L. J. Cooper, and D. A. Lee. 2012. Membrane-bound IL-21 promotes sustained ex vivo proliferation of human natural killer cells. *PLoS One* 7: e30264.

21. Markiewicz, K., K. Zeman, A. Kozar, M. Golebiowska-Wawrzyniak, and W. Wozniak. 2012. [Evaluation of selected parameters of cellular immunity in children with osteosarcoma at diagnosis]. *Med Wieku Rozwoj* 16: 212-221.

22. Luksch, R., D. Perotti, G. Cefalo, C. Gambacorti Passerini, M. Massimino, F. Spreafico, M. Casanova, A. Ferrari, M. Terenziani, D. Polastri, F. Gambirasio, M. Podda, F. Bozzi, F. Ravagnani, G. Parmiani, and F. Fossati Bellani. 2003. Immunomodulation in a treatment program including pre- and post-operative interleukin-2 and chemotherapy for childhood osteosarcoma. *Tumori* 89: 263-268.

23. Mariani, E., A. Tarozzi, A. Meneghetti, L. Cattini, and A. Facchini. 1997. Human osteosarcoma cell susceptibility to natural killer cell lysis depends on CD54 and increases after TNF alpha incubation. *FEBS Lett* 406: 83-88.

24. Buddingh, E. P., M. W. Schilham, S. E. Ruslan, D. Berghuis, K. Szuhai, J. Suurmond, A. H. Taminiau, H. Gelderblom, R. M. Egeler, M. Serra, P. C. Hogendoorn, and A. C. Lankester. 2011. Chemotherapy-resistant osteosarcoma is highly susceptible to IL-15-activated allogeneic and autologous NK cells. *Cancer Immunol Immunother* 60: 575-586.

25. Cho, D., D. R. Shook, N. Shimasaki, Y. H. Chang, H. Fujisaki, and D. Campana. 2010. Cytotoxicity of activated natural killer cells against pediatric solid tumors. *Clin Cancer Res* 16: 3901-3909.

26. Bachmann, M. F., and A. Oxenius. 2007. Interleukin 2: from immunostimulation to immunoregulation and back again. *EMBO Rep* 8: 1142-1148.

27. Henney, C. S., K. Kuribayashi, D. E. Kern, and S. Gillis. 1981. Interleukin-2 augments natural killer cell activity. *Nature* 291: 335-338.

28. Atkins, M. B., M. T. Lotze, J. P. Dutcher, R. I. Fisher, G. Weiss, K. Margolin, J. Abrams, M. Sznol, D. Parkinson, M. Hawkins, C. Paradise, L. Kunkel, and S. A. Rosenberg. 1999. High-dose recombinant interleukin 2 therapy for patients with metastatic melanoma: analysis of 270 patients treated between 1985 and 1993. *J Clin Oncol* 17: 2105-2116.

29. Dutcher, J. P., M. Atkins, R. Fisher, G. Weiss, K. Margolin, F. Aronson, J. Sosman, M. Lotze, M. Gordon, T. Logan, and J. Mier. 1997. Interleukin-2-based therapy for metastatic renal cell cancer: the Cytokine Working Group experience, 1989-1997. *Cancer J Sci Am* 3 Suppl 1: S73-78.

30. Rosenstein, M., S. E. Ettinghausen, and S. A. Rosenberg. 1986. Extravasation of intravascular fluid mediated by the systemic administration of recombinant interleukin 2. *J Immunol* 137: 1735-1742.

31. Khanna, C., P. M. Anderson, D. E. Hasz, E. Katsanis, M. Neville, and J. S. Klausner. 1997. Interleukin-2 liposome inhalation therapy is safe and effective for dogs with spontaneous pulmonary metastases. *Cancer* 79: 1409-1421.

32. Khanna, C., J. C. Waldrep, P. M. Anderson, R. W. Weischelbaum, D. E. Hasz, E. Katsanis, and J. S. Klausner. 1997. Nebulized interleukin 2 liposomes: aerosol characteristics and biodistribution. *J Pharm Pharmacol* 49: 960-971.

33. Lorenz, J., K. Wilhelm, M. Kessler, C. Peschel, U. Schwulera, R. Lissner, W. G. Struff, E. Huland, C. Huber, and W. E. Aulitzky. 1996. Phase I trial of inhaled natural interleukin 2 for treatment of pulmonary malignancy: toxicity, pharmacokinetics, and biological effects. *Clin Cancer Res* 2: 1115-1122.

34. Guma, S. R., D. A. Lee, L. Yu, N. Gordon, D. Hughes, J. Stewart, W. L. Wang, and E. S. Kleinerman. 2014. Natural killer cell therapy and aerosol interleukin-2 for the treatment of osteosarcoma lung metastasis. *Pediatr Blood Cancer* 61: 618-626.

35. Guma, S. R., D. A. Lee, Y. Ling, N. Gordon, and E. S. Kleinerman. 2014. Aerosol interleukin-2 induces natural killer cell proliferation in the lung and combination therapy improves the survival of mice with osteosarcoma lung metastasis. *Pediatr Blood Cancer* 61: 1362-1368.

36. DeRenzo, C., and S. Gottschalk. 2014. Genetically modified T-cell therapy for osteosarcoma. *Adv Exp Med Biol* 804: 323-340.

37. Morgan, R. A., M. E. Dudley, J. R. Wunderlich, M. S. Hughes, J. C. Yang, R. M. Sherry, R. E. Royal, S. L. Topalian, U. S. Kammula, N. P. Restifo, Z. Zheng, A. Nahvi, C. R. de Vries, L. J. Rogers-Freezer, S. A. Mavroukakis, and S. A. Rosenberg. 2006. Cancer regression in patients after transfer of genetically engineered lymphocytes. *Science* 314: 126-129.

38. Robbins, P. F., R. A. Morgan, S. A. Feldman, J. C. Yang, R. M. Sherry, M. E. Dudley, J. R. Wunderlich, A. V. Nahvi, L. J. Helman, C. L. Mackall, U. S. Kammula, M. S. Hughes, N. P. Restifo, M. Raffeld, C. C. Lee, C. L. Levy, Y. F. Li, M. El-Gamil, S. L. Schwarz, C. Laurencot, and S. A. Rosenberg. 2011. Tumor regression in patients with metastatic synovial cell sarcoma and melanoma using genetically engineered lymphocytes reactive with NY-ESO-1. *J Clin Oncol* 29: 917-924.

39. Ahmed, N., V. S. Salsman, E. Yvon, C. U. Louis, L. Perlaky, W. S. Wels, M. K. Dishop, E. E. Kleinerman, M. Pule, C. M. Rooney, H. E. Heslop, and S. Gottschalk.

2009. Immunotherapy for osteosarcoma: genetic modification of T cells overcomes low levels of tumor antigen expression. *Mol Ther* 17: 1779-1787.

40. Huang, G., L. Yu, L. J. Cooper, M. Hollomon, H. Huls, and E. S. Kleinerman. 2012. Genetically modified T cells targeting interleukin-11 receptor alpha-chain kill human osteosarcoma cells and induce the regression of established osteosarcoma lung metastases. *Cancer Res* 72: 271-281.

41. Hoenicke, L., and L. Zender. 2012. Immune surveillance of senescent cells--biological significance in cancer- and non-cancer pathologies. *Carcinogenesis* 33: 1123-1126.

42. Ishida, Y., Y. Agata, K. Shibahara, and T. Honjo. 1992. Induced expression of PD-1, a novel member of the immunoglobulin gene superfamily, upon programmed cell death. *EMBO J* 11: 3887-3895.

43. Raimondi, G., I. Zanoni, S. Citterio, P. Ricciardi-Castagnoli, and F. Granucci. 2006. Induction of peripheral T cell tolerance by antigen-presenting B cells. II. Chronic antigen presentation overrules antigen-presenting B cell activation. *J Immunol* 176: 4021-4028.

44. Keir, M. E., M. J. Butte, G. J. Freeman, and A. H. Sharpe. 2008. PD-1 and its ligands in tolerance and immunity. *Annu Rev Immunol* 26: 677-704.

45. Kinter, A. L., E. J. Godbout, J. P. McNally, I. Sereti, G. A. Roby, M. A. O'Shea, and A. S. Fauci. 2008. The common gamma-chain cytokines IL-2, IL-7, IL-15, and IL-21 induce the expression of programmed death-1 and its ligands. *J Immunol* 181: 6738-6746.

46. Merelli, B., D. Massi, L. Cattaneo, and M. Mandala. 2014. Targeting the PD1/PD-L1 axis in melanoma: biological rationale, clinical challenges and opportunities. *Crit Rev Oncol Hematol* 89: 140-165.

47. Dong, H., G. Zhu, K. Tamada, and L. Chen. 1999. B7-H1, a third member of the B7 family, co-stimulates T-cell proliferation and interleukin-10 secretion. *Nat Med* 5: 1365-1369.

48. Latchman, Y., C. R. Wood, T. Chernova, D. Chaudhary, M. Borde, I. Chernova, Y. Iwai, A. J. Long, J. A. Brown, R. Nunes, E. A. Greenfield, K. Bourque, V. A. Boussiotis, L. L. Carter, B. M. Carreno, N. Malenkovich, H. Nishimura, T. Okazaki, T. Honjo, A. H. Sharpe, and G. J. Freeman. 2001. PD-L2 is a second ligand for PD-1 and inhibits T cell activation. *Nat Immunol* 2: 261-268.

49. Okazaki, T., and T. Honjo. 2007. PD-1 and PD-1 ligands: from discovery to clinical application. *Int Immunol* 19: 813-824.

50. Shi, L., S. Chen, L. Yang, and Y. Li. 2013. The role of PD-1 and PD-L1 in T-cell immune suppression in patients with hematological malignancies. *J Hematol Oncol* 6: 74.

51. Vibhakar, R., G. Juan, F. Traganos, Z. Darzynkiewicz, and L. R. Finger. 1997. Activation-induced expression of human programmed death-1 gene in T-lymphocytes. *Exp Cell Res* 232: 25-28.

52. Zhang, X., J. C. Schwartz, X. Guo, S. Bhatia, E. Cao, M. Lorenz, M. Cammer, L. Chen, Z. Y. Zhang, M. A. Edidin, S. G. Nathenson, and S. C. Almo. 2004. Structural and functional analysis of the costimulatory receptor programmed death-1. *Immunity* 20: 337-347.

53. Okazaki, T., and J. Wang. 2005. PD-1/PD-L pathway and autoimmunity. *Autoimmunity* 38: 353-357.

54. Probst, H. C., K. McCoy, T. Okazaki, T. Honjo, and M. van den Broek. 2005. Resting dendritic cells induce peripheral CD8+ T cell tolerance through PD-1 and CTLA-4. *Nat Immunol* 6: 280-286.

55. Keir, M. E., S. C. Liang, I. Guleria, Y. E. Latchman, A. Qipo, L. A. Albacker, M. Koulmanda, G. J. Freeman, M. H. Sayegh, and A. H. Sharpe. 2006. Tissue expression of PD-L1 mediates peripheral T cell tolerance. *J Exp Med* 203: 883-895.

56. Fife, B. T., K. E. Pauken, T. N. Eagar, T. Obu, J. Wu, Q. Tang, M. Azuma, M. F. Krummel, and J. A. Bluestone. 2009. Interactions between PD-1 and PD-L1 promote tolerance by blocking the TCR-induced stop signal. *Nat Immunol* 10: 1185-1192.

57. Abiko, K., N. Matsumura, J. Hamanishi, N. Horikawa, R. Murakami, K. Yamaguchi, Y. Yoshioka, T. Baba, I. Konishi, and M. Mandai. 2015. IFN-gamma from lymphocytes induces PD-L1 expression and promotes progression of ovarian cancer. *Br J Cancer* 112: 1501-1509.

58. Barber, D. L., E. J. Wherry, D. Masopust, B. Zhu, J. P. Allison, A. H. Sharpe, G. J. Freeman, and R. Ahmed. 2006. Restoring function in exhausted CD8 T cells during chronic viral infection. *Nature* 439: 682-687.

59. Ahmadzadeh, M., L. A. Johnson, B. Heemskerk, J. R. Wunderlich, M. E. Dudley, D. E. White, and S. A. Rosenberg. 2009. Tumor antigen-specific CD8 T cells infiltrating the tumor express high levels of PD-1 and are functionally impaired. *Blood* 114: 1537-1544.

60. Peng, W., C. Liu, C. Xu, Y. Lou, J. Chen, Y. Yang, H. Yagita, W. W. Overwijk, G. Lizee, L. Radvanyi, and P. Hwu. 2012. PD-1 blockade enhances T-cell migration to tumors by elevating IFN-gamma inducible chemokines. *Cancer Res* 72: 5209-5218.

61. Spranger, S., H. K. Koblish, B. Horton, P. A. Scherle, R. Newton, and T. F. Gajewski. 2014. Mechanism of tumor rejection with doublets of CTLA-4, PD-1/PD-L1, or IDO blockade involves restored IL-2 production and proliferation of CD8(+) T cells directly within the tumor microenvironment. *J Immunother Cancer* 2: 3.

62. Gatalica, Z., C. Snyder, T. Maney, A. Ghazalpour, D. A. Holterman, N. Xiao, P. Overberg, I. Rose, G. D. Basu, S. Vranic, H. T. Lynch, D. D. Von Hoff, and O. Hamid. 2014. Programmed cell death 1 (PD-1) and its ligand (PD-L1) in common cancers and their correlation with molecular cancer type. *Cancer Epidemiol Biomarkers Prev* 23: 2965-2970.

63. Okiyama, N., and S. I. Katz. 2014. Programmed cell death 1 (PD-1) regulates the effector function of CD8 T cells via PD-L1 expressed on target keratinocytes. *J Autoimmun* 53: 1-9.

64. Riley, J. L. 2009. PD-1 signaling in primary T cells. *Immunol Rev* 229: 114-125.

65. Francisco, L. M., P. T. Sage, and A. H. Sharpe. 2010. The PD-1 pathway in tolerance and autoimmunity. *Immunol Rev* 236: 219-242.

66. Pardoll, D. M. 2012. The blockade of immune checkpoints in cancer immunotherapy. *Nat Rev Cancer* 12: 252-264.

67. Parsa, A. T., J. S. Waldron, A. Panner, C. A. Crane, I. F. Parney, J. J. Barry, K. E. Cachola, J. C. Murray, T. Tihan, M. C. Jensen, P. S. Mischel, D. Stokoe, and R. O.

Pieper. 2007. Loss of tumor suppressor PTEN function increases B7-H1 expression and immunoresistance in glioma. *Nat Med* 13: 84-88.

68. Marzec, M., Q. Zhang, A. Goradia, P. N. Raghunath, X. Liu, M. Paessler, H. Y. Wang, M. Wysocka, M. Cheng, B. A. Ruggeri, and M. A. Wasik. 2008. Oncogenic kinase NPM/ALK induces through STAT3 expression of immunosuppressive protein CD274 (PD-L1, B7-H1). *Proc Natl Acad Sci U S A* 105: 20852-20857.

69. Khalili, J. S., S. Liu, T. G. Rodriguez-Cruz, M. Whittington, S. Wardell, C. Liu, M. Zhang, Z. A. Cooper, D. T. Frederick, Y. Li, R. W. Joseph, C. Bernatchez, S. Ekmekcioglu, E. Grimm, L. G. Radvanyi, R. E. Davis, M. A. Davies, J. A. Wargo, P. Hwu, and G. Lizee. 2012. Oncogenic BRAF(V600E) promotes stromal cell-mediated immunosuppression via induction of interleukin-1 in melanoma. *Clin Cancer Res* 18: 5329-5340.

70. Gajewski, T. F., J. Louahed, and V. G. Brichard. 2010. Gene signature in melanoma associated with clinical activity: a potential clue to unlock cancer immunotherapy. *Cancer J* 16: 399-403.

71. Taube, J. M., R. A. Anders, G. D. Young, H. Xu, R. Sharma, T. L. McMiller, S. Chen, A. P. Klein, D. M. Pardoll, S. L. Topalian, and L. Chen. 2012. Colocalization of inflammatory response with B7-h1 expression in human melanocytic lesions supports an adaptive resistance mechanism of immune escape. *Sci Transl Med* 4: 127ra137.

72. Thompson, R. H., M. D. Gillett, J. C. Cheville, C. M. Lohse, H. Dong, W. S. Webster, K. G. Krejci, J. R. Lobo, S. Sengupta, L. Chen, H. Zincke, M. L. Blute, S. E. Strome, B. C. Leibovich, and E. D. Kwon. 2004. Costimulatory B7-H1 in renal

cell carcinoma patients: Indicator of tumor aggressiveness and potential therapeutic target. *Proc Natl Acad Sci U S A* 101: 17174-17179.

73. Thompson, R. H., S. M. Kuntz, B. C. Leibovich, H. Dong, C. M. Lohse, W. S. Webster, S. Sengupta, I. Frank, A. S. Parker, H. Zincke, M. L. Blute, T. J. Sebo, J. C. Cheville, and E. D. Kwon. 2006. Tumor B7-H1 is associated with poor prognosis in renal cell carcinoma patients with long-term follow-up. *Cancer Res* 66: 3381-3385.

74. Hino, R., K. Kabashima, Y. Kato, H. Yagi, M. Nakamura, T. Honjo, T. Okazaki, and Y. Tokura. 2010. Tumor cell expression of programmed cell death-1 ligand 1 is a prognostic factor for malignant melanoma. *Cancer* 116: 1757-1766.

75. Mu, C. Y., J. A. Huang, Y. Chen, C. Chen, and X. G. Zhang. 2011. High expression of PD-L1 in lung cancer may contribute to poor prognosis and tumor cells immune escape through suppressing tumor infiltrating dendritic cells maturation. *Med Oncol* 28: 682-688.

76. Nomi, T., M. Sho, T. Akahori, K. Hamada, A. Kubo, H. Kanehiro, S. Nakamura, K. Enomoto, H. Yagita, M. Azuma, and Y. Nakajima. 2007. Clinical significance and therapeutic potential of the programmed death-1 ligand/programmed death-1 pathway in human pancreatic cancer. *Clin Cancer Res* 13: 2151-2157.

77. Zou, W., and L. Chen. 2008. Inhibitory B7-family molecules in the tumour microenvironment. *Nat Rev Immunol* 8: 467-477.

78. Zeng, Z., F. Shi, L. Zhou, M. N. Zhang, Y. Chen, X. J. Chang, Y. Y. Lu, W. L. Bai, J. H. Qu, C. P. Wang, H. Wang, M. Lou, F. S. Wang, J. Y. Lv, and Y. P. Yang. 2011. Upregulation of circulating PD-L1/PD-1 is associated with poor post-cryoablation

prognosis in patients with HBV-related hepatocellular carcinoma. *PLoS One* 6: e23621.

79. Gao, Q., X. Y. Wang, S. J. Qiu, I. Yamato, M. Sho, Y. Nakajima, J. Zhou, B. Z. Li, Y. H. Shi, Y. S. Xiao, Y. Xu, and J. Fan. 2009. Overexpression of PD-L1 significantly associates with tumor aggressiveness and postoperative recurrence in human hepatocellular carcinoma. *Clin Cancer Res* 15: 971-979.

80. Karim, R., E. S. Jordanova, S. J. Piersma, G. G. Kenter, L. Chen, J. M. Boer, C. J. Melief, and S. H. van der Burg. 2009. Tumor-expressed B7-H1 and B7-DC in relation to PD-1+ T-cell infiltration and survival of patients with cervical carcinoma. *Clin Cancer Res* 15: 6341-6347.

81. Konishi, J., K. Yamazaki, M. Azuma, I. Kinoshita, H. Dosaka-Akita, and M. Nishimura. 2004. B7-H1 expression on non-small cell lung cancer cells and its relationship with tumor-infiltrating lymphocytes and their PD-1 expression. *Clin Cancer Res* 10: 5094-5100.

82. Topalian, S. L., F. S. Hodi, J. R. Brahmer, S. N. Gettinger, D. C. Smith, D. F. McDermott, J. D. Powderly, R. D. Carvajal, J. A. Sosman, M. B. Atkins, P. D. Leming, D. R. Spigel, S. J. Antonia, L. Horn, C. G. Drake, D. M. Pardoll, L. Chen, W. H. Sharfman, R. A. Anders, J. M. Taube, T. L. McMiller, H. Xu, A. J. Korman, M. Jure-Kunkel, S. Agrawal, D. McDonald, G. D. Kollia, A. Gupta, J. M. Wigginton, and M. Sznol. 2012. Safety, activity, and immune correlates of anti-PD-1 antibody in cancer. *N Engl J Med* 366: 2443-2454.

83. Garon, E. B., N. A. Rizvi, R. Hui, N. Leighl, A. S. Balmanoukian, J. P. Eder, A. Patnaik, C. Aggarwal, M. Gubens, L. Horn, E. Carcereny, M. J. Ahn, E. Felip, J. S.

Lee, M. D. Hellmann, O. Hamid, J. W. Goldman, J. C. Soria, M. Dolled-Filhart, R. Z. Rutledge, J. Zhang, J. K. Lunceford, R. Rangwala, G. M. Lubiniecki, C. Roach, K. Emancipator, and L. Gandhi. 2015. Pembrolizumab for the treatment of non-small-cell lung cancer. *N Engl J Med* 372: 2018-2028.

84. Herbst, R. S., J. C. Soria, M. Kowanetz, G. D. Fine, O. Hamid, M. S. Gordon, J. A. Sosman, D. F. McDermott, J. D. Powderly, S. N. Gettinger, H. E. Kohrt, L. Horn, D. P. Lawrence, S. Rost, M. Leabman, Y. Xiao, A. Mokatrin, H. Koeppen, P. S. Hegde, I. Mellman, D. S. Chen, and F. S. Hodi. 2014. Predictive correlates of response to the anti-PD-L1 antibody MPDL3280A in cancer patients. *Nature* 515: 563-567.

85. Tumeh, P. C., C. L. Harview, J. H. Yearley, I. P. Shintaku, E. J. Taylor, L. Robert, B. Chmielowski, M. Spasic, G. Henry, V. Ciobanu, A. N. West, M. Carmona, C. Kivork, E. Seja, G. Cherry, A. J. Gutierrez, T. R. Grogan, C. Mateus, G. Tomasic, J. A. Glaspy, R. O. Emerson, H. Robins, R. H. Pierce, D. A. Elashoff, C. Robert, and A. Ribas. 2014. PD-1 blockade induces responses by inhibiting adaptive immune resistance. *Nature* 515: 568-571.

86. Brahmer, J., K. L. Reckamp, P. Baas, L. Crino, W. E. Eberhardt, E. Poddubskaya, S. Antonia, A. Pluzanski, E. E. Vokes, E. Holgado, D. Waterhouse, N. Ready, J. Gainor, O. Aren Frontera, L. Havel, M. Steins, M. C. Garassino, J. G. Aerts, M. Domine, L. Paz-Ares, M. Reck, C. Baudelet, C. T. Harbison, B. Lestini, and D. R. Spigel. 2015. Nivolumab versus Docetaxel in Advanced Squamous-Cell Non-Small-Cell Lung Cancer. *N Engl J Med* 373: 123-135.

87. Gettinger, S. N., L. Horn, L. Gandhi, D. R. Spigel, S. J. Antonia, N. A. Rizvi, J. D. Powderly, R. S. Heist, R. D. Carvajal, D. M. Jackman, L. V. Sequist, D. C. Smith, P.

Leming, D. P. Carbone, M. C. Pinder-Schenck, S. L. Topalian, F. S. Hodi, J. A. Sosman, M. Sznol, D. F. McDermott, D. M. Pardoll, V. Sankar, C. M. Ahlers, M. Salvati, J. M. Wigginton, M. D. Hellmann, G. D. Kollia, A. K. Gupta, and J. R. Brahmer. 2015. Overall Survival and Long-Term Safety of Nivolumab (Anti-Programmed Death 1 Antibody, BMS-936558, ONO-4538) in Patients With Previously Treated Advanced Non-Small-Cell Lung Cancer. *J Clin Oncol* 33: 2004-2012.

88. Topalian, S. L., C. G. Drake, and D. M. Pardoll. 2012. Targeting the PD-1/B7-H1(PD-L1) pathway to activate anti-tumor immunity. *Curr Opin Immunol* 24: 207-212.

89. Robert, C., G. V. Long, B. Brady, C. Dutriaux, M. Maio, L. Mortier, J. C. Hassel, P. Rutkowski, C. McNeil, E. Kalinka-Warzocha, K. J. Savage, M. M. Hernberg, C. Lebbe, J. Charles, C. Mihalcioiu, V. Chiarion-Sileni, C. Mauch, F. Cognetti, A. Arance, H. Schmidt, D. Schadendorf, H. Gogas, L. Lundgren-Eriksson, C. Horak, B. Sharkey, I. M. Waxman, V. Atkinson, and P. A. Ascierto. 2015. Nivolumab in previously untreated melanoma without BRAF mutation. *N Engl J Med* 372: 320-330.

90. Postow, M. A., J. Chesney, A. C. Pavlick, C. Robert, K. Grossmann, D. McDermott, G. P. Linette, N. Meyer, J. K. Giguere, S. S. Agarwala, M. Shaheen, M. S. Ernstoff, D. Minor, A. K. Salama, M. Taylor, P. A. Ott, L. M. Rollin, C. Horak, P. Gagnier, J. D. Wolchok, and F. S. Hodi. 2015. Nivolumab and ipilimumab versus ipilimumab in untreated melanoma. *N Engl J Med* 372: 2006-2017.

91. Voena, C., and R. Chiarle. 2016. Advances in cancer immunology and cancer immunotherapy. *Discov Med* 21: 125-133.

92. Kazandjian, D., D. L. Suzman, G. Blumenthal, S. Mushti, K. He, M. Libeg, P. Keegan, and R. Pazdur. 2016. FDA Approval Summary: Nivolumab for the Treatment of Metastatic Non-Small Cell Lung Cancer With Progression On or After Platinum-Based Chemotherapy. *Oncologist* 21: 634-642.

93. Sul, J., G. M. Blumenthal, X. Jiang, K. He, P. Keegan, and R. Pazdur. 2016. FDA Approval Summary: Pembrolizumab for the Treatment of Patients With Metastatic Non-Small Cell Lung Cancer Whose Tumors Express Programmed Death-Ligand 1. *Oncologist* 21: 643-650.

94. Planchard, D., T. Yokoi, M. J. McCleod, J. R. Fischer, Y. C. Kim, M. Ballas, K. Shi, and J. C. Soria. 2016. A Phase III Study of Durvalumab (MEDI4736) With or Without Tremelimumab for Previously Treated Patients With Advanced NSCLC: Rationale and Protocol Design of the ARCTIC Study. *Clin Lung Cancer* 17: 232-236 e231.

95. Massard, C., M. S. Gordon, S. Sharma, S. Rafii, Z. A. Wainberg, J. Luke, T. J. Curiel, G. Colon-Otero, O. Hamid, R. E. Sanborn, P. H. O'Donnell, A. Drakaki, W. Tan, J. F. Kurland, M. C. Rebelatto, X. Jin, J. A. Blake-Haskins, A. Gupta, and N. H. Segal. 2016. Safety and Efficacy of Durvalumab (MEDI4736), an Anti-Programmed Cell Death Ligand-1 Immune Checkpoint Inhibitor, in Patients With Advanced Urothelial Bladder Cancer. *J Clin Oncol* 34: 3119-3125.

96. Brahmer, J. R., S. S. Tykodi, L. Q. Chow, W. J. Hwu, S. L. Topalian, P. Hwu, C. G. Drake, L. H. Camacho, J. Kauh, K. Odunsi, H. C. Pitot, O. Hamid, S. Bhatia, R. Martins, K. Eaton, S. Chen, T. M. Salay, S. Alaparthy, J. F. Grosso, A. J. Korman, S. M. Parker, S. Agrawal, S. M. Goldberg, D. M. Pardoll, A. Gupta, and J. M.

Wigginton. 2012. Safety and activity of anti-PD-L1 antibody in patients with advanced cancer. *N Engl J Med* 366: 2455-2465.

97. Powles, T., J. P. Eder, G. D. Fine, F. S. Braiteh, Y. Loriot, C. Cruz, J. Bellmunt, H. A. Burris, D. P. Petrylak, S. L. Teng, X. Shen, Z. Boyd, P. S. Hegde, D. S. Chen, and N. J. Vogelzang. 2014. MPDL3280A (anti-PD-L1) treatment leads to clinical activity in metastatic bladder cancer. *Nature* 515: 558-562.

98. Sunshine, J., and J. M. Taube. 2015. PD-1/PD-L1 inhibitors. *Curr Opin Pharmacol* 23: 32-38.

99. Hodi, F. S., S. J. O'Day, D. F. McDermott, R. W. Weber, J. A. Sosman, J. B. Haanen, R. Gonzalez, C. Robert, D. Schadendorf, J. C. Hassel, W. Akerley, A. J. van den Eertwegh, J. Lutzky, P. Lorigan, J. M. Vaubel, G. P. Linette, D. Hogg, C. H. Ottensmeier, C. Lebbe, C. Peschel, I. Quirt, J. I. Clark, J. D. Wolchok, J. S. Weber, J. Tian, M. J. Yellin, G. M. Nichol, A. Hoos, and W. J. Urba. 2010. Improved survival with ipilimumab in patients with metastatic melanoma. *N Engl J Med* 363: 711-723.

100. Margolin, K., M. S. Ernstoff, O. Hamid, D. Lawrence, D. McDermott, I. Puzanov, J. D. Wolchok, J. I. Clark, M. Sznol, T. F. Logan, J. Richards, T. Michener, A. Balogh, K. N. Heller, and F. S. Hodi. 2012. Ipilimumab in patients with melanoma and brain metastases: an open-label, phase 2 trial. *Lancet Oncol* 13: 459-465.

101. Webster, R. M. 2014. The immune checkpoint inhibitors: where are we now? *Nat Rev Drug Discov* 13: 883-884.

102. Preusser, M., M. Lim, D. A. Hafler, D. A. Reardon, and J. H. Sampson. 2015. Prospects of immune checkpoint modulators in the treatment of glioblastoma. *Nat Rev Neurol* 11: 504-514.

103. Lussier, D. M., L. O'Neill, L. M. Nieves, M. S. McAfee, S. A. Holechek, A. W. Collins, P. Dickman, J. Jacobsen, P. Hingorani, and J. N. Blattman. 2015. Enhanced T-cell immunity to osteosarcoma through antibody blockade of PD-1/PD-L1 interactions. *J Immunother* 38: 96-106.

104. Koshkina, N. V., C. Khanna, A. Mendoza, H. Guan, L. DeLauter, and E. S. Kleinerman. 2007. Fas-negative osteosarcoma tumor cells are selected during metastasis to the lungs: the role of the Fas pathway in the metastatic process of osteosarcoma. *Mol Cancer Res* 5: 991-999.

105. Rao-Bindal, K., N. V. Koshkina, J. Stewart, and E. S. Kleinerman. 2013. The histone deacetylase inhibitor, MS-275 (entinostat), downregulates c-FLIP, sensitizes osteosarcoma cells to FasL, and induces the regression of osteosarcoma lung metastases. *Curr Cancer Drug Targets* 13: 411-422.

106. Jia, S. F., L. L. Worth, and E. S. Kleinerman. 1999. A nude mouse model of human osteosarcoma lung metastases for evaluating new therapeutic strategies. *Clin Exp Metastasis* 17: 501-506.

107. Peng, W., G. Lizee, and P. Hwu. 2013. Blockade of the PD-1 pathway enhances the efficacy of adoptive cell therapy against cancer. *Oncoimmunology* 2: e22691.

108. Loi, S., S. Dushyanthen, P. A. Beavis, R. Salgado, C. Denkert, P. Savas, S. Combs, D. L. Rimm, J. M. Giltnane, M. V. Estrada, V. Sanchez, M. E. Sanders, R. S. Cook, M. A. Pilkinton, S. A. Mallal, K. Wang, V. A. Miller, P. J. Stephens, R. Yelensky, F. D. Doimi, H. Gomez, S. V. Ryzhov, P. K. Darcy, C. L. Arteaga, and J. M. Balko. 2016. RAS/MAPK Activation Is Associated with Reduced Tumor-Infiltrating Lymphocytes in Triple-Negative Breast Cancer: Therapeutic Cooperation Between

MEK and PD-1/PD-L1 Immune Checkpoint Inhibitors. *Clin Cancer Res* 22: 1499-1509.

109. John, L. B., C. Devaud, C. P. Duong, C. S. Yong, P. A. Beavis, N. M. Haynes, M. T. Chow, M. J. Smyth, M. H. Kershaw, and P. K. Darcy. 2013. Anti-PD-1 antibody therapy potently enhances the eradication of established tumors by gene-modified T cells. *Clin Cancer Res* 19: 5636-5646.

110. Schadler, K. L., P. A. Zweidler-McKay, H. Guan, and E. S. Kleinerman. 2010. Delta-like ligand 4 plays a critical role in pericyte/vascular smooth muscle cell formation during vasculogenesis and tumor vessel expansion in Ewing's sarcoma. *Clin Cancer Res* 16: 848-856.

111. Shen, J. K., G. M. Cote, E. Choy, P. Yang, D. Harmon, J. Schwab, G. P. Nielsen, I. Chebib, S. Ferrone, X. Wang, Y. Wang, H. Mankin, F. J. Hornicek, and Z. Duan. 2014. Programmed cell death ligand 1 expression in osteosarcoma. *Cancer Immunol Res* 2: 690-698.

112. Koirala, P., M. E. Roth, J. Gill, S. Piperdi, J. M. Chinai, D. S. Geller, B. H. Hoang, A. Park, M. A. Fremed, X. Zang, and R. Gorlick. 2016. Immune infiltration and PD-L1 expression in the tumor microenvironment are prognostic in osteosarcoma. *Sci Rep* 6: 30093.

113. Muhlbauer, M., M. Fleck, C. Schutz, T. Weiss, M. Froh, C. Blank, J. Scholmerich, and C. Hellerbrand. 2006. PD-L1 is induced in hepatocytes by viral infection and by interferon-alpha and -gamma and mediates T cell apoptosis. *J Hepatol* 45: 520-528.

114. Waeckerle-Men, Y., A. Starke, and R. P. Wuthrich. 2007. PD-L1 partially protects renal tubular epithelial cells from the attack of CD8+ cytotoxic T cells. *Nephrol Dial Transplant* 22: 1527-1536.

115. Chinai, J. M., M. Janakiram, F. Chen, W. Chen, M. Kaplan, and X. Zang. 2015. New immunotherapies targeting the PD-1 pathway. *Trends Pharmacol Sci* 36: 587-595.

116. Yamazaki, T., H. Akiba, H. Iwai, H. Matsuda, M. Aoki, Y. Tanno, T. Shin, H. Tsuchiya, D. M. Pardoll, K. Okumura, M. Azuma, and H. Yagita. 2002. Expression of programmed death 1 ligands by murine T cells and APC. *J Immunol* 169: 5538-5545.

117. Atefi, M., E. Avramis, A. Lassen, D. J. Wong, L. Robert, D. Foulad, M. Cerniglia, B. Titz, T. Chodon, T. G. Graeber, B. Comin-Anduix, and A. Ribas. 2014. Effects of MAPK and PI3K pathways on PD-L1 expression in melanoma. *Clin Cancer Res* 20: 3446-3457.

118. Soliman, H., F. Khalil, and S. Antonia. 2014. PD-L1 expression is increased in a subset of basal type breast cancer cells. *PLoS One* 9: e88557.

119. Liu, J., A. Hamrouni, D. Wolowiec, V. Coiteux, K. Kuliczkowski, D. Hetuin, A. Saudemont, and B. Quesnel. 2007. Plasma cells from multiple myeloma patients express B7-H1 (PD-L1) and increase expression after stimulation with IFN-{gamma} and TLR ligands via a MyD88-, TRAF6-, and MEK-dependent pathway. *Blood* 110: 296-304.

120. Spranger, S., R. M. Spaapen, Y. Zha, J. Williams, Y. Meng, T. T. Ha, and T. F. Gajewski. 2013. Up-regulation of PD-L1, IDO, and T(regs) in the melanoma tumor microenvironment is driven by CD8(+) T cells. *Sci Transl Med* 5: 200ra116.

121. Zhang, Y., S. Huang, D. Gong, Y. Qin, and Q. Shen. 2010. Programmed death-1 upregulation is correlated with dysfunction of tumor-infiltrating CD8+ T lymphocytes in human non-small cell lung cancer. *Cell Mol Immunol* 7: 389-395.

122. Krambeck, A. E., H. Dong, R. H. Thompson, S. M. Kuntz, C. M. Lohse, B. C. Leibovich, M. L. Blute, T. J. Sebo, J. C. Cheville, A. S. Parker, and E. D. Kwon. 2007. Survivin and b7-h1 are collaborative predictors of survival and represent potential therapeutic targets for patients with renal cell carcinoma. *Clin Cancer Res* 13: 1749-1756.

123. Ghebeh, H., S. Mohammed, A. Al-Omair, A. Qattan, C. Lehe, G. Al-Qudaihi, N. Elkum, M. Alshabanah, S. Bin Amer, A. Tulbah, D. Ajarim, T. Al-Tweigeri, and S. Dermime. 2006. The B7-H1 (PD-L1) T lymphocyte-inhibitory molecule is expressed in breast cancer patients with infiltrating ductal carcinoma: correlation with important high-risk prognostic factors. *Neoplasia* 8: 190-198.

124. Ghebeh, H., A. Tulbah, S. Mohammed, N. Elkum, S. M. Bin Amer, T. Al-Tweigeri, and S. Dermime. 2007. Expression of B7-H1 in breast cancer patients is strongly associated with high proliferative Ki-67-expressing tumor cells. *Int J Cancer* 121: 751-758.

125. Hamanishi, J., M. Mandai, M. Iwasaki, T. Okazaki, Y. Tanaka, K. Yamaguchi, T. Higuchi, H. Yagi, K. Takakura, N. Minato, T. Honjo, and S. Fujii. 2007. Programmed cell death 1 ligand 1 and tumor-infiltrating CD8+ T lymphocytes are prognostic factors of human ovarian cancer. *Proc Natl Acad Sci U S A* 104: 3360-3365.

126. Borghaei, H., L. Paz-Ares, L. Horn, D. R. Spigel, M. Steins, N. E. Ready, L. Q. Chow, E. E. Vokes, E. Felip, E. Holgado, F. Barlesi, M. Kohlhaufl, O. Arrieta, M. A.

Burgio, J. Fayette, H. Lena, E. Poddubskaya, D. E. Gerber, S. N. Gettinger, C. M. Rudin, N. Rizvi, L. Crino, G. R. Blumenschein, Jr., S. J. Antonia, C. Dorange, C. T. Harbison, F. Graf Finckenstein, and J. R. Brahmer. 2015. Nivolumab versus Docetaxel in Advanced Nonsquamous Non-Small-Cell Lung Cancer. *N Engl J Med* 373: 1627-1639.

127. Okudaira, K., R. Hokari, Y. Tsuzuki, Y. Okada, S. Komoto, C. Watanabe, C. Kurihara, A. Kawaguchi, S. Nagao, M. Azuma, H. Yagita, and S. Miura. 2009. Blockade of B7-H1 or B7-DC induces an anti-tumor effect in a mouse pancreatic cancer model. *Int J Oncol* 35: 741-749.

128. Iwai, Y., S. Terawaki, and T. Honjo. 2005. PD-1 blockade inhibits hematogenous spread of poorly immunogenic tumor cells by enhanced recruitment of effector T cells. *Int Immunol* 17: 133-144.

129. Curran, M. A., W. Montalvo, H. Yagita, and J. P. Allison. 2010. PD-1 and CTLA-4 combination blockade expands infiltrating T cells and reduces regulatory T and myeloid cells within B16 melanoma tumors. *Proc Natl Acad Sci U S A* 107: 4275-4280.

130. Zhou, Q., H. Xiao, Y. Liu, Y. Peng, Y. Hong, H. Yagita, P. Chandler, D. H. Munn, A. Mellor, N. Fu, and Y. He. 2010. Blockade of programmed death-1 pathway rescues the effector function of tumor-infiltrating T cells and enhances the antitumor efficacy of lentivector immunization. *J Immunol* 185: 5082-5092.

131. Lin, D. Y., Y. Tanaka, M. Iwasaki, A. G. Gittis, H. P. Su, B. Mikami, T. Okazaki, T. Honjo, N. Minato, and D. N. Garboczi. 2008. The PD-1/PD-L1 complex resembles

the antigen-binding Fv domains of antibodies and T cell receptors. *Proc Natl Acad Sci U S A* 105: 3011-3016.

132. Freeman, G. J., A. J. Long, Y. Iwai, K. Bourque, T. Chernova, H. Nishimura, L. J. Fitz, N. Malenkovich, T. Okazaki, M. C. Byrne, H. F. Horton, L. Fouser, L. Carter, V. Ling, M. R. Bowman, B. M. Carreno, M. Collins, C. R. Wood, and T. Honjo. 2000. Engagement of the PD-1 immunoinhibitory receptor by a novel B7 family member leads to negative regulation of lymphocyte activation. *J Exp Med* 192: 1027-1034.

133. Jurikova, M., L. Danihel, S. Polak, and I. Varga. 2016. Ki67, PCNA, and MCM proteins: Markers of proliferation in the diagnosis of breast cancer. *Acta Histochem* 118: 544-552.

134. Scholzen, T., and J. Gerdes. 2000. The Ki-67 protein: from the known and the unknown. *J Cell Physiol* 182: 311-322.

135. Gown, A. M., and M. C. Willingham. 2002. Improved detection of apoptotic cells in archival paraffin sections: immunohistochemistry using antibodies to cleaved caspase 3. *J Histochem Cytochem* 50: 449-454.

136. Resendes, A. R., N. Majo, J. Segales, J. Espadamala, E. Mateu, F. Chianini, M. Nofrarias, and M. Domingo. 2004. Apoptosis in normal lymphoid organs from healthy normal, conventional pigs at different ages detected by TUNEL and cleaved caspase-3 immunohistochemistry in paraffin-embedded tissues. *Vet Immunol Immunopathol* 99: 203-213.

137. Modak, S. P., and F. J. Bollum. 1970. Terminal lens cell differentiation. 3. Initiator activity of DNA during nuclear degeneration. *Exp Cell Res* 62: 421-432.

138. Gavrieli, Y., Y. Sherman, and S. A. Ben-Sasson. 1992. Identification of programmed cell death in situ via specific labeling of nuclear DNA fragmentation. *J Cell Biol* 119: 493-501.

139. Mangili, F., C. Cigala, and G. Santambrogio. 1999. Staining apoptosis in paraffin sections. Advantages and limits. *Anal Quant Cytol Histol* 21: 273-276.

140. Labat-Moleur, F., C. Guillermet, P. Lorimier, C. Robert, S. Lantuejoul, E. Brambilla, and A. Negoescu. 1998. TUNEL apoptotic cell detection in tissue sections: critical evaluation and improvement. *J Histochem Cytochem* 46: 327-334.

141. Williams, G. T., and C. A. Smith. 1993. Molecular regulation of apoptosis: genetic controls on cell death. *Cell* 74: 777-779.

142. Alenzi, F. Q. 2004. Links between apoptosis, proliferation and the cell cycle. *Br J Biomed Sci* 61: 99-102.

143. Gerard, C., and A. Goldbeter. 2014. The balance between cell cycle arrest and cell proliferation: control by the extracellular matrix and by contact inhibition. *Interface Focus* 4: 20130075.

144. de la Puente, P., B. Muz, A. Jin, F. Azab, M. Luderer, N. N. Salama, and A. K. Azab. 2016. MEK inhibitor, TAK-733 reduces proliferation, affects cell cycle and apoptosis, and synergizes with other targeted therapies in multiple myeloma. *Blood Cancer J* 6: e399.

145. Wolchok, J. D., H. Kluger, M. K. Callahan, M. A. Postow, N. A. Rizvi, A. M. Lesokhin, N. H. Segal, C. E. Ariyan, R. A. Gordon, K. Reed, M. M. Burke, A. Caldwell, S. A. Kronenberg, B. U. Agunwamba, X. Zhang, I. Lowy, H. D. Inzunza, W. Feely, C. E. Horak, Q. Hong, A. J. Korman, J. M. Wigginton, A. Gupta, and M.

Sznol. 2013. Nivolumab plus ipilimumab in advanced melanoma. *N Engl J Med* 369: 122-133.

146. Hamid, O., C. Robert, A. Daud, F. S. Hodi, W. J. Hwu, R. Kefford, J. D. Wolchok, P. Hersey, R. W. Joseph, J. S. Weber, R. Dronca, T. C. Gangadhar, A. Patnaik, H. Zarour, A. M. Joshua, K. Gergich, J. Elassaiss-Schaap, A. Algazi, C. Mateus, P. Boasberg, P. C. Tumeh, B. Chmielowski, S. W. Ebbinghaus, X. N. Li, S. P. Kang, and A. Ribas. 2013. Safety and tumor responses with lambrolizumab (anti-PD-1) in melanoma. *N Engl J Med* 369: 134-144.

147. Curiel, T. J., S. Wei, H. Dong, X. Alvarez, P. Cheng, P. Mottram, R. Krzysiek, K. L. Knutson, B. Daniel, M. C. Zimmermann, O. David, M. Burow, A. Gordon, N. Dhurandhar, L. Myers, R. Berggren, A. Hemminki, R. D. Alvarez, D. Emilie, D. T. Curiel, L. Chen, and W. Zou. 2003. Blockade of B7-H1 improves myeloid dendritic cell-mediated antitumor immunity. *Nat Med* 9: 562-567.

148. Hirano, F., K. Kaneko, H. Tamura, H. Dong, S. Wang, M. Ichikawa, C. Rietz, D. B. Flies, J. S. Lau, G. Zhu, K. Tamada, and L. Chen. 2005. Blockade of B7-H1 and PD-1 by monoclonal antibodies potentiates cancer therapeutic immunity. *Cancer Res* 65: 1089-1096.

149. Woo, S. R., M. E. Turnis, M. V. Goldberg, J. Bankoti, M. Selby, C. J. Nirschl, M. L. Bettini, D. M. Gravano, P. Vogel, C. L. Liu, S. Tangsombatvisit, J. F. Grosso, G. Netto, M. P. Smeltzer, A. Chaux, P. J. Utz, C. J. Workman, D. M. Pardoll, A. J. Korman, C. G. Drake, and D. A. Vignali. 2012. Immune inhibitory molecules LAG-3 and PD-1 synergistically regulate T-cell function to promote tumoral immune escape. *Cancer Res* 72: 917-927.

150. Ohaegbulam, K. C., A. Assal, E. Lazar-Molnar, Y. Yao, and X. Zang. 2015. Human cancer immunotherapy with antibodies to the PD-1 and PD-L1 pathway. *Trends Mol Med* 21: 24-33.

151. Blackburn, S. D., H. Shin, W. N. Haining, T. Zou, C. J. Workman, A. Polley, M. R. Betts, G. J. Freeman, D. A. Vignali, and E. J. Wherry. 2009. Coregulation of CD8+ T cell exhaustion by multiple inhibitory receptors during chronic viral infection. *Nat Immunol* 10: 29-37.

152. Alvarez, I. B., V. Pasquinelli, J. O. Jurado, E. Abbate, R. M. Musella, S. S. de la Barrera, and V. E. Garcia. 2010. Role played by the programmed death-1-programmed death ligand pathway during innate immunity against Mycobacterium tuberculosis. *J Infect Dis* 202: 524-532.

153. Norris, S., A. Coleman, L. Kuri-Cervantes, M. Bower, M. Nelson, and M. R. Goodier. 2012. PD-1 expression on natural killer cells and CD8(+) T cells during chronic HIV-1 infection. *Viral Immunol* 25: 329-332.

154. Benson, D. M., Jr., C. E. Bakan, A. Mishra, C. C. Hofmeister, Y. Efebera, B. Becknell, R. A. Baiocchi, J. Zhang, J. Yu, M. K. Smith, C. N. Greenfield, P. Porcu, S. M. Devine, R. Rotem-Yehudar, G. Lozanski, J. C. Byrd, and M. A. Caligiuri. 2010. The PD-1/PD-L1 axis modulates the natural killer cell versus multiple myeloma effect: a therapeutic target for CT-011, a novel monoclonal anti-PD-1 antibody. *Blood* 116: 2286-2294.

155. Lee, S. J., W. Y. Kang, Y. Yoon, J. Y. Jin, H. J. Song, J. H. Her, S. M. Kang, Y. K. Hwang, K. J. Kang, K. M. Joo, and D. H. Nam. 2015. Natural killer (NK) cells inhibit

systemic metastasis of glioblastoma cells and have therapeutic effects against glioblastomas in the brain. *BMC Cancer* 15: 1011.

156. Huang, X., F. Venet, Y. L. Wang, A. Lepape, Z. Yuan, Y. Chen, R. Swan, H. Kherouf, G. Monneret, C. S. Chung, and A. Ayala. 2009. PD-1 expression by macrophages plays a pathologic role in altering microbial clearance and the innate inflammatory response to sepsis. *Proc Natl Acad Sci U S A* 106: 6303-6308.

157. Cho, H. Y., E. K. Choi, S. W. Lee, K. O. Jung, S. K. Seo, I. W. Choi, S. G. Park, and I. Choi. 2009. Programmed death-1 receptor negatively regulates LPS-mediated IL-12 production and differentiation of murine macrophage RAW264.7 cells. *Immunol Lett* 127: 39-47.

158. Said, E. A., F. P. Dupuy, L. Trautmann, Y. Zhang, Y. Shi, M. El-Far, B. J. Hill, A. Noto, P. Ancuta, Y. Peretz, S. G. Fonseca, J. Van Grevenynghe, M. R. Boulassel, J. Bruneau, N. H. Shoukry, J. P. Routy, D. C. Douek, E. K. Haddad, and R. P. Sekaly. 2010. Programmed death-1-induced interleukin-10 production by monocytes impairs CD4+ T cell activation during HIV infection. *Nat Med* 16: 452-459.

159. Zhang, M., G. Hutter, S. A. Kahn, T. D. Azad, S. Gholamin, C. Y. Xu, J. Liu, A. S. Achrol, C. Richard, P. Sommerkamp, M. K. Schoen, M. N. McCracken, R. Majeti, I. Weissman, S. S. Mitra, and S. H. Cheshier. 2016. Anti-CD47 Treatment Stimulates Phagocytosis of Glioblastoma by M1 and M2 Polarized Macrophages and Promotes M1 Polarized Macrophages In Vivo. *PLoS One* 11: e0153550.

160. Routes, J. M., K. Morris, M. C. Ellison, and S. Ryan. 2005. Macrophages kill human papillomavirus type 16 E6-expressing tumor cells by tumor necrosis factor alpha- and nitric oxide-dependent mechanisms. *J Virol* 79: 116-123.

161. Vitale, M., C. Cantoni, G. Pietra, M. C. Mingari, and L. Moretta. 2014. Effect of tumor cells and tumor microenvironment on NK-cell function. *Eur J Immunol* 44: 1582-1592.

162. Mukhtar, R. A., A. P. Moore, O. Nseyo, F. L. Baehner, A. Au, D. H. Moore, P. Twomey, M. J. Campbell, and L. J. Esserman. 2011. Elevated PCNA+ tumor-associated macrophages in breast cancer are associated with early recurrence and non-Caucasian ethnicity. *Breast Cancer Res Treat* 130: 635-644.

163. Mosser, D. M. 2003. The many faces of macrophage activation. *J Leukoc Biol* 73: 209-212.

164. Gordon, S. 2003. Alternative activation of macrophages. *Nat Rev Immunol* 3: 23-35.

165. Vasiliadou, I., and I. Holen. 2013. The role of macrophages in bone metastasis. *J Bone Oncol* 2: 158-166.

166. Sica, A., T. Schioppa, A. Mantovani, and P. Allavena. 2006. Tumour-associated macrophages are a distinct M2 polarised population promoting tumour progression: potential targets of anti-cancer therapy. *Eur J Cancer* 42: 717-727.

167. Pahl, J. H., K. M. Kwappenberg, E. M. Varypataki, S. J. Santos, M. L. Kuijjer, S. Mohamed, J. T. Wijnen, M. J. van Tol, A. M. Cleton-Jansen, R. M. Egeler, W. Jiskoot, A. C. Lankester, and M. W. Schilham. 2014. Macrophages inhibit human osteosarcoma cell growth after activation with the bacterial cell wall derivative liposomal muramyl tripeptide in combination with interferon-gamma. *J Exp Clin Cancer Res* 33: 27.

168. Meazza, R., B. Azzarone, A. M. Orengo, and S. Ferrini. 2011. Role of common-gamma chain cytokines in NK cell development and function: perspectives for immunotherapy. *J Biomed Biotechnol* 2011: 861920.

169. Michel, T., A. Poli, O. Domingues, M. Mauffray, M. Theresine, N. H. Brons, F. Hentges, and J. Zimmer. 2012. Mouse lung and spleen natural killer cells have phenotypic and functional differences, in part influenced by macrophages. *PLoS One* 7: e51230.

170. Malhotra, A., and A. Shanker. 2011. NK cells: immune cross-talk and therapeutic implications. *Immunotherapy* 3: 1143-1166.

171. Habu, S., H. Fukui, K. Shimamura, M. Kasai, Y. Nagai, K. Okumura, and N. Tamaoki. 1981. In vivo effects of anti-asialo GM1. I. Reduction of NK activity and enhancement of transplanted tumor growth in nude mice. *J Immunol* 127: 34-38.

172. Maruyama, T., K. Watanabe, I. Takei, A. Kasuga, A. Shimada, T. Yanagawa, T. Kasatani, Y. Suzuki, K. Kataoka, Saruta, and et al. 1991. Anti-asialo GM1 antibody suppression of cyclophosphamide-induced diabetes in NOD mice. *Diabetes Res* 17: 37-41.

173. Monnier, J., and B. A. Zabel. 2014. Anti-asialo GM1 NK cell depleting antibody does not alter the development of bleomycin induced pulmonary fibrosis. *PLoS One* 9: e99350.

174. Robinson-Smith, T. M., I. Isaacsohn, C. A. Mercer, M. Zhou, N. Van Rooijen, N. Husseinzadeh, M. M. McFarland-Mancini, and A. F. Drew. 2007. Macrophages mediate inflammation-enhanced metastasis of ovarian tumors in mice. *Cancer Res* 67: 5708-5716.

175. Kasai, M., T. Yoneda, S. Habu, Y. Maruyama, K. Okumura, and T. Tokunaga. 1981. In vivo effect of anti-asialo GM1 antibody on natural killer activity. *Nature* 291: 334-335.

176. Di Carlo, E., A. Comes, S. Basso, A. De Ambrosis, R. Meazza, P. Musiani, K. Moelling, A. Albini, and S. Ferrini. 2000. The combined action of IL-15 and IL-12 gene transfer can induce tumor cell rejection without T and NK cell involvement. *J Immunol* 165: 3111-3118.

177. Bellora, F., R. Castriconi, A. Dondero, G. Reggiardo, L. Moretta, A. Mantovani, A. Moretta, and C. Bottino. 2010. The interaction of human natural killer cells with either unpolarized or polarized macrophages results in different functional outcomes. *Proc Natl Acad Sci U S A* 107: 21659-21664.

178. Shi, Y., X. Fan, H. Deng, R. J. Brezski, M. Rycyzyn, R. E. Jordan, W. R. Strohl, Q. Zou, N. Zhang, and Z. An. 2015. Trastuzumab triggers phagocytic killing of high HER2 cancer cells in vitro and in vivo by interaction with Fcgamma receptors on macrophages. *J Immunol* 194: 4379-4386.

179. Xu, M., M. Liu, X. Du, S. Li, H. Li, X. Li, Y. Li, Y. Wang, Z. Qin, Y. X. Fu, and S. Wang. 2015. Intratumoral Delivery of IL-21 Overcomes Anti-Her2/Neu Resistance through Shifting Tumor-Associated Macrophages from M2 to M1 Phenotype. *J Immunol* 194: 4997-5006.

180. Huang, W., Z. Chen, L. Zhang, D. Tian, D. Wang, D. Fan, K. Wu, and L. Xia. 2015. Interleukin-8 Induces Expression of FOXC1 to Promote Transactivation of CXCR1 and CCL2 in Hepatocellular Carcinoma Cell Lines and Formation of Metastases in Mice. *Gastroenterology* 149: 1053-1067 e1014.

181. Kleffel, S., C. Posch, S. R. Barthel, H. Mueller, C. Schlapbach, E. Guenova, C. P. Elco, N. Lee, V. R. Juneja, Q. Zhan, C. G. Lian, R. Thomi, W. Hoetzenecker, A. Cozzio, R. Dummer, M. C. Mihm, Jr., K. T. Flaherty, M. H. Frank, G. F. Murphy, A. H. Sharpe, T. S. Kupper, and T. Schatton. 2015. Melanoma Cell-Intrinsic PD-1 Receptor Functions Promote Tumor Growth. *Cell* 162: 1242-1256.

182. Salas, S., C. Jiguet-Jiglaire, L. Campion, C. Bartoli, F. Frassineti, J. L. Deville, A. Maues De Paula, F. Forest, P. Jezequel, J. C. Gentet, and C. Bouvier. 2014. Correlation between ERK1 and STAT3 expression and chemoresistance in patients with conventional osteosarcoma. *BMC Cancer* 14: 606.

183. Ryu, K., E. Choy, C. Yang, M. Susa, F. J. Hornicek, H. Mankin, and Z. Duan. 2010. Activation of signal transducer and activator of transcription 3 (Stat3) pathway in osteosarcoma cells and overexpression of phosphorylated-Stat3 correlates with poor prognosis. *J Orthop Res* 28: 971-978.

184. Jiang, X., J. Zhou, A. Giobbie-Hurder, J. Wargo, and F. S. Hodi. 2013. The activation of MAPK in melanoma cells resistant to BRAF inhibition promotes PD-L1 expression that is reversible by MEK and PI3K inhibition. *Clin Cancer Res* 19: 598-609.

185. Fossey, S. L., A. T. Liao, J. K. McCleese, M. D. Bear, J. Lin, P. K. Li, W. C. Kisseberth, and C. A. London. 2009. Characterization of STAT3 activation and expression in canine and human osteosarcoma. *BMC Cancer* 9: 81.

186. Xiong, H., Z. G. Zhang, X. Q. Tian, D. F. Sun, Q. C. Liang, Y. J. Zhang, R. Lu, Y. X. Chen, and J. Y. Fang. 2008. Inhibition of JAK1, 2/STAT3 signaling induces

apoptosis, cell cycle arrest, and reduces tumor cell invasion in colorectal cancer cells. *Neoplasia* 10: 287-297.

187. Ritter, J., and S. S. Bielack. 2010. Osteosarcoma. *Ann Oncol* 21 Suppl 7: vii320-325.

188. Chen, X., A. Bahrami, A. Pappo, J. Easton, J. Dalton, E. Hedlund, D. Ellison, S. Shurtleff, G. Wu, L. Wei, M. Parker, M. Rusch, P. Nagahawatte, J. Wu, S. Mao, K. Boggs, H. Mulder, D. Yergeau, C. Lu, L. Ding, M. Edmonson, C. Qu, J. Wang, Y. Li, F. Navid, N. C. Daw, E. R. Mardis, R. K. Wilson, J. R. Downing, J. Zhang, and M. A. Dyer. 2014. Recurrent somatic structural variations contribute to tumorigenesis in pediatric osteosarcoma. *Cell Rep* 7: 104-112.

189. Helman, L. J., and P. Meltzer. 2003. Mechanisms of sarcoma development. *Nat Rev Cancer* 3: 685-694.

190. Stephens, P. J., C. D. Greenman, B. Fu, F. Yang, G. R. Bignell, L. J. Mudie, E. D. Pleasance, K. W. Lau, D. Beare, L. A. Stebbings, S. McLaren, M. L. Lin, D. J. McBride, I. Varela, S. Nik-Zainal, C. Leroy, M. Jia, A. Menzies, A. P. Butler, J. W. Teague, M. A. Quail, J. Burton, H. Swerdlow, N. P. Carter, L. A. Morsberger, C. Iacobuzio-Donahue, G. A. Follows, A. R. Green, A. M. Flanagan, M. R. Stratton, P. A. Futreal, and P. J. Campbell. 2011. Massive genomic rearrangement acquired in a single catastrophic event during cancer development. *Cell* 144: 27-40.

191. Perry, J. A., A. Kiezun, P. Tonzi, E. M. Van Allen, S. L. Carter, S. C. Baca, G. S. Cowley, A. S. Bhatt, E. Rheinbay, C. S. Pedamallu, E. Helman, A. Taylor-Weiner, A. McKenna, D. S. DeLuca, M. S. Lawrence, L. Ambrogio, C. Sougnez, A. Sivachenko, L. D. Walensky, N. Wagle, J. Mora, C. de Torres, C. Lavarino, S. Dos Santos Aguiar, J. A. Yunes, S. R. Brandalise, G. E. Mercado-Celis, J. Melendez-Zajgla, R. Cardenas-

Cardos, L. Velasco-Hidalgo, C. W. Roberts, L. A. Garraway, C. Rodriguez-Galindo, S. B. Gabriel, E. S. Lander, T. R. Golub, S. H. Orkin, G. Getz, and K. A. Janeway. 2014. Complementary genomic approaches highlight the PI3K/mTOR pathway as a common vulnerability in osteosarcoma. *Proc Natl Acad Sci U S A* 111: E5564-5573.

192. Song, M., D. Chen, B. Lu, C. Wang, J. Zhang, L. Huang, X. Wang, C. L. Timmons, J. Hu, B. Liu, X. Wu, L. Wang, J. Wang, and H. Liu. 2013. PTEN loss increases PD-L1 protein expression and affects the correlation between PD-L1 expression and clinical parameters in colorectal cancer. *PLoS One* 8: e65821.

193. Lastwika, K. J., W. Wilson, 3rd, Q. K. Li, J. Norris, H. Xu, S. R. Ghazarian, H. Kitagawa, S. Kawabata, J. M. Taube, S. Yao, L. N. Liu, J. J. Gills, and P. A. Dennis. 2016. Control of PD-L1 Expression by Oncogenic Activation of the AKT-mTOR Pathway in Non-Small Cell Lung Cancer. *Cancer Res* 76: 227-238.

194. Boland, J. M., E. D. Kwon, S. M. Harrington, J. A. Wampfler, H. Tang, P. Yang, and M. C. Aubry. 2013. Tumor B7-H1 and B7-H3 expression in squamous cell carcinoma of the lung. *Clin Lung Cancer* 14: 157-163.

195. McLaughlin, J., G. Han, K. A. Schalper, D. Carvajal-Hausdorf, V. Pelekanou, J. Rehman, V. Velcheti, R. Herbst, P. LoRusso, and D. L. Rimm. 2016. Quantitative Assessment of the Heterogeneity of PD-L1 Expression in Non-Small-Cell Lung Cancer. *JAMA Oncol* 2: 46-54.

196. Velcheti, V., K. A. Schalper, D. E. Carvajal, V. K. Anagnostou, K. N. Syrigos, M. Sznol, R. S. Herbst, S. N. Gettinger, L. Chen, and D. L. Rimm. 2014. Programmed death ligand-1 expression in non-small cell lung cancer. *Lab Invest* 94: 107-116.

197. Dong, H., S. E. Strome, D. R. Salomao, H. Tamura, F. Hirano, D. B. Flies, P. C. Roche, J. Lu, G. Zhu, K. Tamada, V. A. Lennon, E. Celis, and L. Chen. 2002. Tumor-associated B7-H1 promotes T-cell apoptosis: a potential mechanism of immune evasion. *Nat Med* 8: 793-800.

198. Akbay, E. A., S. Koyama, J. Carretero, A. Altabef, J. H. Tchaicha, C. L. Christensen, O. R. Mikse, A. D. Cherniack, E. M. Beauchamp, T. J. Pugh, M. D. Wilkerson, P. E. Fecci, M. Butaney, J. B. Reibel, M. Soucheray, T. J. Cohoon, P. A. Janne, M. Meyerson, D. N. Hayes, G. I. Shapiro, T. Shimamura, L. M. Sholl, S. J. Rodig, G. J. Freeman, P. S. Hammerman, G. Dranoff, and K. K. Wong. 2013. Activation of the PD-1 pathway contributes to immune escape in EGFR-driven lung tumors. *Cancer Discov* 3: 1355-1363.

199. Chen, Y., R. R. Ramjiawan, T. Reiberger, M. R. Ng, T. Hato, Y. Huang, H. Ochiai, S. Kitahara, E. C. Unan, T. P. Reddy, C. Fan, P. Huang, N. Bardeesy, A. X. Zhu, R. K. Jain, and D. G. Duda. 2015. CXCR4 inhibition in tumor microenvironment facilitates anti-programmed death receptor-1 immunotherapy in sorafenib-treated hepatocellular carcinoma in mice. *Hepatology* 61: 1591-1602.

200. Kennedy, J. D., C. W. Pierce, and J. P. Lake. 1992. Extrathymic T cell maturation. Phenotypic analysis of T cell subsets in nude mice as a function of age. *J Immunol* 148: 1620-1629.

201. Italiani, P., and D. Boraschi. 2014. From Monocytes to M1/M2 Macrophages: Phenotypical vs. Functional Differentiation. *Front Immunol* 5: 514.

202. Burkholder, B., R. Y. Huang, R. Burgess, S. Luo, V. S. Jones, W. Zhang, Z. Q. Lv, C. Y. Gao, B. L. Wang, Y. M. Zhang, and R. P. Huang. 2014. Tumor-induced

perturbations of cytokines and immune cell networks. *Biochim Biophys Acta* 1845: 182-201.

203. Patera, A. C., A. M. Drewry, K. Chang, E. R. Beiter, D. Osborne, and R. S. Hotchkiss. 2016. Frontline Science: Defects in immune function in patients with sepsis are associated with PD-1 or PD-L1 expression and can be restored by antibodies targeting PD-1 or PD-L1. *J Leukoc Biol*.

204. He, G., H. Zhang, J. Zhou, B. Wang, Y. Chen, Y. Kong, X. Xie, X. Wang, R. Fei, L. Wei, H. Chen, and H. Zeng. 2015. Peritumoural neutrophils negatively regulate adaptive immunity via the PD-L1/PD-1 signalling pathway in hepatocellular carcinoma. *J Exp Clin Cancer Res* 34: 141.

205. MacMicking, J., Q. W. Xie, and C. Nathan. 1997. Nitric oxide and macrophage function. *Annu Rev Immunol* 15: 323-350.

206. Xie, K., S. Huang, Z. Dong, S. H. Juang, M. Gutman, Q. W. Xie, C. Nathan, and I. J. Fidler. 1995. Transfection with the inducible nitric oxide synthase gene suppresses tumorigenicity and abrogates metastasis by K-1735 murine melanoma cells. *J Exp Med* 181: 1333-1343.

207. Bournazou, E., and J. Bromberg. 2013. Targeting the tumor microenvironment: JAK-STAT3 signaling. *JAKSTAT* 2: e23828.

208. Iwai, Y., M. Ishida, Y. Tanaka, T. Okazaki, T. Honjo, and N. Minato. 2002. Involvement of PD-L1 on tumor cells in the escape from host immune system and tumor immunotherapy by PD-L1 blockade. *Proc Natl Acad Sci U S A* 99: 12293-12297.

209. Zheng, W., H. Xiao, H. Liu, and Y. Zhou. 2015. Expression of programmed death 1 is correlated with progression of osteosarcoma. *APMIS* 123: 102-107.

210. MacFarlane, A. W. t., M. Jillab, E. R. Plimack, G. R. Hudes, R. G. Uzzo, S. Litwin, E. Dulaimi, T. Al-Saleem, and K. S. Campbell. 2014. PD-1 expression on peripheral blood cells increases with stage in renal cell carcinoma patients and is rapidly reduced after surgical tumor resection. *Cancer Immunol Res* 2: 320-331.

211. Khanna, C., J. Prehn, C. Yeung, J. Caylor, M. Tsokos, and L. Helman. 2000. An orthotopic model of murine osteosarcoma with clonally related variants differing in pulmonary metastatic potential. *Clin Exp Metastasis* 18: 261-271.

212. Carmenate, T., A. Pacios, M. Enamorado, E. Moreno, K. Garcia-Martinez, D. Fuente, and K. Leon. 2013. Human IL-2 mutein with higher antitumor efficacy than wild type IL-2. *J Immunol* 190: 6230-6238.

213. Roth, M., M. Linkowski, J. Tarim, S. Piperdi, R. Sowers, D. Geller, J. Gill, and R. Gorlick. 2014. Ganglioside GD2 as a therapeutic target for antibody-mediated therapy in patients with osteosarcoma. *Cancer* 120: 548-554.

214. Poon, V. I., M. Roth, S. Piperdi, D. Geller, J. Gill, E. R. Rudzinski, D. S. Hawkins, and R. Gorlick. 2015. Ganglioside GD2 expression is maintained upon recurrence in patients with osteosarcoma. *Clin Sarcoma Res* 5: 4.

215. Yu, A. L., M. M. Uttenreuther-Fischer, C. S. Huang, C. C. Tsui, S. D. Gillies, R. A. Reisfeld, and F. H. Kung. 1998. Phase I trial of a human-mouse chimeric anti-disialoganglioside monoclonal antibody ch14.18 in patients with refractory neuroblastoma and osteosarcoma. *J Clin Oncol* 16: 2169-2180.

216. Heiner, J. P., F. Miraldi, S. Kallick, J. Makley, J. Neely, W. H. Smith-Mensah, and N. K. Cheung. 1987. Localization of GD2-specific monoclonal antibody 3F8 in human osteosarcoma. *Cancer Res* 47: 5377-5381.

217. Hubert, P., A. Heitzmann, S. Viel, A. Nicolas, X. Sastre-Garau, P. Oppezzo, O. Pritsch, E. Osinaga, and S. Amigorena. 2011. Antibody-dependent cell cytotoxicity synapses form in mice during tumor-specific antibody immunotherapy. *Cancer Res* 71: 5134-5143.

218. Guillaume, T., D. B. Rubinstein, and M. Symann. 1998. Immune reconstitution and immunotherapy after autologous hematopoietic stem cell transplantation. *Blood* 92: 1471-1490.

219. Jing, W., R. J. Orentas, and B. D. Johnson. 2007. Induction of immunity to neuroblastoma early after syngeneic hematopoietic stem cell transplantation using a novel mouse tumor vaccine. *Biol Blood Marrow Transplant* 13: 277-292.

VITA

Pooja M. Dhupkar was born in India and graduated with a bachelor's degree in Pharmaceutical Sciences from the University of Mumbai, India, in June 2005. She came to the United States to pursue her graduate education in August 2005. She completed her Masters in Pharmacology and Toxicology from the University of Sciences in Philadelphia, Philadelphia, PA in July 2008. Her masters' thesis involved studying the effects of the anti-EGFR antibody Cetuximab in prostate cancer cells. This work led to her first author publication in *Anticancer Res.* 2010 Jun; 30(6):1905-10. After her masters, she worked as a Research Technician at Temple University, Philadelphia, where she gained expertise in biochemistry and molecular biology. Pooja joined the Graduate School of Biomedical Sciences at the University of Health Science Center and University of Texas M. D. Anderson Cancer Center. She then joined Dr. Eugenie Kleinerman's laboratory in the Department of Pediatrics to pursue her thesis research. Her work so far in graduate school has resulted in a co-author paper in *Mol Cancer Ther*. 2015 Mar; 14(3):681-91 and a first author publication in *Biochemistry and* Biophysics Reports, http://dx.doi.org/10.1016/j.bbrep.2016.10.009. She has also written a book chapter on 'Interleukin-2', which is currently under review.